Estrogen Decreases Inflammatory Responses by Dampening Glial Cell Activation

by

Tina Mathew

A dissertation submitted to the Graduate Faculty in Psychology in partial fulfillment of the requirements for the degree of Doctor of Philosophy

The City University of New York

2013

This manuscript has been read and accepted for the Graduate Faculty in Psychology in satisfaction of the dissertation requirement for the degree of Doctor of Philosophy.

Vanya Quinones-Jenab, Ph.D.

_____ _____

Date Chair of Examining Committee

Maureen O'Connor, Ph.D.

_____ _____

Date Chair of Examining Committee

Vanya Quinones-Jenab, Ph.D._____

Shirzad Jenab, Ph.D._____

Peter Serrano, Ph.D._____

Jim Gordon, Ph.D._____

Jesus Angulo, Ph.D._____

Supervisory Committee

THE CITY UNIVERSITY OF NEW YORK

ABSTRACT

Estrogen Decreases Inflammatory Responses by Dampening Glial Cell Activation

by

Tina Mathew

Advisor**:** Dr. Vanya Quinones-Jenab

Important sex differences in the development and perception of pain have been found by numerous epidemiological studies. This dimorphic response to pain is attributed to distinct endocrinological profiles in males and females. For example, in females, 17β-estradiol has been shown to diminish behavioral responses to nociception induced by inflammation in various pain models. However, estrogen's anti-hyperalgesic mechanism during the nervous system's inflammatory response is yet to be clearly defined. Glial cells, in particular microglia and astrocytes, have been shown to play an influential role in the establishment of pain states. The objective of this study is to determine if estrogen exerts its anti-hyperalgesic effects by reducing glial cell responses in the dorsal horn of the spinal cord and/or immune cell responses at the injury site, and how this in turn influences intracellular signaling pathways that regulate pro-inflammatory events. To this end, the Cg model of inflammatory pain was used with eight-week old ovariectomized Sprague-Dawley female rats that were subcutaneously implanted with a silastic capsule containing either 20% 17β-estradiol or cholesterol (vehicle), and at varying time periods, they received an injection of either carrageenan or saline (vehicle). Hindpaw withdrawal latencies in response to different heat stimuli (4.5 mV, 4.9 mV, and 5.3 mV) were measured using the Hargreaves Paw Thermal Stimulator. The rats were then sacrificed, spinal cords were dissected, and immunohistochemistry was performed on paws to observe CD68 macrophage activity and on spinal cord sections to observe glial cell responses and IL-1β

cytokine activity. Additionally, glial activation was correlation with levels of intracellular markers using Western blot analyses. Results reveal significantly dampened behavioral responses coupled with reduced glial activation in animals that received the estradiol treatment compared to animals that received the vehicle treatment. Additionally, estradiol treatment significantly reduced CD68 macrophage activity and IL-1β cytokine activity colocalized with glial activation. Correlations with intracellular markers did not reveal significant relationships with glial activity, but both the MAPK/ERK and JAK/STAT pathways were implicated in the estradiol-mediated inflammatory response in behavioral correlations. Taken together, our results suggest that estradiol's anti-inflammatory effects are mediated through the reduction of glial cell activity and consequent down-regulation of inflammatory mediators at the injury site and in the central nervous system.

ACKNOWLEDGEMENTS

Few have been as fortunate as I to have so many people in my life who have helped me throughout my graduate career. I offer sincere thanks to all of you for your wisdom and support throughout the years that have helped me reach this proud moment in my life.

To my mentor, Dr. Vanya Quinones-Jenab, thank you for your valuable mentorship and guidance during my time here at Hunter. You were always available to give me advice and motivation when I needed it, and I greatly appreciate the recommendations you gave me on all aspects of my project. I would also like to extend thanks to my dissertation committee members for taking part in my thesis. To Drs. Shirzad Jenab and Peter Serrano, thank you for helping me with the design of my experiments. To Drs. Jim Gordon and Jesus Angulo, thank you for being involved in the completion of my thesis and my defense.

To the members of the Quinones lab, thank you for all your help on my projects throughout the years. Thanks go to Drs. Kai Shivers and Lisa Abrams for helping train me and assist me with my experiments. Thanks also go to Stephanie Nygard and Zane Ferguson for their constant support, friendly advice, and comic relief amid stacks and stacks of SPSS outputs. Thank you also to all of the undergraduate students who helped me with my bench work.

I would also like to thank my friends and family for their unwavering support and understanding. I would especially like to thank Liddy, Joanne, and Cristina for always believing in me and making me laugh even when I didn't feel like it. To Anil: thank you for being my real-life knight in shining armor. To my parents: words cannot describe how grateful I am for all the love and support you have given me throughout my life, thank you. To my sister, Reena: thank you for always being there for me. And to my adorable nephew, Benjamin: thank you for

always knowing how to put a smile on my face! I love you all very much. Finally, above all, I thank God for giving me the strength and wisdom to meet every challenge.

TABLE OF CONTENTS

LIST OF FIGURES

LIST OF TABLES

ABBREVIATIONS

AMPA	α-amino-3-hydroxy-5-methylisoxazole
Ca^{2+}	calcium
Cg	carrageenan
CNS	central nervous system
COX	cyclooxygenase
DRG	dorsal root ganglia
E	estradiol
ER	estrogen receptor
ERK	extracellular signal-regulated kinase
GFAP	glial fibrillary acidic protein
IFN	Interferon
IL	interleukin
IL-1ra	IL-1 receptor antagonist
JAK	Janus Kinase
LPS	lipopolysaccharide
MAPK	mitogen active protein kinase
Mg^{2+}	magnesium
Na^{+}	sodium
NFκB	nuclear transcription factor kappa B
NMDA	N-methyl-D-aspartate
NGF	nerve growth factor
NO	nitric oxide
NOS	nitric oxide synthase
OVX	ovariectomy
pKA	protein kinase A
PG	prostaglandin
PGE_2	prostaglandin E_2
PWL	paw withdrawal latency
RA	rheumatoid arthritis
SP	substance P
STAT	signal transducer and activator of transcription
TMD	temporomandibular disorder
TNF	tumor necrosis factor
TNFR1	TNF receptor type 1
TNFR2	TNF receptor type 2
TRPV1	transient receptor potential vanilloid-1
TTXr	tetrodotoxin-resistant

Chapter 1: Introduction

Background and Significance

As human beings we all strive for health and happiness, but these two fundamental goals of life sometimes evade us because of pain. Whether it is emotional, mental, physical, or an intricate combination of all of the above, pain is the most ubiquitous complaint that doctors receive from patients. Unsurprisingly, the susceptibility to painful ailments like arthritis and fibromyalgia tends to increase with age (Campbell, 2004). This is because the vital hormones that once saturated our bodies with neuroprotective nourishment begin to dwindle. When the body's hormones are no longer at optimal levels, DNA is not optimally transcribed and autonomic homeostasis is not as well maintained-- this adverse chain of events creates a breeding ground for illness. Hormones perform critical functions that keep us healthy. For example, testosterone is necessary for optimal muscle growth and repair, cortisol is indispensable for efficient immune system function, and estrogen is essential for the growth and repair of neurons (Lewis et al., 2008). Recognizing and treating hormonal imbalances is key to maintaining good health and enhancing the quality of life well past one's prime.

Nowhere does this principle manifest itself more clearly than in the consideration of postmenopausal women who, as a result of decreased levels of endogenous estrogen, are prime targets for painful, degenerative illnesses. According to the National Institutes of Health, an estimated 40 million women across the United States will experience menopause during the next 20 years, and women today are living roughly one-third of their life after menopause (NIH.gov). Despite the controversial nature of using hormone replacement therapy (HRT), fueled by the recent recommendation against its use for the prevention of chronic illnesses in postmenopausal women, anywhere from 20-45% of women between the ages of 50 and 75 in the United States

today undergo some form of HRT (NIH.gov). In addition, HRT use is not limited to postmenopausal women, but is also used to treat hypo-estrogenic adolescent and young adult females. The prevalence of HRT use, in spite of conflicting reports about its efficacy in scientific literature, highlights the rising population of suffering patients and the growing need for more research on the effects of hormones on inflammation, a hallmark of degenerative disease.

Extensive research has been conducted to understand the influence of hormones on different pain states and these studies have revealed significant gender differences in pain discrimination and perception. To further our understanding of this dimorphic response to pain, current studies should investigate the role of gonadal hormones in the modulation of pain and inflammation. This investigation aims to, by gaining insight into hormonal regulatory influences on immunocompetent cells and specific biochemical markers involved in the inflammatory response, shed light on the sources of gender disparities in pain, which can in turn enhance our understanding of how to use HRT in the treatment of postmenopausal women with painful disorders.

Pain Classified

Pain is a multifarious sensory experience with strong cognitive and emotional counterparts. It is inherently unpleasant and conjures up the image of someone who is hurting or aching. Due to its diverse nature, pain can present itself with varying quality, intensity, duration, and location: for example, the sharp, severe pain you may experience for a few seconds right after stubbing the tip of your toe on a big rock differs greatly from the dull, throbbing pain you may experience an hour later around the whole toe. Even though pain is essentially classified as a physiological sensation, it can also translate to distress and anguish in its cognitive and emotional analogues. More specifically, the perception of pain at the psychological level

involves both a cognitive analysis of the painful incident and an emotional response to it (Riedel & Neeck, 2001).

While it is an altogether aversive experience, pain performs a crucial role in preserving the life of an organism. By immediately warning the organism of a potentially detrimental stimulus in its environment, the sensation of pain allows the organism to take appropriate action to withdraw from the stimulus and minimize damage to itself. This kind of pain can be termed adaptive (Millan, 1999). It serves as the cautionary reminder that motivates an individual to protect or treat an injury and to avoid such damaging stimuli in the future. As such, pain is also tied to motor reflexes in avoidance behaviors and changes in autonomic output. These widespread effects contribute to the elaborate mosaic of the pain experience (Kidd and Urban, 2001).

Pain can be broadly divided into acute and chronic pain. Acute pain usually resolves quickly when the noxious stimulus is removed (Saab, Waxman & Hains, 2008), lasting for only a brief period of time due to antinociceptive mechanisms induced by the stimulus that dissipate the painful sensation. (Riedel & Neeck, 2001). Normally occurring acute pain also reflects the timing, localization and intensity of a stimulus quite accurately (Kidd & Urban, 2001). Conversely, chronic pain, also known as clinical or pathological pain, has no benefit to the individual and can endanger one's survival (Costigan & Woolf, 2000). In contrast to acute pain, which accurately reflects aspects of the noxious stimulus such as intensity and duration, chronic pain is often amplified and can be experienced unprompted, without an external trigger (Kidd & Urban, 2001). Patients with this condition can develop long-term behavioral effects such as anhedonia (the inability to experience pleasure from once pleasurable activities), withdrawal, or a loss of interest in one's surroundings. Provoked by a persistent state of unavoidable stress,

these behavioral consequences of chronic pain emulate depressive conditions, and are therefore maladaptive (Millan, 1999).

A more precise classification of pain can produce the following categories: nociceptive pain, inflammatory pain, neuropathic pain, and functional pain. A noxious stimulus that is mediated by an intricate high-threshold sensory system, called the nociceptive system, causes the sensory experience of acute pain. From the periphery, this system reaches through the spinal cord, brainstem and thalamus to the cerebral cortex where perception takes place. Noxious stimuli are associated with the unpleasant side effect of pain that commands immediate attention so that we can build avoidance behaviors that protect against tissue damage (Basbaum & Julius, 2001). As such, nociceptive pain functions as a critical early warning system that announces an alarm in the face of a potentially harmful stimulus. It is an essential sensation that should not be disabled, except in particular clinical circumstances like surgery, because without it, we would lose the ability to protect ourselves against tissue injury, which can ultimately be fatal (McHugh & McHugh, 2000). Sufferers of the CIP disorder, congenital insensitivity to pain, face this very challenge because they lack high-threshold sensory neurons due to a mutation of the tyrosine kinase A receptor (Miranda et al., 2002).

When tissue injury is sustained in spite of the nociceptive defense mechanism—as in inflammatory illness, trauma, or surgery—our body responds by switching its protective role from defender to healer. Now the priority is to encourage repair of the damaged tissue and that is where inflammatory pain takes center stage. Inflammatory pain encourages injury repair by forming an area of hypersensitivity surrounding the injury, known as inflammation. This functions to decrease movement and contact with the injured area while it undergoes healing (Basbaum & Jessell, 2000). Although most pain is resolved soon after the harmful stimulus is

removed and the injury has healed, some types of pain persist, while others arise in the absence of any observable damaging stimulus.

With no apparent evolutionary benefit to the individual, pain of this nature can be termed maladaptive, as described earlier. Maladaptive pain occurs without an apparent noxious stimulus and is therefore pathological. Because it presents itself as irregular sensory processing, this kind of pain can be recurring. For example, chronic inflammation due to arthritis is induced by neuropathic pain, which is pain that results from damage to the nervous system. Other examples of neuropathic pain include patients with diabetic or AIDS-related polyneuropathy who suffer from lesions in the peripheral nervous system (Koltzenburg & Scadding, 2001). A more esoteric manifestation of maladaptive pain is functional pain, in which not only is there no observable noxious stimulus or peripheral aberration, but also no apparent damage to the nervous system. Functional pain is characterized by a heightened sensitivity of the sensory machinery that magnifies pain symptoms due to abnormal functioning of the nervous system. Conditions like fibromyalgia and irritable bowel syndrome display features that fit this particular pain profile (Costigan & Woolf, 2000).

Nociception

Although the terms "pain" and "nociception" are often used synonymously, it is important to note that there is a key difference between them. As discussed earlier, pain consists of both the physiological and psychological aspects of the sensation; however, nociception refers to the neural mechanism underlying the perception of pain. In this manner, nociception is defined as the physiological response to actual or perceived tissue damage, and does not include any psychological aspects of pain (Basbaum & Jessel, 2000). Since it is solely the neural recognition of a noxious stimulus (Weiseler-Frank, Maier & Watkins, 2004), nociception has no

connotation to an unpleasant feeling, like the term pain. For example, studies have shown that pain may arise in the absence of any tissue damage, and it may be exaggerated well beyond actual tissue injury (McHugh & McHugh, 2000).

In the nervous system, primary afferent neurons are sensory fibers that innervate cutaneous and deep somatic tissues, conveying information about both noxious and innocuous stimuli to the central nervous system (CNS). More specifically, the sensory fibers that transmit pain information are known as nociceptive afferent neurons, or nociceptors. Through three main functions, nociceptors provide the central nervous system with information about the state of the organism and its environment (Meyer, Ringkamp, Campbell, & Raja, 2005). First, via transduction, nociceptors detect noxious stimuli; second, via conduction, these afferents convey this sensory message from their peripheral nerve terminals to the spinal cord; and third, via transmission, this information is then communicated to the appropriate neurons residing within specific laminae in the dorsal horn of the spinal cord (Kidd & Urban, 2001).

Since research has shown that loss of these afferent fibers produces a pain-free phenotype, nociceptors have concretely been implicated in pain (Abrahamsen et al., 2008). These highly specialized sensory receptors respond most robustly to noxious stimuli affecting peripheral tissues (Basbaum & Jessell, 2000). Many nociceptors are actually free nerve endings that form arborizations in peripheral tissue. They carry proteins in their membranes that can transform different types of noxious stimuli, such as thermal, mechanical, and chemical types, into an electrical potential that is used to then transmit this information to the spinal cord (Coutaux, et. al, 2005; Basbaum & Jessell, 2000). Nociceptors are characterized by long distal projections with small diameter cell bodies that terminate in the dorsal root ganglia (DRG) located in close proximity to the spinal cord (McHugh & McHugh, 2000; Meyer, et. al, 2005).

They are also characterized by a high-threshold nature that requires high intensity stimuli to induce activation: a fact that increases the risk for tissue damage. Nociceptors are uniquely different from other sensory receptors, as illustrated by their particular sensitivity to the chemical, capsaicin, which is the fundamental ingredient in spicy foods (Kidd & Urban, 2001). Another characteristic that distinguishes them from other primary sensory afferents is their response to constant stimulation; while most sensory fibers demonstrate adaptation to a constant stimulus, nociceptors actually sensitize to constant stimulization, thereby creating an increase in response over time (Meyer, et al., 2005). While some nociceptors only respond to certain kinds of noxious stimuli (i.e. thermal, mechanical, chemical), most nociceptors display polymodality by responding to all different kinds (Meyer, et. al, 2005; Costigan & Woolf, 2000). It is this varying quality that is responsible for producing the wide array of pain sensations, like aching, pricking, and burning pain (Meyer et al., 2005).

Primary afferent fibers in the nervous system have varied functions in detecting noxious and innocuous stimuli based on their structural differences, such as axon diameter size and myelination thickness, which translates into conduction velocity (Costigan & Woolf, 2000). According to these differences, they can be categorized into three main groups. Aα and Aβ fibers have axons with relatively large diameters (>10μM) and thick myelination, which allows for fast conduction speeds (30+ m/s). Since these fibers are structured to have a low-threshold nature, under normal conditions they only transmit innocuous signals such as vibration and light touch (Costigan & Woolf, 2000). Aδ fibers have axons with medium-sized diameters (2-6μM), thin myelination, and consequently an intermediate conduction velocity (4-30 m/s). Conversely, C fibers are characterized by very thin axon diameters (0.4-1.2μM), no myelination, and therefore slow signal transmission (0.4-2 m/s) [(Milligan & Watkins, 2009; Basbaum & Jessell,

2000; Millan, 1999)]. In contrast with Aα and Aβ fibers, both Aδ and C fibers have free nerve endings and they only respond to and conduct information arising from noxious stimuli, under normal conditions (Kidd & Urban, 2001). Due to their structural implications for slower conduction velocity, both of these fiber types transmit information slowly, at approximately 10% the rate of that of motor fibers (McHugh & McHugh, 2000).

C fibers are primarily polymodal in nature, responding to thermal, mechanical, and chemical stimuli (Coutaux et. al, 2005; Millan, 1999; Meyer, et. al, 2005), and they are deeply embedded along vein walls (Millan, 1999). Studies have also revealed the existence of some C fibers that fire only in response to chemical stimulation (Kidd & Urban, 2001). When C fibers are active above threshold level, they will induce a slow, diffuse, painful burning sensation (McHugh & McHugh, 2000; Meyer, et. al, 2005), following the initial rapid phase of pain transmitted by Aδ fibers (Millan, 1999). Studies have implicated C fibers in thermal nociceptive sensation, showing that in glabrous skin, C fibers fire in response to a heat stimulus of short duration (less than 5 seconds) at a temperature close to human pain threshold (~45ºC). Patients with congenital insensitivity to pain have been shown to lack C fibers; a finding that serves to further support the role of C fibers in nociception (Meyer, et. al, 2005).

A subdivision of C-fiber afferents have been identified in human skin that, under normal conditions, are inactive and unresponsive to characteristic nociceptive stimuli. These fibers, known as silent nociceptors, have very high mechanical thresholds that surpass those of typical C fibers (Meyer et al., 2005). Studies have implicated this particular class of afferents in inflammation, showing that they are recruited and activated in a gradual manner during the inflammatory response and may also play a role in the development of post-inflammation hypersensitivity (Coutaux et al., 2005).

With a higher activation threshold than C fibers, Aδ nociceptive fibers carry out all the functions of C fibers, but are considered to so in a more robust manner (Coutaux et al., 2005). These fibers are implicated in the induction of sharp, pricking pain and perhaps aching pain (Meyer et al., 2005). Aδ fibers are also characterized by a more frequent discharge rate, and information they transmit to the CNS is more discriminable (Meyer, et. al, 2005). However, their precise function in the inflammatory process still remains to be clarified (Coutaux, et. al, 2005). Studies have confirmed the existence of two different classes of Aδ fibers: Type I and Type II Aδ fibers. Found in both hairy and glabrous skin (Meyer et al., 2005), Type I fibers have a high thermal threshold and therefore respond weakly to heat stimuli, but respond strongly to mechanical stimuli of high intensity such as pinching. Due to their polymodal nature, Type I fibers may also respond to chemical stimulation (Millan, 1999). Found mainly in hairy skin, Type II fibers respond robustly to heat stimulation and are considered to be the first in line for signal transmission of heat or capsaicin stimuli to the CNS. These kinds of stimuli induce a twofold pain response in Type II fibers: a quick, sharp pricking sensation is followed by a slower burning sensation. Also, unlike their Type I counterparts, Type II fibers are insensitive to mechanical stimulation (Meyer et al., 2005).

Studies have demonstrated that the vanilloid receptor 1 (TRPV1), a non-selective channel with preference for calcium (Ca^{2+}), is most likely responsible for the mediation of heat sensitivity in Aδ fibers (Meyer, et. al, 2005; Coutaux, et al., 2005). This is a sensible conclusion in light of the fact that this receptor is expressed primarily in small neurons with myelinated axons and has a high activation threshold for heat, similar to Aδ fibers. Vanilloids, including capsaicin, piperine, and zingerone, are naturally occurring chemicals responsible for the spicy taste in foods (Coutaux et al., 2005). Vanilloids, heat, and protons activate TRPV1 receptors,

indicating that their activation may be augmented by a decrease in pH of the environment in the inflamed tissue (Kidd & Urban, 2001; Meyer, et. al, 2005). This theory has been supported by studies that discovered that the loss of thermal hyperalgesia is correlated with a significant loss of cells expressing the TRPV1 receptor (Abrahamsen et al., 2008).

Organization of pain pathway

Pain is consciously experienced once neural signals reach the limbic and cortical centers of the brain. Figure 1 illustrates the intricate network of mechanisms involved in the transmission of a noxious stimulus into a nociceptive signal that is then hierarchically propagated through the nervous system (Millan, 1999). Far from being a straightforward relay of signals from the periphery to the brain, pain processing is an active system of several, repeating pathways. This dynamic nature of neural communication allows for the suppression or augmentation of pain to occur at any or all levels of synaptic connection (Milligan & Watkins, 2009). In this manner, it is important to be familiar with the types of connections that nociceptive neurons make throughout all levels of the nervous system so that we can best understand how hormones may influence the perception of pain. This research will concentrate primarily on the branch of the nociceptive pathway that extends from the peripheral afferents to the spinal cord.

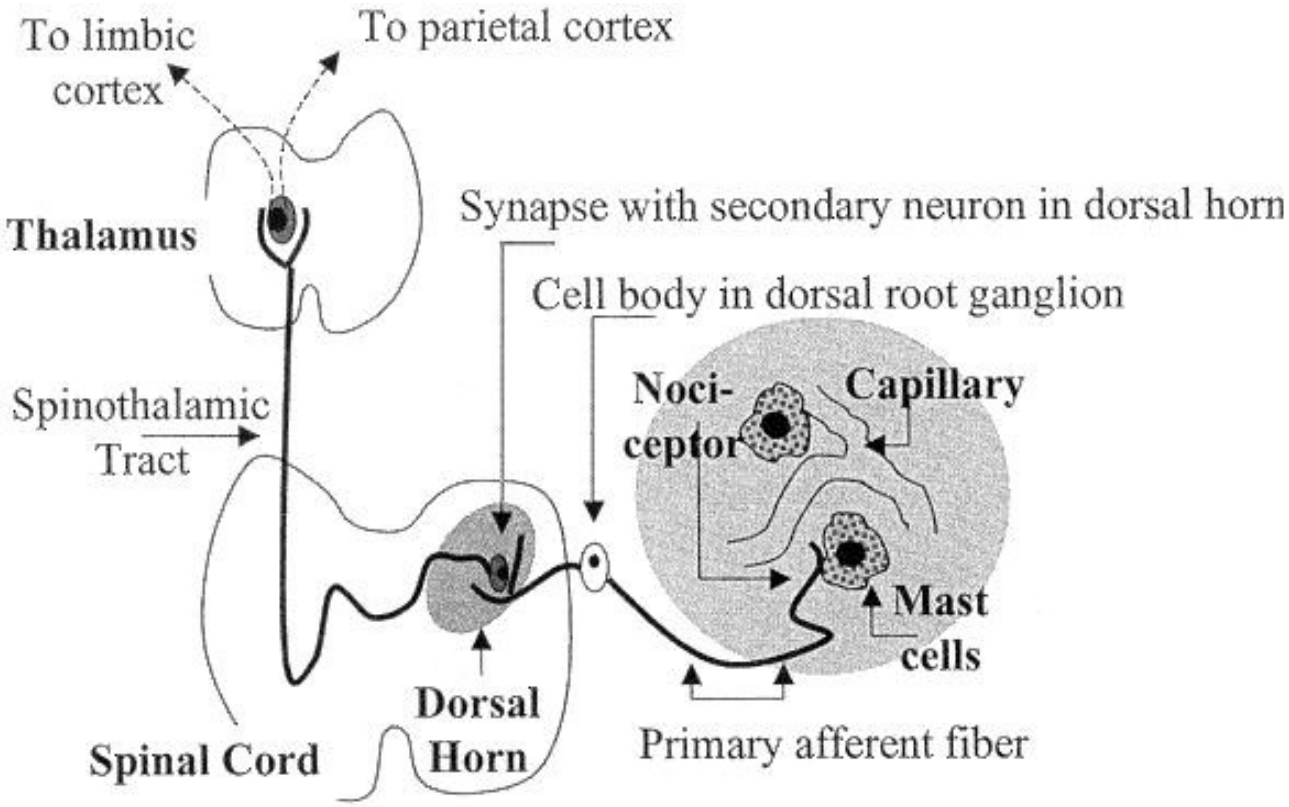

Figure 1.1. Organization of the pain pathway. Primary nociceptive fibers, located next to capillaries and mast cells, respond to tissue injury in a systematic manner. The series of events surrounding this response, including cell injury, mast cell degranulation, plasma exudation, and capillary dilation, result in nociceptor stimulation. These pain signals travel along the nociceptor, pass through the dorsal root ganglion, and continue to the dorsal horn in the spinal cord. Before reaching the thalamic centers in the brain, the signals then cross over to the spinal thalamic tracts on the contralateral side. When pain information finally arrives at the thalamus and higher brain centers like the limbic and parietal cortices, pain becomes a conscious experience to which meaning and emotions are attributed.
From: McHugh & McHugh (2000), AACN CLIN ISSUES ADV PRACT ACUTE CRIT CARE, VOL 11(2), 168-178.

When a stimulus that conveys potential or actual tissue damage is identified by the primary nociceptive afferents, a pain signal is generated (Milligan & Watkins, 2009). As depicted in Figure 2, the axons of these primary nociceptive neurons congregate onto the dorsal horn area of the spinal cord; more specifically, most of these nociceptors synapse in Laminae I and II of the dorsal horn area, while some synapse in Laminae V, VI, and X (Milligan & Watkins, 2009; Weiseler-Frank, et al., 2004; Riedel & Neeck, 2001). At this location, the first site of synaptic communication between the primary nociceptive afferents and the CNS, the pain signal is susceptible to both local and descending modulation of either an excitatory or inhibitory nature (Riedel & Neeck, 2001). In light of this fact, the dorsal horn is a potentially significant area for the investigation of the attenuation or amplification of nociceptive signals.

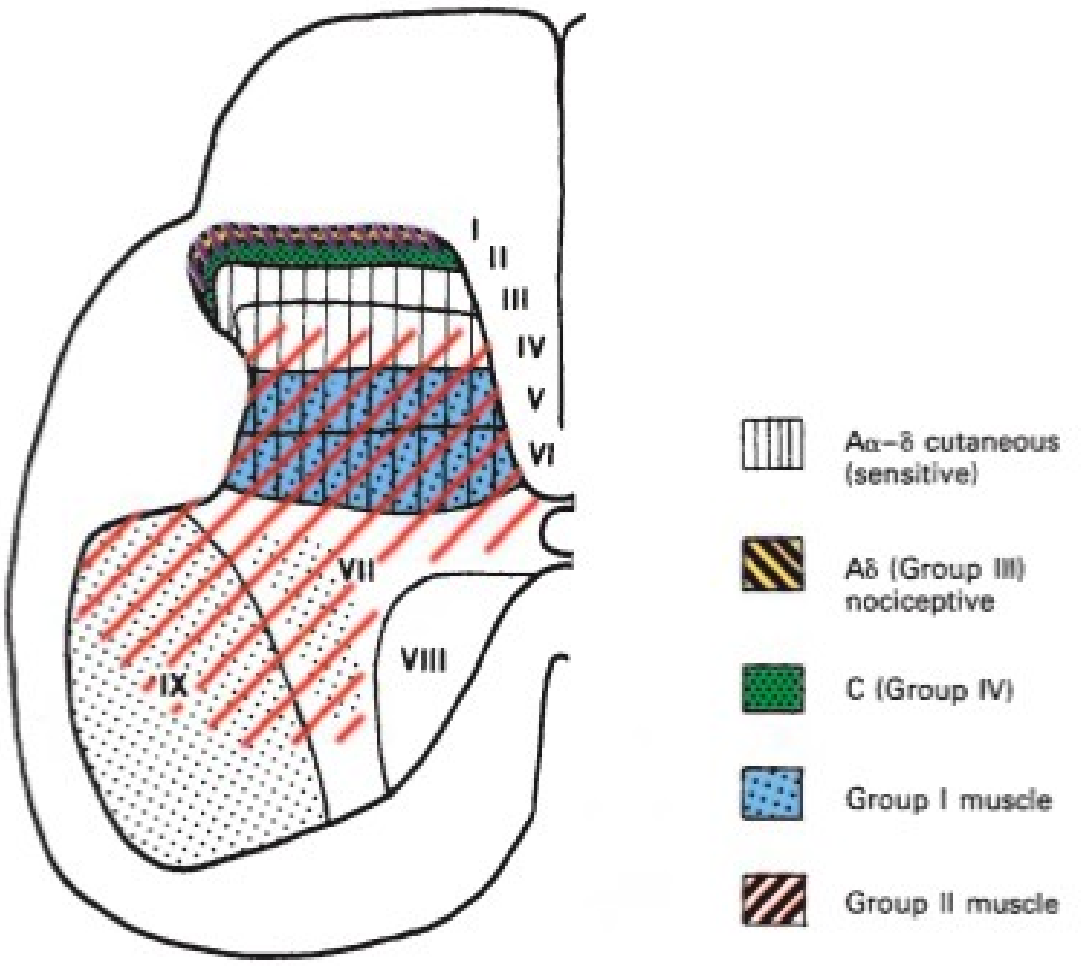

Figure 1.2. Spinal cord grey matter distribution of afferent fibers. Nociception-related fibers synapse at various superficial levels of the spinal cord's dorsal horn. From: (Riedel & Neeck, 2001), Z RHEUMATOL, VOL. 60, 404-415.

Once the neurons in the dorsal horn receive nociceptive information from the primary afferents, they transmit it to higher-order centers of the nervous system (McMahon, Cafferty, & Marchand, 2005). Second-order nociceptors intersect at the level of the spinal cord (McHugh & McHugh, 2000), transmit signals to thalamic and brainstem neurons (Riedel & Neeck, 2001; Kidd & Urban, 2001), and finally synapse onto cortical neurons that function to produce conscious pain experience. Coordination in the pain pathway is key to the successful production of an adaptive response to a painful stimulus; if even one part of the pathway is interrupted, the result is an alteration of pain perception that can grow to be pathological, as illustrated by the example of chronic inflammation (Milligan & Watkins, 2009).

Inflammation

Inflammation, marked by the characteristic symptom of pain, can manifest as chronic inflammatory pain in serious illnesses such as rheumatoid arthritis (McMahon, et al., & Marchand, 2005). Pathological in nature, chronic inflammatory pain is maladaptive as it can occur unprompted, devoid of external noxious stimuli (Coutaux, et. al, 2005; Basbaum & Jessell, 2000), and no longer promotes healing (Miligans & Watkins, 2009). At the physiological level, inflammation materializes as heat and rubor (redness), which are caused by peripheral blood vessel dilation coupled with swelling due to plasma extraversion (Basbaum & Jessell, 2000), at the site of tissue injury (Costigan & Woolf, 2000). At the neurological level, the activation of the nociceptive unit initiates the inflammatory response. The nociceptive unit consists of capillaries, mast cells, and nociceptors (McHugh & McHugh, 2000).

Painful stimuli can result in cell injury, dilation of capillaries, mast cell degranulation, and plasma exudation (McHugh & McHugh, 2000). Exaggerated pain responses can occur if nociceptive messages are amplified during inflammation. The resulting tissue damage triggers a

cascade of events, associated with the inflammatory process, which can extend the activation of nociceptive afferents and consequently heighten their sensitivity (Coutaux et. al, 2005). The plastic nature of the nervous system permits it to modify its functions in accordance with its surrounding conditions: this very nature accounts for the nociceptive system's ability to engage in hypersensitivity in response to inflammation (Kidd & Urban, 2001).

Following inflammation, the nociceptive system can depict allodynia, a condition in which nociceptors are activated by usually benign stimuli (Riedel & Neeck, 2001; Ren & Dubner, 1999), or more typically hyperalgesia, which is marked by an extreme response to a noxious stimulus (Coutaux, et. al, 2005; Riedel & Neeck, 2001). Hyperalgesia, occurring at both the site of tissue damage (primary hyperalgesia) and the in the surrounding area (secondary hyperalgesia) [(Coutaux, et al., 2005)], is the characteristic symptom of inflammation associated with hypersensitivity (Kidd & Urban, 2001). In this type of neural response, the pain threshold is lowered such that pain exhibited in response to a suprathreshold stimulus is heightened (Meyer et al., 2005).

Our endogenous opioid system significantly modulates pain responses as well. Researchers discovered that exogenous administration of u-opioid receptor agonists increase metabolic activity in brain regions rich in u-opioid receptors like the anterior cingulate cortex (ACC), PFC (prefrontal cortex), thalamus, basal ganglia, and amygdala, in a dose-dependent manner (Firestone et al 1996, Schlaepfer et al 1998, Wagner at al 2001). In a study using a painful cold stimulus, rCBF responses were recorded in response to fentanyl, a u-opioid agonist. The results showed that rCBF increases elicited by the stimulus were dampened considerably by the u-opioid agonist in many regions (Casey et al 2000).

Multiple different mechanisms have been implicated in the development of hyperalgesia,

such as sensitization at the peripheral level, central level, or both (Ren & Dubner, 1999). Noxious stimuli cause both chemical and neural changes at two locations: the site of injury, specifically at the nerve endings and axon projections of local nociceptors, and the first-order synapses in the spinal cord's dorsal horn (Milligan & Watkins, 2009). Evidence of increased nociceptor response to test stimuli after hyperalgesia is induced indicates that primary hyperalgesia may be linked to the sensitization of peripheral nociceptive afferents (Riedel & Neeck, 2001; Meyer, et. al, 2005). By decreasing the depolarization threshold, this sensitization successfully increases response rate to a constant stimulus (Coutaux, et. al, 2005; Sweitzer, Arruda, & DeLeo, 2001; Gold, Reichling, Shuster, & Levine, 1996). Secondary hyperalgesia, alternatively, is thought to be a result of central sensitization (Meyer at al., 2005), which takes place centrally at the dorsal horn in the spinal cord and is marked by neural and chemical changes in pain information processing (Milligan & Watkins, 2009). This particular process may be linked to chronic pain development that is devoid of external origin (Coutaux, et al., 2005).

Peripheral Sensitization

Peripheral tissue injury in response to some noxious stimulus, be it chemical, mechanical, or thermal, begets the release of a complex concoction of chemical substances, including prostaglandins (PGs), cytokines, nerve growth factor (NGF), adenosine, leukotrienes, bradykinin, serotonin, thromboxanes, nitric oxide (NO), and histamine (McMahon, et. al, 2005; Kidd & Urban, 2001; McHugh & McHugh, 2000; Costigan & Woolf, 2000; Basbaum & Woolf, 1999; Meyer, et. al, 2005). These chemicals are discharged when the nervous and immune systems encounter and interact with foreign noxious stimuli (Riedel & Neeck, 2001). While some of these inflammatory mediators aid in the recovery of injured tissues (Millan, 1999),

others galvanize the activation of nociceptors that then transmit pain information to the spinal cord (Milligan & Watkins, 2009; McHugh & McHugh, 2000). Acting synergistically, these latter mediators function through both indirect initiation of the release of more mediators from immune cells and nociceptors, and by direct activation of chemosensitive nociceptors (Saab, et. al, 2008; Coutaux, et. al, 2005). In this manner, the process of peripheral sensitization is spurred by the action of the aforementioned inflammatory mediators that induce peripheral nerve terminals to respond to a noxious stimulus by lowering their depolarization thresholds (Kidd & Urban, 2001; Meyer, et. al, 2005).

One of the specific mechanisms that accounts for peripheral sensitization is the induction of post-translational changes in voltage-gated ion channels, particularly sodium (Na^+) channels (Kidd & Urban, 2001; Costigan & Woolf, 2000). More specifically, researchers have proposed that the tetrodotoxin-resistant (TTXr) Na^+ channel plays a modulatory role in peripheral nociceptive afferents (Meyer, et. al, 2005). This channel is considered to have a unique role in nociception due to its particular location on small-diameter sensory neurons, many of which are located in the DRG (Kidd & Urban, 2001; Gold, et. al, 1996). Chemicals discharged at the location of tissue injury initiate a chain of events that result in modified ionic conductances in peripheral terminals of nociceptors, thereby causing sensitization (Gold, et al., 1996). Specifically, researchers found that hyperalgesic substances, such as prostaglandin E_2 (PGE_2), adenosine, and serotonin, modify the TTXr Na^+ current in a dose-dependent manner that corresponds to common patterns of nociceptor sensitization. These alterations may explain hallmark features of sensitization like an increased number of action potentials in response to a constant stimulus, in addition to the lowering of nociceptor thresholds (Gold, et al., 1996).

A second mechanism that may be implicated in the increase of nociceptor action

potentials is the transfer of nociceptive activity to usually innocuous, large-diameter afferents like Aβ fibers. NGF, one of the many agents released in response to peripheral tissue injury, is a growth factor that has been found to not only sensitize nociceptors, but to also shift nociceptive function to formerly non-nociceptive fibers (Meyer, et. al, 2005). Specifically, during the process of inflammation, both medium and large-sized A fiber DRG neurons begin to mimic C fiber activity by generating and releasing neuropeptides like substance P. By doing so, now non-nociceptive Aβ fibers and nociceptive Aδ fibers engage in a phenotypic exchange for C fiber function (Milligan & Watkins, 2009; Costigan & Woolf, 2000). Studies testing this theory have shown that inflammation can indeed induce an increase in the number of Aβ fibers expressing substance P, which translates to a change at the functional level as well (Neumann, et. al, 1996). Through the mediation of cytokines and growth factors, these newly recruited C fibers can stimulate excitation centrally and peripherally, inducing further changes in nociceptor response (Kidd & Urban, 2001).

Central Sensitization

The heightened excitability of spinal cord nociceptive neurons are linked to atypical pain states like allodynia and hyperalgesia (McMahon, et. al, 2005; Kidd & Urban, 2001). Specific neuromodulators operating at the synapse between the primary nociceptor and second order neurons in the dorsal horn bring about important changes to central nociceptor activity (Milligan & Watkins, 2009; Kidd & Urban, 2001).

One well-researched mechanism involved in central sensitization is associated with the altered functioning of N-methyl-D-aspartate (NMDA) receptors in dorsal horn neurons. NMDA receptors, widespread in the spinal cord's dorsal horn, are well known for their role in nociceptive transmission (Riedel & Neeck, 2001; Kidd & Urban, 2001). The spinal cord

responds to non-injurious noxious stimuli with the glutamate, an excitatory neurotransmitter that functions via the α-amino-3-hydroxy-5-methylisoxazole (AMPA) receptors (Kidd & Urban, 2001). However, under nociceptive conditions marked by continuous activation of peripheral nociceptors associated with inflammation, NMDA receptors are expressed and activated instead.

Specifically, the discharge of glutamate and substance P results in the depolarization of pain-projection neurons in the spinal cord, which in turn induces the removal of the magnesium ion (Mg^{2+}) that typically blocks the NMDA channel. This chain of events triggers increased Ca^{2+} influx, enhanced signal transmission, and increased generation and release of NO through Ca^{2+}-activated nitric oxide synthase (NOS) (Milligan & Watkins, 2009). The presynaptic terminals of sensory neurons then release neuromodulators in greater numbers due to enhanced excitability of spinal cord neurons induced by NO and PGs. This can also encourage phenotypic alterations of non-nociceptive fibers as mentioned in peripheral sensitization (Kidd & Urban, 2001). Taken together, these changes produce intensified pain messages that are being transmitted through the spinal cord.

Glia: Key Players in Mediating Pain

After a long history of playing second fiddle to neurons, glia are now emerging as influential nervous system cells in their own right as they are increasingly implicated in a variety of brain functions, such as learning and memory, once thought to be solely the domain of neuronal cells (Temburni & Jacob, 2001). Glia have also recently been identified as powerful modulators of pain signaling, significantly contributing to the development of pathological pain states that underlie progressive neurodegenerative disorders (Arevalo, 2011). Studies clearly implicate glia in nociceptive processes, modulating neurotransmission at the synaptic level (Bacci, et al., 1999). Furthermore, glial cells have been found to express estrogen receptors

(ERs) whose expression they increase in response to many different pathological conditions: a potential neuroprotective event by which estrogen exerts its anti-inflammatory effect. Making up a whopping ninety percent of our brain cells, glial cells are now thought to play a far more consequential role in the brain such as mediating the development of degenerative illnesses like Alzheimer's and Parkinson's diseases. Glial cells can be divided into two main categories: microglia and macroglia, which include astrocytes and oligodendrocytes (Moalem & Tracey, 2006).

Microglia

Following the onset of peripheral tissue injury, microglia are activated and release pro-inflammatory cytokines like interleukin-1β (IL-1β), interleukin-6 (IL-6), and tumor necrosis factor-α (TNF-α), which initiates the cascade of events that produce the inflammatory response. This process is propagated through the recruitment of other microglia and the eventual activation of neighboring astrocytes (Watkins et al., 2001). Microglia make up about 5-10% of all glial cells (DeLeo & Colburn, 1998; Moalem & Tracey, 2006). While myeloid progenitor cells that travel to the peripheral nervous sytem (PNS) differentiate into macrophages or dendritic cells, these same progenitor cells differentiate into microglia when they migrate to the central nervous system (CNS). Microglia behave similarly to macrophages upon activation (Lawson, et. al., 1990; Nakajim & Kohsaka, 2001; Stoll & Jander, 1999). During normal basal conditions, microglia are in a sessile state and are characterized by a small soma surrounded by fine, hair-like branched processes. When activated, these cells transform themselves both morphologically and functionally: these changes in cell mobilization and activation allow microglia to mimic phagocytic functions. Specifically, through an ATP-mediated elongation mechanism, activated microglia are able to project processes so as to isolate damaged cells and to faciliate the

eradication of potential pathogens (Davalos, et al., 2005). Although microglia are evenly dispersed in the CNS, the cells that are- activated in response to peripheral nerve injury are only the microglia in the spinal cord (Zhang et al., 2008).

Studies have shown a activation of microglia on the ipsilateral dorsal horn following peripheral nerve injury, in comparison to faint microglial activation on the contralateral dorsal horn and in naïve subjects (Beggs & Salter, 2007; Jergova & Cizkova, 2007). An alteration of surface markers, proteins that are either membrane-bound or embedded, was also observed in activated microglia versus basal microglia. These surface markers, such as complement receptor 3 (also known as CD11b), aid in phagocytic functions of microglia (Coyle, 1998; Wieseler-Frank, et al., 2005). Activated microglia release a diverse group of neuroinflammatory mediators like chemokines, neurotrophic factors, and cytokines. In particular, microglia production and release of pro-inflammatory cytokines such as IL-1β, IL-6, and TNF-α initiate the activation of nearby astrocytes (Watkins & Maier, 2003).

Astrocytes

Astrocytes are a type of macroglial cell that constitute the great majority of glial cells in the CNS, but their specific development and function has yet to be clearly defined. For the most part, astrocytes exhibit phagocytosis, perform a crucial role in neuronal development, and help to create and preserve the blood brain barrier (BBB) (Cahoy, et al., 2008). During a resting state, astrocytes are characterized by thin processes and they isolate oligodendrocytes and neurons in order to help maintain the CNS microenvironment, via regulation of extracellular K^+ and Ca^{2+} concentrations and neutrotransmitter concentrations through uptake. When activated, astrocytes experience activation, hypertrophy, and heightened expression of intermediate filaments like the glial fibrillary acidic protein, which is an astrocyte-specific activation marker (Wieseler-Frank, et

al., 2005; Garrison, et al., 1994).

Astrocyte activation causes persistence of a pain state. Inactive astrocytes express resting state levels of cytokine receptors. IL-1β, and potentially IL-18, when released from microglia, bind to IL-1 receptors on the astrocyte membrane; this results in a sequence of cellular events leading to activation of the astrocyte (Miyoshi, et al., 2008; Dinarello, 1999). Microglial cells express TLR, which may initiate the production of IL-18 (part of the IL-1 family) through the activation of p38 mitogen activated protein kinase (p38MAPK): this substance is responsible for inducing expression of pro-inflammatory cytokines like IL-1β and IL-6. Researchers have found that intrathecal injection of IL-18 induces astrocyte activation and tactile allodynia (Miyoshi, et al., 2008). All of these cellular events lead to greater expression of pro-inflammatory cytokines as well as inducible nitric oxide (NO) synthetase, which further extends the inflammatory response.

Astrocytes are also involved in the modulation of glutamate concentrations, via synthesis of glutamate from glucose as well as the uptake of extracellular glutamate, resulting in decreased glutaminergic activity (Hertz & Hansson, 2007). During chronic pain states, this major excitatory neurotransmitter increases its concentration in the dorsal horn of the spinal cord. This is evidenced by astrocyte expression of pyruvate carboxylase, an enzyme associated with glutamate synthesis that is not found in neurons (Hertz & Hansson, 2007). Glutamate makes an important contribution to pain processes through its activation of many ionotropic and metabotropic receptors; the ionotropic N-methyl-D-aspartate (NMDA) receptor is particularly significant due to its pivotal role in central sensitization of nociceptive neurons in the spinal cord. NMDA is also responsible for astrocyte activation through Ca^{2+} influx (Petrenko, et al., 2003). Ca^{2+} influx encourages neutrotransmitter release and alters cell membrane excitability, thereby

playing an influential role in pain signaling.

Following a peripheral injury, nociceptive neurons transmit pain signals to the dorsal horn of the spinal cord, where ATP and neurotransmitters like substance P, serotonin, glutamate, gamma amino butyric acid, and calcitonin gene-related protein (CGRP) are released (Watkins & Maier, 2003). This cascade of events stimulates glial cell activation in the synaptic area, which further enhances sensitivity of postsynaptic neurons.

Different mechanisms have been proposed for glial cell activation. One such mechanism is the release of chemical mediators that influence both synaptic transmission and glial activation. Substances secreted at the onset of injury—like CGRP, glutamate, NO, endogenous opioid peptides, substance P, and ATP—cross through or between afferent neurons, causing a sequence of events that result in glial cell activation and prolonged neuroinflammation. Specifically, ATP stimulates the migration and activation of microglia within 50-100 μm, which leads to an intracellular increase of Ca^{2+} and brain-derived neurotrophic factor (BDNF). This causes the activation and transfer of NF-κB to the nucleus-initiating expression for many pro-inflammatory mediators. Behaving similarly to NF-κB, NO also affects gene expression and stimulates activation (Guo, et al., 2007; Holguin, et al., 2004; Meller, et al., 1993; Brahmachari, et al., 2006). This cascade of events is illustrated in Figure 3. Glial cells in the CNS can also be activated by substance P via neurokinin-1 (NK-1) receptors and through direct interaction of particular cell membrane receptors with other chemical agents like glutamate and opioid peptides.

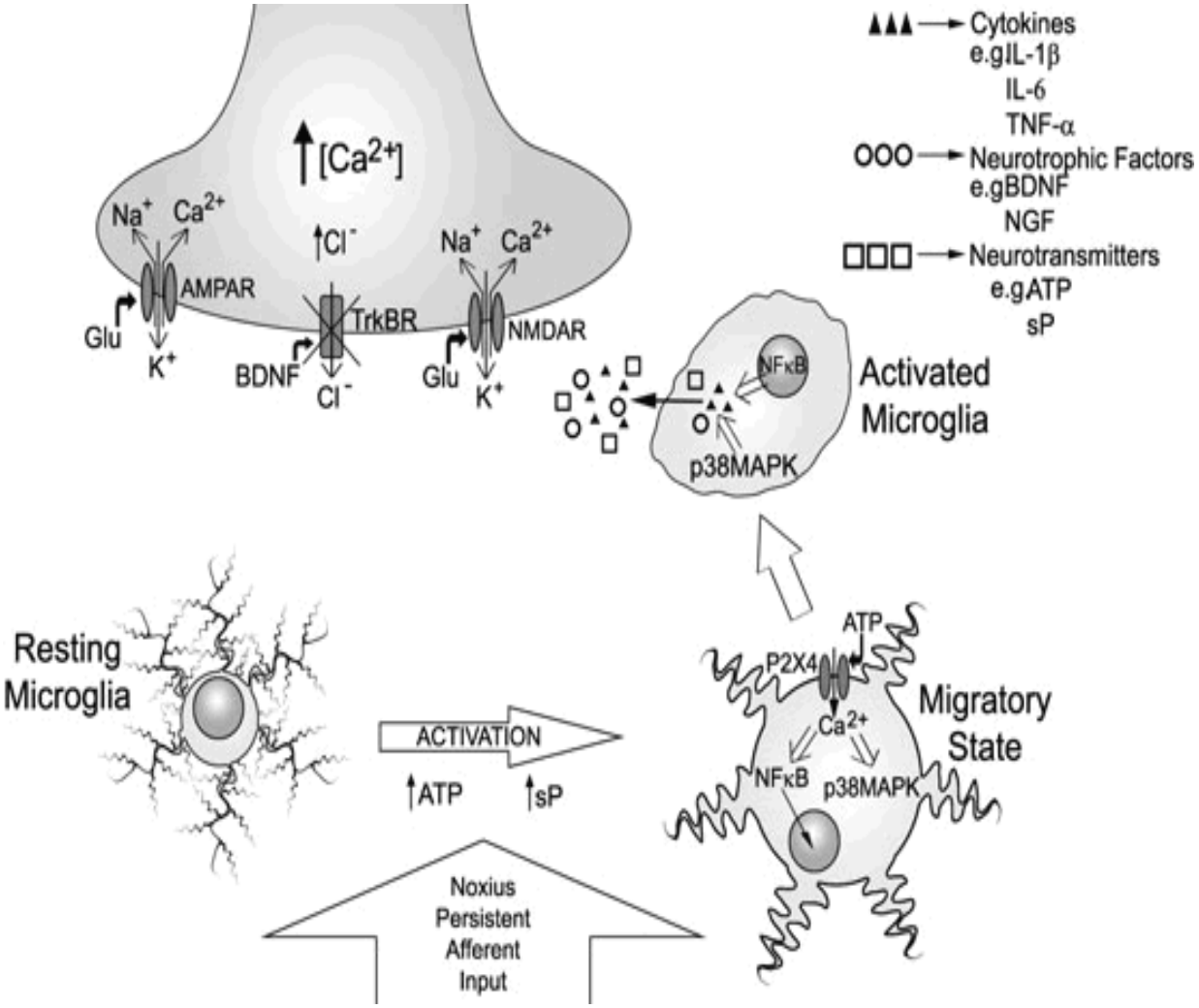

Figure 1.3. Glial activation via chemical mediators. Microglial cells at the resting state are activated by noxious afferent inputs, which cause them to migrate to the source of ATP. The subsequent binding of ATP to the P2X4 receptors on the microglial surface leads to Ca^{2+} influx that causes NFkB to translocate to the nucleus, which then induces the p38MAPK pathway. These events stimulate transcription of diverse neuroinflammatory mediators such as neurotrophic factors, neurotransmitters, and cytokines. These mediators are released into the synaptic cleft and, upon binding to different receptors, produce a rise in intracellular concentration of Ca^{2+} and Cl^- ions which consequently depolarize and sensitize the neuron. AMPA and NMDA are two major receptors associated with Ca^{2+} influx. BDNF has been found to bind to the TrkB receptor, which results in the inhibition of Cl^- efflux.
From: (Vallejo et al., 2010) PAIN PRACTICE, Vol 10, Issue 3, 167-184

A second mechanism involves intracellular and extracellular modulations of K^+ and Ca^{2+} concentrations. Specifically, greater nociceptive afferent input results in the increase of extracellular K^+, which causes greater K^+ uptake by astrocytes. This leads to membrane depolarization, changes in morphology, as well as potential activation (Hansson, 2006). Studies have also implicated K^+ in the induction of microglial activation in rat hippocampal tissue *in vitro* (Abraham, et al., 2001). Likewise, the rise of intracellular Ca^{2+} concentration leads to both microglia and astrocyte activation, coupled with functional and morphological changes, and this can be propagated through the production and release of pro-inflammatory mediators. This mechanism is illustrated in Figure 4.

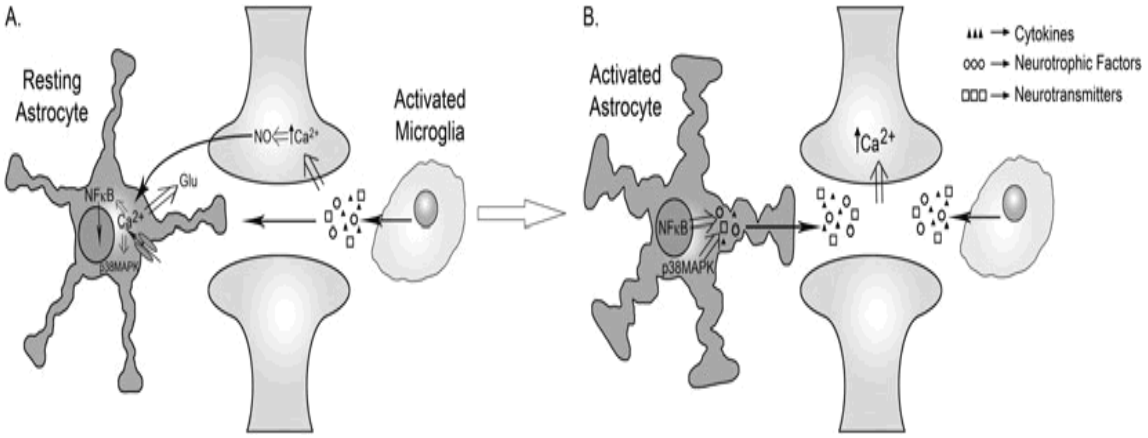

Figure 1.4. Glial activation via shifts in intracellular and extracellular ion concentrations. (A) When neuroinflammatory mediators are released into the synaptic cleft by activated microglial cells, the surface receptors of neighboring astrocytes bind to these mediators and cause Ca^{2+} influx. Microglial cells can also cause NO synthase expression in the postsynaptic neuron, which also leads to astrocyte activation and subsequent Ca^{2+} influx. Raised levels of intracellular Ca^{2+} cause NFkB to translocate to the astrocyte nucleus; this initiates both the p38MAPK pathway and a dose-dependent release of glutamate. (B) Once the astrocyte is activated, it undergoes hypertrophy along with an increased generation of neuroinflammatory mediators that are released into the synaptic cleft. Astrocyte activation coupled with microglial activation results in significant depolarization of the neuron, enhancing its sensitivity and prolonging the pain state.
From: (Vallejo et al., 2010) PAIN PRACTICE, Vol 10, Issue 3, 167-184

Inflammatory Mediators

When tissue injury is incurred, the inflammatory process is initiated by the generation of local mast cells, neutrophils, macrophages and other cells like leukocytes that migrate to the site of injury (Moalem & Tracey, 2006; Sommer & Kress, 2004). When these cells become activated, they release an onslaught of inflammatory mediators such as substance P, bradykinin, PGs, and cytokines (Saab, et al., 2008; Angst, et al., 2008; Chichorro, et al., 2004). By either promoting healing or galvanizing pain sensation through the sensitization of primary nociceptive afferents, these mediators play a vital role in the inflammatory response (Hopkins, 2007; Rittner & Stein, 2005). Cytokines are of particular interest to this study.

Cytokines

In response to tissue damage, cytokines are generated and released in glia and the peripheral system of the CNS by a diverse group of cell types that include neutrophils, macrophages, mast cells and white blood cells (Moalem & Tracey, 2006; Angst, et al., 2008; Cunha, Verri, Silva, Poole, Cunha, & Ferreira, 2005). These small polypeptides mostly act in either a pro-inflammatory or anti-inflammatory manner, although some can express both functions based on factors like their concentrations and cellular environment (Uceyler & Sommer, 2008). Functioning at two levels, cytokines impact local cell receptors to produce autocrine effects and also receptors of other cells to produce paracrine effects. Hormonal effects have been accounted for as a result of cytokine action due to their influence on more remote tissue as well (Verri, Jr., et al., 2006). Most cytokines, however, are responsible for local neuromodulation in injured tissue (Hopkins, 2007). Previous research has established that cytokine action bridges the gap between tissue damage followed by immune response, and subsequent nociception. However, the mechanisms underlying the nervous and immune

systems' relationship are yet to be clearly defined (Coutaux, et al., 2005). Current literature supports a bi-directional relationship between the two systems in which immune cells responding to inflammation relay information back to neurons, which in turn modify their activity (Watkins & Maier, 1999).

When a peripheral injury is incurred, mast cells respond by degranulating and recruiting macrophages and neutrophils to the site of tissue damage, where cytokines are then released in a highly mechanistic manner (Coutaux, et al., 2005). In addition, other inflammatory mediators like bradykinin are brought to the site and activated, and this in turn induces the drift of leukocytes into the damaged tissue (Sommer & Kress, 2004; Rittner, Machelska, & Stein, 2005). Cytokines produce tumor necrosis factor-α (TNF-α), and this particular mediator catalyzes the following cascade of cytokine production: TNF-α induces the secretion of interleukin-1β (IL-1β), followed by interleukin-6 (IL-6) and interleukin-8 (IL-8) (Hopkins, 2007; Wieseler-Frank, Maier, & Watkins, 2005). Figure 3 illustrates this cascade, highlighting two separate pathways of inflammatory mediation: the sympathetic amine and the COX pathway (Loram, Fuller, Fick, Cartmell, Poole, & Mitchell, 2006). Specifically, IL-6 and IL-1β cause the activation of cyclooxygenase-2 (COX-2), which is then followed by the release of nociceptor-sensitizing prostanoids like PG. In conjunction with the hypersensitivity of the damaged tissue, the diverse mediators that are discharged during the inflammatory response work together to produce heightened pain states like allodynia and hyperalgesia.

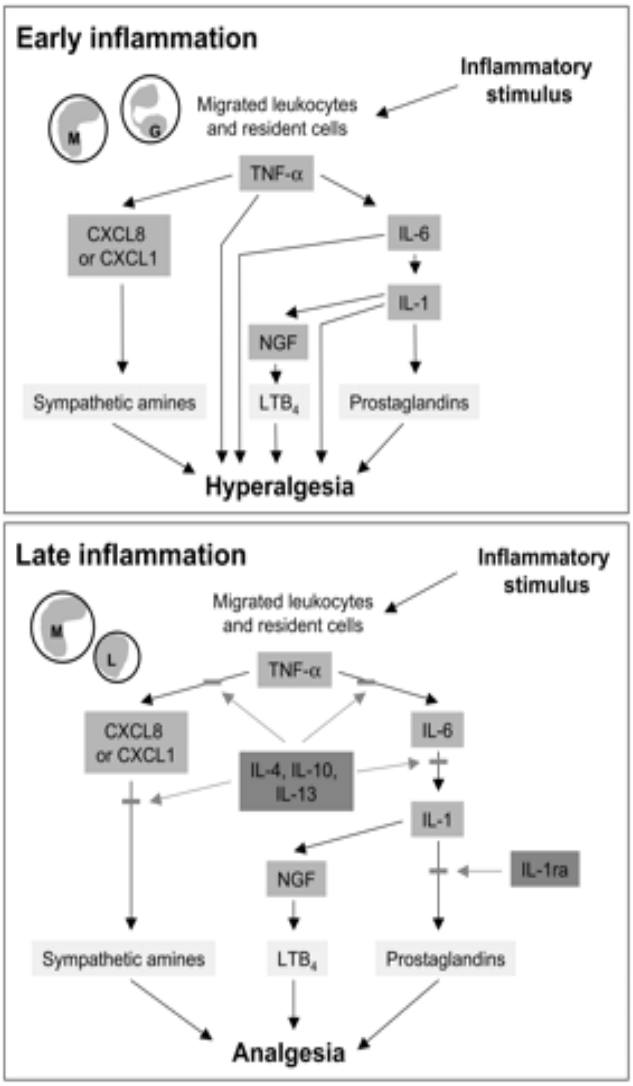

Figure 1.5. Mechanisms of pro- and anti-inflammation during early and late stages of inflammation. In early inflammation, leukocytes like monocytes (M) and granulocytes (G) migrate to damaged tissue in response to a noxious stimulus. Here, they trigger a cascade of pro-inflammatory cytokines such as TNF-α and IL-1 and -6, as well as chemokines (e.g. CXC chemokine ligand 8 [CXCL8] and CXCL1), and NGF. Next, secondary mediators, like sympathetic amines, prosataglandins, and leukotriene B4 (LTB_4), are released and activated, producing a hyperalgesic state. In later stages of inflammation, lymphocytes (L) generate anti-inflammatory cytokines, like IL-4, -10, -13, and -1ra, and these mediators function to inhibit the generation of pro-inflammatory cytokines which thwarts further development of hyperalgesia. *From: Rittner, Machelska, & Stein (2005): JOURNAL OF LEUKOCYTE BIOLOGY, VOL 78(6), 1215-1222.*

Pro-inflammatory cytokines

There are several cytokines that exhibit pro-inflammatory function by acting through direct sensitization of primary nociceptive afferents or through indirect generation of PGs and sympathetic amines (Verri, Jr., et al., 2006; Uceyler & Sommer, 2008). TNF-α, IL-1β, and IL-6 have all been identified as pro-inflammatory cytokines, and can enhance neural activity and mechanosensitivity at the dorsal root ganglia.

TNF-α

TNF-α is an exemplary pro-inflammatory cytokine in that it jumpstarts the cascade of activation and release of other cytokines following inflammation (Schafers & Sorkin, 2008; Rittner, Machelska, & Stein, 2005). While TNF-α is constitutively expressed by mast cells, during the inflammatory response, it may be secreted by other cell types like Schwann cells, neutrophils, and macrophages (Moalem & Tracey, 2006; Sommer & Kress, 2004). This can occur in response to various noxious stimuli such as bacterial, viral, and parasitic products, trauma, ischemia, as well as other cytokines (Rittner, et al., 2005). In addition to its role in initiating the cytokine cascade following inflammation, TNF-α is also responsible for killing specific types of tumor cells (DeLeo, Colburn, & Rickman, 1997).

TNF-α carries out its functions through two kinds of receptors that are involved in different pathways: tumor necrosis factor receptor-1 (TNFR1), which is constitutively expressed and connected to pathways for cell death, and TNFR2, which can be induced (Rittner, et al., 2005; Moalem & Tracey, 2006). Inflammatory cells express both of these receptor types, which are upregulated in the DRG during inflammation (Rittner, et al., 2005). When either receptor is activated via TNF-α binding , the following chain of events follow: p38MAPK also becomes

activated, NF-κB is translocated to the nucleus, and COX-2-dependent prostanoid release is stimulated (Moalem & Tracey, 2006). TNF-α binding also stimulates the generation of IL-1β, which in turn induces the expression of other pro-inflammatory cytokines like IL-6.

IL-1β

IL-1β is another pro-inflammatory cytokine that is known to perform a significant role in chronic pain development. When IL-1β binds to its receptor (IL-1R), found in both the CNS and PNS, a sequence of intracellular biochemical events are triggered that are associated with the expression of IL-6, p38MAPK, and NF-κB: these agents ultimately induce gene expression of COX-2 and type II phospholipase A2 (Dinarello, 1998). Following the induction of COX-2, many of IL-1β's activites are mediated by PG E2, which is heavily generated and subsequently induces nociceptor sensitization (Rivest, 1999). Many studies have demonstrated that PG expression, induced via intraplantar injection of IL-1β, resulted in a dose-dependent bilateral thermal and mechanical hyperalgesia (Ferreira, et al., 1998; Safieh-Garabedian, et al., 1995; Perkins, et al., 1995).

IL-6

IL-6 is considered to be a pro-inflammatory cytokine that can induce hyperalgesia through the stimulation of arachidonic acid release. Curiously, studies have shown that IL-6 suppresses *in vitro* production of IL-1β by monocytes/macrophages stimulated with lipopolysaccharide (LPS). However, *in vivo* it stimulates the production of two anti-inflammatory proteins : soluble TNF-α receptor and IL-1β receptor antagonist. These two agents behave like decoys at the receptor sites, inhibiting binding of IL-1β or TNF-α with their cell receptors (Schindler, et al., 1990; Miller, et al., 1997; Tilg, et al., 1994).

Anti-inflammatory cytokines

Certain mediators exhibit analgesic properties by limiting the production of pro-inflammatory cytokines through the suppression of genes that code for the generation of IL-1, IL-6 and TNF-α (Angst, et al., 2008; Moalem & Tracey, 2006; Rittner, et al., 2005). Acting later in the inflammatory response, these anti-inflammatory cytokines, like IL-4 and IL-10, act independently of endogenous opioid production to counteract the hyperalgesia produced by pro-inflammatory cytokines (Rittner & Stein, 2005).

IL-4

IL-4 is a model anti-inflammatory cytokine that is mainly generated by T cells (te Velde, et al., 1990), as well as monocytes, mast cells, and macrophages (Cunha, et al., 1999). Studies have shown that IL-4 acts by suppressing the release of pro-inflammatory cytokines such as TNF-α, IL-1α, IL-1β, and IL-6 in response to lipopolysaccharide (LPS)- or IFN-γ-induced inflammation: this was evidenced by the the restoration of normal cytokine production with the administration of anti-IL-4 antiserum (te Velde, et al., 1990).

Researchers have also demonstrated the inhibition of pain behavioral responses to intraplantar injection of Cg, bradykinin, or TNF-α, when preceded by IL-4 administration 30 minutes before injection. It was also found that when IL-4 was administered 12-14 hours before IL-1β injection, the resulting hyperalgesia was inhibited (Cunha, Poole, Lorenzetti, Veiga, & Ferreira, 1999). These results indicate that, by inhibiting TNF-α during an earlier stage of inflammation and IL-1β in the later stages, IL-4 acts in a time-dependent manner.

IL-10

IL-10 is another characteristic anti-inflammatory cytokine that is generated and released by several different immune cells, such as macrophages, mononcytes, T-lymphocytes, natural killer cells, and B cells (Wagner ,et al., 1998; Marshall, Berumen, Nielsen, Gibetic, & Jordana,

1996; Mertz, DeWitt, Stetler-Stevenson, & Wahl, 1994). Studies have shown that IL-10 functions to enhance cell development, working with IL-3 and IL-4 (Marshall, et al., 1996), modulate B cell function (Mertz, et al., 1994), and decrease macrophage and mast cell production of pro-inflammatory cytokines (Wagner, et al., 1998). Similar to IL-4, IL-10 pretreatment has been found to attenuate pain response associated with IL-10-dependent decreases in TNF-α and IL-1β. Vale and colleagues demonstrated related findings in their study in which the administration of anti-IL-10 antiserum exacerbated the writhing response and debilitation of the knee joint in rats (2003).

Prostanoids and Cyclooygenases

Prostanoid synthesis is an important mediator of pain at the level of the periphery as well as the CNS. By inducing second messenger pathways involving cAMP and protein kinase A to reduce nociceptor thresholds and enhance membrane excitability, prostanoids increase nociceptor activation and transmission in primary afferent fibers (Burian & Gesslinger, 2005; Moalem & Tracey, 2006). Cyclooxygenase (COX) enzymes synthesize prostaglandins from arachidonic acid. The two isoforms of COX, COX-1 and COX-2, carry out different enzymatic functions. While COX-1 is a constitutive enzyme that is primarily responsible for homeostatic prostaglandin production, COX-2 shows low basal expression and is stimulated by various inflammatory mediators (Moalem & Tracey, 2006). Prostaglandins are part of a family of arachidonic acid metabolites called the eicosanoids, which include thromboxanes and leukotrienes as well (Meyer et al., 2005). These mediators are implicated in the sensitization of nociceptors in the skin to natural stimuli and different endogenous inflammatory mediators, which results in increased sensitivity to pain (Kidd & Urban, 2001). Sensitization is achieved by raising levels of cyclic AMP and lowering activation thresholds of primary afferents through

TTX-R sodium channels and the protein kinase A (PKA) pathway (Kidd & Urban, 2001; Basbaum & Jessell, 2000). PGs carry out their functions by acting on G-protein-coupled receptors, including the IP receptor for PGI_2 and $EP_{1\text{-}4}$ for PGE_2 (Moalem & Tracey, 2006). Current research acknowledges significant influences of prostanoids on pain processing at both the peripheral and central levels (McMahon, et al., 2005).

Key Intracellular Markers in Nociceptor Signaling Pathways

cAMP and Protein Kinase A (PKA)

Pain researchers identified cAMP as the first cellular second messenger to be involved in nociceptor sensitization, as evidenced by the presence of hyperalgesia and increased sensitivity of nociceptor fibers to the administration of membrane permeable cAMP analogs (Ferreira et al., 1990). Inflammatory mediators like prostaglandins produce hyperalgesia by causing an increase of intracellular cAMP, which stimulates evoked neurotransmitter release and alters both voltage and ligand-gated channels involved in pain (Gold et al., 1998). Past research has shown that intracellular cAMP levels in nociceptive neurons can be decreased by the endogenous activation of various opioid receptors (Stein et al., 1989) that engage in anti-nociceptive activity.

The second messenger, protein kinase A (pKA) is cAMP's binding partner and is therefore highly associated with cAMP activity, such that pKA inhibition decreases hyperalgesic behavioral responses and nociceptor activity (Zhang et al., 2002). The precise mechanisms of pKA signaling are yet to be established, but studies have shown that the mutation of PKA phophorylation on a primary afferent nociceptor-specific, tetrodotoxin-resistant sodium channel (TTX-R INa) (Fitzgerald et al., 1999) and the ligand-gated ion channel TRPV abolishes fluctuations in channels caused by cAMP signalling (Bhave et al., 2002). Recent research has

discovered cAMP's role in activating other molecules like channels involved in Ca^{2+} signaling (Kaupp & Seifert, 2002). This modulation Ca^{2+} signaling may have unique implications for glial cell interaction in the development of hyperalgesic inflammation.

Mitogen-Activated Protein Kinases (MAPK)

Mitogen-activated protein kinases (MAPKs) have also been identified as key players in nociceptor sensitization and the development of pathological pain states. For example, ERK1/2 activation by b2-adrenergic agonists contributes to the development of mechanical hyperalgesia (Aley et al., 2001). ERK is also activated in nociceptors by noxious stimuli like electrical stimulation, NGF, and capsaicin (Delcroix et al., 2003; Dai et al., 2002). When peripheral inflammation occurs, MAPK p38 activation results in TRPVI activation which ultimately leads to p38-dependent hyperalgesia (Mizushima et al., 2005).

Nitric Oxide (NO)

Another important second messenger involved in pain sensitization is nitric oxid (NO), produced by nitic oxide synthase (NOS). Noxious stimuli has been shown to increase immunoreactivity in DRG neurons (Vizzard et al., 1996). Also, NOS inhibitors were found to partially hinder PGE2-induced increase of TTX-R INa (Aley et al., 1998). However, it is important to note that NO is unique in that it has the ability to induce anti-nociceptive effects as well (Vivancos et al., 2003).

STAT 3 (79)

Yet another intracellular protein of interest is STAT3 (79), which belongs to the mammalian JAK protein family (including JAK1, JAK2, JAK3, and TYK2) (Levy and Darnell, 2002). This protein group enables the tyrosine kinase activity that is necessary for STAT to activate cytokine receptors. When STAT3 is inactive, it is localized in the cytoplasm. Once

activated by a noxious stimulus through receptor-ligand coupling, STAT3 enters the cell through the receptor through domain-specific binding (Liu et al., 2005). Researchers have shown that STAT3 activation is triggered by peripheral nerve injury within 15 minutes (Lee et al., 2004). Furthermore, some studies have demonstrated that STAT3 is activated in a time-dependent manner relative to the time of the peripheral nerve injury (Schwaiger et al., 2000; Qiu et al., 2005; Bareyre et al., 2011).

Carrageenan Model of Inflammation

Carrageenan (Cg) is a glycoprotein obtained from seaweed and it is typically used in animal research to induce inflammation (Rittner, Machelska, & Stein, 2005; Bennet, 2001). Depending on the injection site, the administration of carrageenan (Cg) can cause inflammation in the muscle and hind paw (Loram, Fuller, Fick, Cartmell, Poole, & Mitchell, 2006). When compared to injection of formalin, injection of Cg stimulates more lasting pain and greater hyperalgesia in a rodent's footpad (Ren & Dubner, 1999). Specifically, previous research has shown that Cg administration in the hind paw results in an acute inflammation, associated with mechanical hyperalgesia, which reaches maximum sensitivity within 2-4 hours post injection. Dose-dependent inflammation and hyperalgesia induced by Cg is alleviated with 24 hours (Loram, et al., 2006). The Cg model of inflammation corresponds to the time course for chronic pain states (Ren & Dubner, 1999).

Estrogen and Pain

Variations in sex exist in a plethora of neural mechanisms and the inflammatory response is no different. Both males and females have estrogens, which are gonadal hormones whose

receptors are located throughout the PNS and CNS (Ceccarelli, et al., 2003; Gaumond, et al., 2005). Some key locations of interest include neurons in the lumbar section of the dorsal horn in the spinal cord (Kuba, et al., 2006) and small-diameter dorsal root ganglion (DRG) neurons in the periphery (Kuba, et al., 2005). These hormone receptors develop differently in males and females (Berkley, 1997).

Intricate endogenous hormonal fluctuations characterize the estrous/menstrual cycle in females, in which estrogen levels rise and fall cyclically (Kuba & Quinones-Jenab, 2005). Specifically, the 14-35 day human menstrual cycle is marked by low levels of estrogen during the early-mid follicular phase, stable levels during the mid-luteal phase, and declined levels again just prior to menstruation (Martin & Behbehani, 2006). In the 4-day rodent estrous cycle, estrogen levels peak during the proestrus phase and fall during estrous (Martin & Behbehani, 2006). Research has shown that these fluctuations in hormones have important consequences for pain processing.

Studies have found that both menstrual phase and reproductive status (including pre-, peri-, and post-menopausal) influence the intensity and incidence of chronic pain (Gaumond, et al., 2005), as well as responses to pain (Kuba, et al., 2006; Macfarlane, et al., 2002). In particular, an increase in migraine attacks have been linked to reduced estrogen levels during the menstrual cycle (Gupta, et al., 2007). Research has also demonstrated that postmenopausal women, compared to premenopausal women, have greater plasma levels of pro-inflammatory cytokines such as TNF-α and IL-1β. Moreover, when treated with physiological concentrations of estrogen, postmenopausal women were found to have significantly decreased levels of IL-6, TNF-α, and IL-1β (Berg et al., 2002; Uemura et al., 2005; Rogers et al., 2001). Studies have demonstrated attenuated nociceptive responses using the Cg model of inflammation in female

rats in proestrus, a stage characterized by high levels of estrogen (Tall and Crisp, 2004). Research on opioid receptor action observed during different stages of the estrous cycle shows temporal variations in activity, which further support the cycle-dependent fluctuation of pain sensitivity (Berkeley, 1997). Exogenous estrogens also play a significant role in pain processing. For example, studies have shown that women suffering from migraines experienced an increase in attacks during oral contraceptive use (Martin & Behbehani, 2006), and post-menopausal women treated with estrogen-replacement therapy suffered a greater incidence of temporomandibular joint pain (Ceccarelli, et al., 2003b).

Studies using animal models have shown that estrogen attenuates levels of IL-6 and TNF-α, following injuries associated with trauma-hemorrhage, experimental autoimmune encephalomyelitis, and adipose and cardiac tissues (Suzuki et al., 2007; Morales et al., 2006; Xu et al., 2006; Bruun et al., 2003). Studies have also demonstrated estrogen's inhibition of inflammatory reactions in neuronal tissues, which is linked to reduced neuronal damage in several neurological illnesses, such as Alzheimer's and Parkinson's diseases, stroke, multiple sclerosis, and amyotrophic lateral sclerosis (Czlonkska et al., 2006). Researchers have corroborated these findings showing that during Phase II of the formalin test, estradiol attenuated flinching responses following the administration of 1% formalin (Kuba, et al., 2006; Manino et al., 2007). This attenuation effect is mediated via estrogen receptor activation, given that tamoxifen (an estrogen receptor modulator), but not α-estradiol (an inactive isomer of estradiol), attenuates estradiol's antihyperalgesic effects (Kuba et al., 2005; Manino et al., 2007). Cuzzocrea and colleagues (2000; 2001) demonstrated that estradiol replacement attenuates inflammation and tissue damage related to paw edema and pleurisy, as well. Researchers investigating peripheral inflammation found that the selective estrogen receptor modulators

(SERMs), raloxifene and tamoxifen, reduce carrageenan-induced inflammation (Cuzzocrea et al., 2007; Esposito et al., 2005).

Other studies further reinforce this significant interaction between the endocrine and immune systems in inflammatory processes. For example, it has been shown that estradiol attenuates the development of inflammation and tissue injury associated with spinal cord trauma (Cuzzocrea et al., 2008), and it also inhibits the spread of damage to the surrounding tissue during the crucial first week after spinal cord injury (Ritz and Hausmann, 2008). Furthermore, Gardell and colleagues (2008) showed that ERb-131, a β-estrogen receptor agonist, alleviates chronic but not acute inflammatory pain states. While these studies provide valuable support for the role of estradiol in different pain models, the specific mechanisms underlying estradiol's anti-inflammatory effects are yet to be clarified.

Estrogen's Reduction of Glial Cells: Possible Role in Antinociception

It is well known that inflammatory pain results from increased prostaglandin (PG) release and the initiation of various known immunologic molecules, such as cytokines, in response to tissue injury. Specifically, a peripheral injury induces macrophages and other immune cells to release IL-1β and TNF-α, which are pro-inflammatory cytokines. In turn, these cytokines induce the release of PGs via activation of the COX-2/mPGES enzymatic pathway, and this induction activates PG receptors at the dorsal root ganglia (DRG) neurons. Meanwhile, after crossing the blood-brain barrier, TNF-α increases PG levels and contributes to additional release of IL-1β by activating glial cells at the spinal cord. This further amplifies neuronal activity at the dorsal horn. Simultaneously, the levels of IL-10, an anti-inflammatory cytokine, are increased at the site of injury and its periphery, and this serves to down-regulate the secretion of other cytokines.

The activation of glial cells, specifically astrocytes and microglia, are closely linked to inflammatory processes. For example, microglia secrete pro-inflammatory cytokines that may play an important part in the enhancement of response in spinal cord neurons during lasting inflammation (Saab et al., 2008). Microglia express the estrogen receptors, ERβ and ERα, which function as endogenous mediators of estrogen action. Researchers have demonstrated that the responsiveness of microglia to pro-inflammatory agents, like lipopolysaccharide (LPS), is regulated by 17-β estradiol (Pozzi, et al., 2006). Additionally, studies using blood cultures have shown that the normal response to injury, local microglial activation coupled with an increase in the inflammatory cytokine IL-1β, is considerably dampened in ovariectomized young adult females replaced with estrogen. Recently, glial cells have also been highlighted as novel drug targets for SERMs because of their ER sensitivity and important contribution to the development of chronic inflammation (Arevalo, 2011).

Proposed Model

In light of the known effects of estrogen on glial activation and the previous reports of estrogen-mediated reduction of cytokine production on cancer and ovarian cells, a strong candidate for estrogen's underlying mechanism of inflammatory response mediation in the CNS is the dampening of glial activation. We postulate that a reduction in glial activation via estrogen treatment will in turn decrease cytokine levels at the spinal cord dorsal horn and DRG. Our hypothesis is that estrogen attenuates inflammation-induced pain responses by decreasing glial activation, which in turn reduces the levels of pro-inflammatory cytokines, (IL)-1β and TNF-α, in the central nervous system. Moreover, estrogen's influence on the aforementioned cytokines will also further reduce levels of other pro-inflammatory cytokines, like IL-6 and PGs, and

resident immune cells like tissue macrophages. Through the use of Western blots and immunocytochemical analyses, we aim to determine how estradiol alters the expression pattern of cytokine and PG receptors in glial cells of the dorsal horn at different time points after administration of carrageenan or saline. Estradiol's anti-inflammatory activity at the injury site will also be analyzed through a tissue macrophage marker. Finally, using markers for identification of active glial cells, we will discover if estradiol changes cytokine levels through the activation of microglia and astrocytes in the spinal cord dorsal horn.

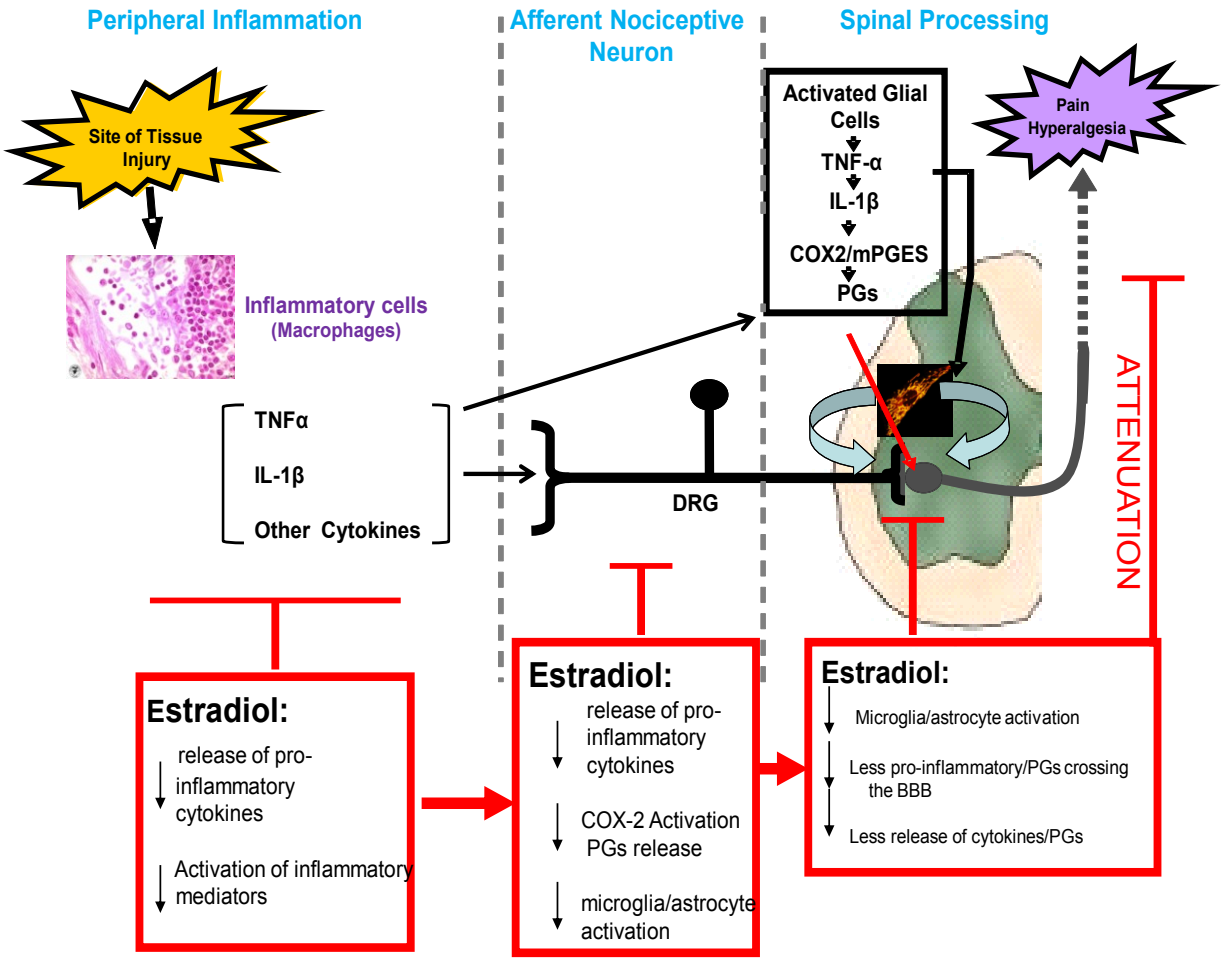

Figure 1.6. Model of hypothetical mechanism by which estradiol mediates analgesic responses to inflammatory pain. The inverted T's represent inhibition, the arrows represent activation and/or stimulation, the gray dotted lines denote the three levels of estradiol action examined during the inflammatory response, and the red boxes contain the effects of estradiol at each of these levels. These summative effects result in the decrease of inflammatory-induced behavioral responses.

Specific Aims

Postmenopausal women are subject to estrogen deficiency, which leave them highly predisposed to degenerative disorders like osteoporosis, atherosclerosis, rheumatoid arthritis, and Alzheimer's disease. Further supporting the significant role of estrogen in women's health is research that associates a decreased severity of age-related neurodegenerative disorders with the presence of estrogen through a process that results in reduced immuno-inflammation. However, estrogen's specific mechanism of decreasing inflammatory-mediated pain responses is yet to be determined. Elucidating estrogen's mechanism bears a strong clinical relevance because it will allow us to improve our knowledge of both the development and treatment of painful pathological ailments that afflict the 8 million women undergoing estrogen-alone replacement therapy.

Research has shown that the anti-cytokine actions of estrogen in blood cultures from postmenopausal women and the analgesic effects of estrogen replacement in ovariectomized rats are blocked by an estrogen receptor antagonist (Rogers et al, 2001; Kuba et al., 2006, 2005; Mannino et al., 2007). These findings suggest that estrogen replacement may wield a protective shield against neurodegenerative illnesses and that its analgesic actions are ER-mediated (Morales et al., 2006). Many of the current studies investigating estradiol's role in the inflammatory response report results that are conflicting and inadequate, and the rising development of novel drug targets for SERMs along with the growing population of HRT patients necessitate further research into estrogen's anti-inflammatory activity (Arevalo, 2011). Since the issue of how estrogen reduces inflammatory pain is one that is neglected in the current literature, it is our aim to understand the specific mechanisms behind the potentially significant consequence of pain mediation in estrogen-alone hormonal therapy.

The objective of my dissertation work is to determine to what extent the anti-hyperalgesic effects of estradiol on inflammatory pain are mediated through the attenuation of the inflammatory response at the injury site compared to in the nervous system. We postulate that estradiol treatment will dampen glial activation, which will in turn decrease cytokine levels at the spinal cord dorsal horn. Specifically, we hypothesize that *estradiol attenuates inflammation-induced pain responses by decreasing glial activation at the spinal cord dorsal horn, which in turn reduces levels of the pro-inflammatory cytokines, (IL)-1β, while concurrently reducing macrophage activation at the injury site.* To test this hypothesis, the following aims are proposed:

Aim 1: To determine to what extent estrogen's attenuation of behavioral responses to inflammation occurs by reducing immune cell responses at the injury site compared to reducing glial cell responses at the spinal cord dorsal horn.

To this end, ovariectomized (OVX) rats will receive s.c. Silastic administration of estradiol (20% estradiol/ 80% cholesterol) or vehicle (100% cholesterol). The following are the four experimental groups: OVX naïve rats plus estradiol, OVX naïve rats plus vehicle, OVX carrageenan-treated rats plus estradiol, and OVX carrageenan-treated rats plus vehicle. After one week following surgery, the rats will either be sacrificed (naïve OVX groups) or receive an interplanar injection of carrageenan (1%; 100 uL) in the right hind paw. The time course for tissue collection is at 1, 5 and 24 hour intervals, which represents the maximal attenuation of inflammatory-induced behavioral responses. The rats will be sacrificed, perfused, and spinal cord tissue will be collected and rapidly stored at -80 °C until use. Paws will also be removed and stored at -80 °C until use.

Immunohistochemistry analyses will be performed to examine paw expression of CD68

macrophage marker levels in comparison with spinal cord dorsal horn expression of activated glial cells using GFAP and OX-6. GFAP is glial fibrilliary acidic protein, a selective label considered to be a marker of astrocyte activation (Dong and Beneveniste, 2001) and OX-6 is an MHC-encoded antigen protein that indicates phenotypic shift in microglial cells from a quiescent state to an activated state (Aloisi, 2001; Frank et al., 2006). Since glial cells and macrophages undergo extreme activation during activation by inflammatory mediators, morphological changes will be quantified and described in microglial and astrocyte cells in the dorsal horn and macrophages in the paw.

Aim 2: To determine if estradiol alters the pattern of cytokine expression in glial cells of the spinal cord dorsal horn.

To test this hypothesis, we will use double-label immunohistochemistry to compare dorsal horn expression of IL-1β with GFAP-expressing astrocyte activation and with OX-6-expressing microglial activation. In addition, these markers will be analyzed via Western blots so that protein levels can be correlated with the amount of marker expression in the cells. Additionally, correlation of behavioral responses with expression levels of these markers will be made.

Aim 3: To determine to what extent intracellular responses associated with inflammatory responses in glial cells (MAP-ERK mediated responses and/or PKA signaling) mediate estrogen analgesia of inflammatory pain.

To examine this potentially significant relationship between glial cells and estrogen, we can analyze and correlate the inflammation-induced morphological changes in glial cells to estrogen's anti-inflammatory activity. Western Blot analyses will be performed to measure

values of these intracellular markers at 1, 5, and 24 hours after carrageenan and/or estradiol administration. In addition, correlation analyses of the expression levels of these intracellular markers and behavioral responses to carrageenan will be made.

Chapter 2: Methods and Materials

Animals

One hundred and forty 8-week old OVX female Sprague-Dawley rats were purchased from Taconic (Germantown, NY). Rats arrived in multiple cohorts to minimize variability associated with any one particular batch. Rats were double-housed with a 12-hour light/dark photoperiod (lights on at 8 A.M. EST). The temperature of the room was maintained at approximately 25°C. Food and water were available ad libitum, and NIH guidelines for care of laboratory animals were followed.

Hormone Replacement Paradigm

One week after ovariectomy, a SILASTIC capsule (1 cm, 0.058 in. ID x 0.077 in. OD, Dow Corning) was inserted beneath the skin at the nape of the neck in all animals. These capsules contained either 20% Beta-Estradiol (1, 3, 5 [10]-Estratriene-3, 17 Beta-diol; Sigma Aldrich) mixed with 80% Cholesterol for the experimental group, or Cholesterol (5-Cholestin-3Beta-ol; Sigma-Aldrich, St. Louis, MO) for the vehicle group. All rats were randomly assigned to either the experimental or vehicle groups; however, both animals in each cage received the same treatment. All animal procedures were approved by the Institutional Animal Care and Use Committee of Hunter College, CUNY.

Behavioral Apparatus & Analysis

The behavioral apparatus used for testing paw withdrawal latency (PWL) is the Hargreaves Box, a Paw Thermal Stimulator purchased from the Department of Anesthesiology at

the University of California, San Diego. It consists of 6 3x8 plexiglass enclosures situated on a heated glass surface with a stable temperature of 30°C ±1°C. A mobile infrared heat lamp produced varying heat intensities ranging from 4.0-6.0mV. For this experiment, the following three heat intensities were tested: low = 4.5 mV; medium = 4.9 mV; and, high = 5.3 mV. Heat intensity, though initially configured as bulb current (5.0, 5.5, and 6.0 amps) in the Hargreaves system, was measured as voltage (mV) because voltage readings were taken before each testing session using a multimeter to ensure uniform heat intensities across the experimental testing period. This is because taking voltage readings is the least intrusive measure of the thermal stimuli—in other words, measuring voltage does not disturb the preset current flow. Taking into account the starting temperature of the outer glass of 30°C ±1°C, the heating rates over the first ten seconds were 2.6, 4.2, and 5.2°C/second at bulb current settings of 5.0, 5.5, and 6.0 amps, respectively. In this manner, the low heat intensity is comparable to 62.6°C, medium to 79.6°C, and high to 88.9°C (Dirig et al., 1997). To assess PWL, the mobile heat lamp was pinpointed onto the plantar surface of the hindpaw, such that the amount of time (in seconds) in took for the animal to withdraw its paw from the heat source was automatically recorded as PWL. In this manner, animals were free to shift their paw at the moment of discomfort.

Prior to carrageenan or saline injection, rats were placed in the plexiglass chambers for 30 minutes in order to get them acclimated to their testing environment. After a baseline reading of PWL for each hind paw, rats were then given either a 100uL carrageenan injection (1% Carrageenan; Sigma) or 100uL saline injection (100% Saline; Braun Medical, Irving, CA) into the intraplantar region of their right hind paw. Immediately after injection, animals in the 1-hour group were placed back into their plexiglass testing chambers, while animals in the 5 and 24-hour groups were placed back into their cages. For the 1-hour group, PWL readings were taken

for the second time at exactly 1 hour after injection. For the 5 and 24-hour groups, rats were placed back into their testing chambers 30 minutes prior to testing for acclimation purposes, and they were tested for the second time at exactly 5 and 24 hours after injection. The table below summarizes the hormone and pain treatment groups for each time condition:

INJECTION	**HORMONE**
Saline	Vehicle
Saline	Estradiol
Carrageenan	Vehicle
Carrageenan	Estradiol

Tissue Collection

Rats were anesthetized and sacrificed using a perfusion procedure by which tissue was fixed and then removed. First, paw width measurements in millimeters were taken using a dial caliper (General Tools, New York, NY), and then paws were removed post-mortem, measured, weighed, and immediately frozen on dry ice. Spinal cord tissue was collected and stored in formalin solution in the refrigerator for one week, after which the tissue was transferred to a sucrose solution until sectioning.

Before analyses were run on spinal cord tissue, the lumbar regions (Figure 2.1A) were removed and sectioned using a cryostat. Once removed, the lumbar regions of the spinal cord were frozen in a tissue freezing medium (Tissue Tek OCT) and mounted for sectioning (30 μm). The sections were then stored in cryoprotectant solution (anti-freeze) solution (30% Glycerol, 30% Ethylene Glycol, and 40% Phosphate-Buffered Saline) at -20°C until immunohistochemical (IHC) analyses. In a similar manner, paws were dissected to isolate the intraplantar region

(Figure 2.1B), frozen in tissue freezing medium, mounted for sectioning (30 µm), and stored in anti-freeze solution until IHC analyses.

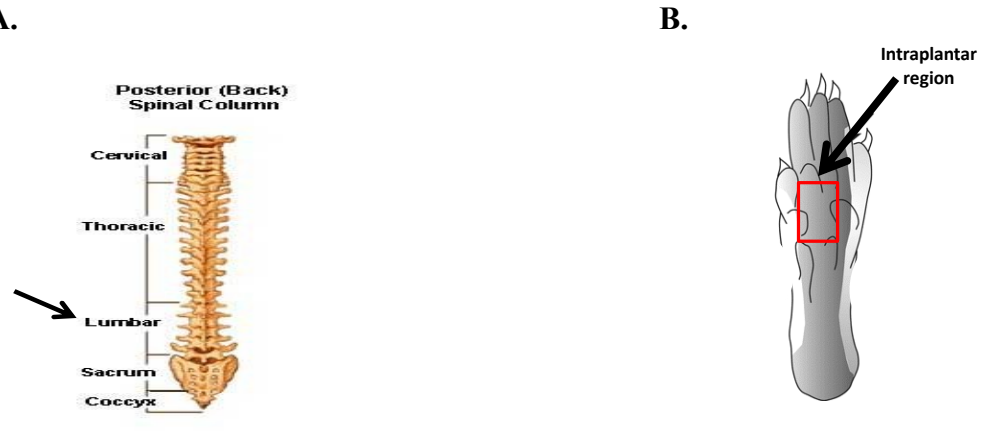

Figure 2.1. Diagram of tissue dissections: A. Spinal cord lumbar region; B. Rat intraplantar hindpaw region.

IHC- Immunohistochemistry with double-label fluorescence

Lumbar region sections of 30 µm (at least 10 serial sections per animal) were washed 3 times in ice-cold phosphate-buffered saline (PBS; Sigma).. The sections were then incubated with 5% Goat Serum (100 µl normal goat serum in 2 ml 0.2% Tx-PBS; Millipore) for 1 hour, followed by overnight incubation at 4°C with the first set of primary antibodies: mouse monoclonal anti-rat Glial Fibrillary Acidic Protein (GFAP, 1:200 dilution; Millipore) and mouse monoclonal anti-rat OX-6 (1:150 dilution; Millipore). The next day, sections were washed 3 times in ice-cold phosphate-buffered saline (PBS) and then incubated overnight with the second primary antibody, rabbit polyclonal IgG IL-1β (1:50 dilution; Santa Cruz Biotech). On the third day, sections were again washed 3 times in PBS and reacted with the first secondary antibody, goat anti-mouse Cy3 (1: 250; Millipore) for 1 hour, washed with PBS, then reacted with the second secondary antibody, goat anti-rabbit FITC (1:400; Santa Cruz Biotech) for 1 hour, and

finally washed again with PBS. The sections were then mounted on slides using 4',6-Diamidino-2-phenylindole, hydrochloride (DAPI; Fisher Scientific), which stains nuclei in fluorescent blue. The following table summarizes the set of treatments applied to each experimental condition.

Astrocytes/Cytokines	**Microglia/Cytokines**
GFAP	***OX-6***
IL-1β	IL-1β
Cy3	Cy3
FITC	FITC

Cy3 fluoresces red, revealing astrocytes detected by GFAP and microglia detected by OX-6, while FITC fluoresces green, revealing cytokine levels detected by IL-1β. Double-labeled cells show colocalization of increased astrocyte/microglia activation (GFAP/OX-6) with higher cytokine levels (IL-1β).

Intraplantar region hindpaw sections were treated in a similar fashion, with at least 10 sections at 30 μm/each analyzed per animal, except the IHC analysis was for single-label fluorescence. Specifically, FITC was used to detect CD68 (also known as ED1), which is a tissue macrophage marker.

IHC Image Quantification

Images were captured using an Olympus Spinning Disk Confocal microscope and the quantification of glial activation was performed on *Volocity*, an image analysis software, using pixel intensity values in the following manner. In fluorescence microscopy, a pixel's intensity value is related to the number of fluorophores (components of a molecule that cause it to be

fluorescent) in the corresponding area of a particular tissue sample. As such, fluorescence microscopy images can be analyzed for fluorescence intensity, which can then be used to determine the local concentration of fluorophores in a specimen.

Images of ipsilateral spinal cord dorsal horn sections were photographed at 20X magnification and cropped to uniform-sized boxes, and four images were taken per section to average results. Although the number of cells was not quantified, the visual representation of approximately consistent numbers of cells among images, as illustrated by DAPI-stained nuclei, support standardized analyses using uniform-sized boxes. The images were adjusted in a consistent manner to subtract background intensity and maximize contrast. In order to avoid "saturation" effects, the threshold pixel intensity values were determined based on regions of interest (ROIs), obtained through visual inspection, in untreated (saline/vehicle) tissue. Pictures were then analyzed for fluorescence intensity values above these predetermined thresholds. This method yields a quantitative measurement of the relative degree of staining exceeding that which exists in normal, untreated tissue. Paw macrophage marker activation was also quantified using this method.

Co-localization was quantified in a similar manner by which the ROI, a double-labeled cell depicting an overlay of fluorophores, was selected in the untreated condition and threshold values were accordingly determined for each channel. Then, images were analyzed on *Volocity* using the thresholded Pearson's Correlation Coefficient (PCC), a standard statistical analysis that measures the strength of a linear relationship between two variables. The two variables in this case are the fluorescent intensities within each channel.

Western Blot Analyses

Protein samples (40 μg) were boiled in Lammeli buffer containing 5% β-mercaptoethanol and loaded onto 10% SDS-PAGE. Gels were electrophoresed, transferred to nitrocellulose membranes, and blocked for 60 minutes with 5% non-fat dry milk in tris-buffer-saline-tween (TBST, pH= 7.4) at room temperature. Membranes were probed overnight at 4°C, for GFAP (1:2000), pKa (1:3000), pERK (1:3000), tERK (1:3000), and stat-3 (1:3000). After three washes with TBST, membranes were then incubated with their appropriate secondary antibody (1:1000) for 60 minutes at room temperature, followed by three more washes with TBST.

The resulting films were scanned and quantified using the Image J Analysis program. Samples were loaded onto gels in such a way that the time course of changes in protein levels in estradiol and vehicle-treated rats after saline or carrageenan treatment can be determined. Proteins were quantified against c- and α-tubulin (1:1000) using the untreated (saline vehicle) condition as a reference to the treated one.

Statistical Analyses

For the behavioral assay, a univariate ANOVA was performed to test for significance of time condition (1 hour, 5 hour, or 24 hour), injection treatment (carrageenan or saline), hormone condition (estradiol or vehicle), and any relevant interactions on paw withdrawal latencies (PWL). PWL values were normalized through percent baseline correction. Fisher's LSD was used to compare differences in PWL for each heat intensity channel (low, medium, and high) between treatment groups (saline/vehicle, saline/estradiol, carrageenan/vehicle, and carrageenan/estradiol) across time condition (1, 5, and 24 hour). Error bars on graphs represent standard deviation.

For the IHC analyses, univariate ANOVAs were performed to test for significance of time condition (1 hour, 5 hour, or 24 hour), injection treatment (carrageenan or saline), hormone condition (estradiol or vehicle), and any relevant interactions on mean fluorescence intensity values of each antibody and colocalization pair (GFAP, OX-6, IL-1B, GFAP/IL-1B, OX-6/IL-1B, and CD68). Specific differences between treatment groups across time condition were compared using Fisher's LSD. Also, the extent of estradiol-mediated activation at the injury site was compared with that at the spinal cord by analyzing CD68 with GFAP and CD68 with OX-6 using percentage to control values and a simple t-test. Error bars on graphs represent standard deviation. Additionally, Pearson's r correlations and linear regression analyses were performed to test for possible correlations between IHC and behavior.

For the Western blot analyses, univariate ANOVAs were performed for each protein, followed by Fisher's LSD for comparison of differences in protein levels between treatment groups across time condition. Error bars on graphs represent standard deviation. Additionally, Pearson's r correlations and linear regression analyses were performed to test for possible relationships between protein levels and behavior, and protein levels of glial activation and intracellular markers.

Chapter 3. Results

Aim 1: Determination of the extent to which estradiol's attenuation of behavioral responses to inflammation occurs by reducing immune cell responses at the injury site compared to glial cell responses at the spinal cord dorsal horn.

Effects of estradiol and carrageenan administration on behavioral responses and paw size.

Effects of estradiol administration on baseline PWL.

Figure 3.1 shows PWL for both estradiol- and vehicle-treated OVX rats at low, medium, and high heat intensities in both paws prior to Cg administration. No significant main effects or interaction effects were observed for hormone or heat intensity.

Effects of estradiol administration on PWL at 1, 5, and 24 hours after Cg administration in the ipsilateral (injected) and contralateral (not injected) paws at the low heat intensity (4.5 mV).

Figure 3.2 shows PWL for both estradiol- and vehicle-treated OVX rats at the low heat intensity at 1, 5, and 24 hours after Cg or saline administration in the ipsilateral (3.2A) and contralateral (3.2B) paw. In the ipsilateral paw (Figure 3.2A), significant main effects of injection and time were observed [Injection: $F(1,83)=10.40$, $p<0.01$; Time: $F(2,83)=4.56$, $p<0.05$]. Specifically, the group that received Cg administration ($M=83.1$) showed significantly decreased PWL compared with the group that received saline administration ($M=95.4$; $p<0.05$). PWL was significantly shorter 1 hour ($M=81.760$) post-Cg/saline administration compared with 24 hours ($M=96.3$) post-injection ($p<0.05$). In addition, a significant interaction of hormone and

time was observed [$F(2,83)=3.29$, $p<0.05$]. The vehicle-treated group displayed significantly decreased PWL 1 hour ($M=73.8$) after injection compared with both 5 hours ($M=93.9$) and 24 hours post-injection ($M=97.5$; $p<0.01$). Also, the vehicle-treated group ($M=73.8$) had significantly shorter PWL compared with the estradiol-treated group ($M=89.7$) 1 hour post-injection ($p<0.05$).

In the contralateral paw (Figure 3.2B), a significant main effect of injection was observed [Injection: $F(1,72)=4.00$,$p<0.05$)]; the group that received saline administration ($M=99.7$) showed significantly decreased PWL compared with the group that received Cg administration ($M=106.2$;$p<0.05$).

Table 3.1 displays corresponding PWL values for ipsilateral and contralateral paws.

Effects of estradiol administration on PWL at 1, 5, and 24 hours after Cg administration in the ipsilateral and contralateral paws at the medium heat intensity (4.9 mV).

Figure 3.3 shows PWL for both estradiol- and vehicle-treated OVX rats at the medium heat intensity at 1, 5, and 24 hours after Cg or saline administration in the ipsilateral (3.3A) and contralateral (3.3B) paw. In the ipsilateral paw (Figure 3.3A), a significant main effect of injection was observed [$F(1,86)=6.03$; $p<.05$]. The group that received Cg administration ($M=74.6$) showed significantly decreased PWL compared with the group that received saline administration ($M=87.8$; $p<0.05$).

In the contralateral paw (Figure 3.3B), a significant interaction of hormone, injection, and time was observed [$F(2,76)=3.23$; $p<0.05$]. Specifically, the vehicle-treated group that received saline administration ($M=86.8$) showed significantly decreased PWL compared with the estradiol-treated group that received saline administration ($M=104.2$), 5 hours post-injection

($p<0.05$). Also, the vehicle-treated group that received saline administration had significantly shorter PWL compared with the vehicle-treated group that received Cg administration ($M=107.3$; $p<0.05$).

Table 3.1 displays corresponding PWL values for ipsilateral and contralateral paws.

Effects of estradiol administration on PWL at 1, 5, and 24 hours after Cg administration in the ipsilateral and contralateral paws at the high heat intensity (5.3 mV).

Figure 3.4 shows PWL for both estradiol- and vehicle-treated OVX rats at the high heat intensity at 1, 5, and 24 hours after Cg or saline administration in the ipsilateral (3.4A, injected) and contralateral (3.4B, not injected) paw.

In the ipsilateral paw (Figure 3.4A), a significant interaction of injection and time was observed [$F(2,890=4.91$; $p<0.05$]. The group that received Cg administration displayed significantly increased PWL 1 hour ($M=109.2$) post-injection compared with 5 and 24 hours post-injection ($M=71.8$ and 86.9, respectively; $p<0.05$). Also, a significantly decreased PWL was observed for the group that received Cg administration ($M=71.8$) compared with the group that received saline administration ($M=100.5$), 5 hours post-injection ($p<0.01$). No significant main effects or interaction effects were observed for hormone, time, or injection were found in the contralateral paw.

Table 3.1 displays corresponding PWL values for ipsilateral and contralateral paws.

Effects of estradiol on paw size in OVX rats.

Figure 3.5 shows mean paw size for both estradiol- and vehicle-treated OVX rats after Cg or saline administration. Significant main effects of injection site, hormone, injection, and time

were observed: [Injection Site: $F(1,12)=147.61$, $p<0.001$; Hormone: $F(1,12)=10.12$, $p<0.05$; Injection: $F(1,12)=87.79$, $p<0.001$; Time: $F(2,12)=5.53$, $p<0.05$]. Specifically, ipsilateral paw size ($M=42.44$) was significantly larger than contralateral paw size ($M=28.47$) across all treatment groups ($p<0.001$). Also, the vehicle-treated group ($M=37.92$) showed significantly increased paw size compared with the estradiol-treated group ($M=32.99$, $p<0.01$). The group that received Cg administration ($M=42.71$) showed significantly larger paw size than the group that received saline ($M=28.20$, $p<0.001$). Additionally, paw size was significantly larger at both 1 and 5 hours ($M=36.66$ and $M=37.82$, respectively) after Cg/saline administration compared with 24 hours ($M=31.88$) post-injection ($p<0.05$).

A significant interaction of injection site and hormone was observed [$F(1,12)=7.94$, $p<0.05$], where ipsilateral paw size ($M=46.52$) was larger than contralateral paw size ($M=29.31$) within the vehicle-treated group ($p<0.05$). Also, injection site and injection conditions were found to interact significantly [$F(1,12)=148.05$, $p<0.001$], where ipsilateral paw size ($M=56.69$) was larger than contralateral paw size ($M=28.73$) in the group that received Cg administration ($p<0.001$). Further, a significant interaction was observed between injection site and time conditions [$F(2,12)=13.80$, $p<0.01$]. Post hoc analyses reveal that ipsilateral paw size was significantly larger than contralateral paw size at 1 hour (Ipsi: $M=42.94$; Contra: $M=30.38$) and 5 hours (Ipsi: $M=42.94$; Contra: $M=30.38$) after injection ($p<0.01$).

Additionally, a significant interaction was observed between hormone, injection, and injection site [$F(1,12)=8.67$, $p<0.05$]. Post-hoc analyses show that ipsilateral paw size was significantly larger in the vehicle treated group administered Cg ($M=64.54$) compared with the estradiol-treated group administered Cg ($M=48.83$, $p<0.05$). A final significant interaction was observed between injection, time, and injection site [$F(2,12)=12.57$, $p<0.01$]. Of the group that

received Cg administration, the ipsilateral paw size was significantly larger 1 hour (Ipsi: M=54.94; Contra: M=30.00), 5 hours (Ipsi: M=71.75; Contra: M=28.06), and 24 hours (Ipsi: M=28.13; Contra: M=43.38) post injection ($p<0.01$).

Table 3.2 displays corresponding paw size values for ipsilateral and contralateral paws across time condition.

Effects of estradiol and carrageenan administration on immune cell response at injury site and comparison to paw size.

Effects of estradiol on macrophage expression at injury site.

Figure 3.6 displays representative immunostained images demonstrating positive labeling of CD68 for macrophages in ipsilateral (injected), plantar-region hindpaw tissue in OVX vehicle- and estradiol-treated rats in saline and carrageenan treatment groups, across different time conditions. FITC, the secondary antibody used to detect CD68, varies in fluorescence intensity from panel A to panel J, indicating varied levels of CD68-expressing macrophage activation.

Figure 3.7 quantifies this information by showing mean fluorescence intensity of CD68-detecting FITC in ipsilateral, plantar-region hindpaw tissue of estradiol- and vehicle-treated OVX rats at 1, 5, and 24 hours after Cg or saline administration. Significant main effects of hormone, injection, and time were observed [Hormone: $F(1,36)=1353.21$, $p<0.001$; Injection: $F(1,36)=2447.21$, $p<0.001$; Time: $F(2,36)=240.35$, $p<0.001$]. Specifically, the mean fluorescence intensity for the vehicle-treated group (M=0.81) was significantly greater compared with the estradiol-treated group (M=0.65, $p<0.001$). The group that received Cg administration

(M=0.84) also showed significantly increased fluorescence intensity than the group that received saline (M=0.62, $p<0.001$). Additionally, significant differences in fluorescent intensity were found among all three time conditions: intensity was increased 1 hour post-injection (M=0.79) compared with 5 hours (M=0.67) and 24 hours post-injection (24: M=0.72, $p<0.001$) and intensity was increased 24 hours post-injection compared with 5 hours post-injection ($p<0.001$).

Additionally, a significant interaction of hormone and injection was observed [$F(1,36)=34.07$, $p<0.001$]. Specifically, the vehicle-treated group that received saline administration (M=0.69) had significantly decreased mean fluorescence intensity compared with the vehicle-treated group that received Cg administration (M=0.93) and the estradiol-treated group that received saline (M=0.55) had significantly decreased intensity compared with the estradiol-treated group that received Cg (M=0.74; $p<0.001$). Further, the estradiol-treated group that received saline had significantly decreased intensity compared with the vehicle-treated group that received saline ($p<0.001$) and the estradiol-treated group that received Cg had significantly decreased intensity compared with the vehicle-treated group that received Cg ($p<0.001$).

A significant interaction was also found between hormone and time [$F(2,36)=14.59$, $p<0.001$]. Post hoc analyses show that in the vehicle-treated group, mean fluorescence intensity was significantly increased 1 hour post-Cg/saline administration (M=0.88) compared with 5 hours (M=0.74) and 24 hours post-injection (M=0.80), and intensity was increased 24 hours post-injection compared with 5 hours post-injection ($p<0.001$). In the estradiol-treated group, a similar pattern was observed where intensity was significantly increased 1 hour post-Cg/saline administration (M=0.70) compared with 5 hours (M=0.61) and 24 hours post-injection (M=0.64), and intensity was increased 24 hours post-injection compared with 5 hours post-injection

($p<0.001$). Further, intensity was significantly increased within each time point in the vehicle-treated group compared with the estradiol-treated group ($p<0.001$).

Correlations between ipsilateral paw size and macrophage expression at the injury site in estradiol- and vehicle-treated OVX rats after Cg or saline administration.

Significant positive correlations were observed between ipsilateral paw size and CD68-expression of macrophages at the injury site. Specifically, paw size was significantly correlated with CD68 across all treatment groups [$r=0.40$, $p<0.05$] and within the estradiol-treated group [$r=0.45$, $p<0.05$; Table 3.3].

Correlations between ipsilateral PWL at the low heat intensity and macrophage expression at the injury site in estradiol- and vehicle-treated OVX rats after Cg or saline administration.

PWL correlated significantly with CD68 expression levels across all three heat intensities. Specifically, PWL correlated negatively with CD68 across all treatment groups at the lowest heat intensity, [$r=0.33$, $p<0.05$], at the medium heat intensity, [$r=0.31$, $p<0.05$] and at the highest heat intensity [$r=0.57$, $p<0.001$]. Also, PWL correlated negatively with CD68 in the vehicle-treated group at the medium heat intensity [$r=0.68$, $p<0.05$] and at the high heat intensity [$r=0.73$, $p<0.001$]. Finally, PWL correlated negatively with CD68 in the estradiol-treated group [$r=0.43$, $p<0.05$; Table 3.5]. Although linear regression analyses failed to show a statistically significant relationship between PWL and CD68, the linear relationships were negative for both vehicle- ($\beta=-33.32$) and estradiol-treated groups ($\beta=-49.71$; Figure 3.8).

Effects of estradiol and carrageenan administration on glial cell responses at the spinal cord dorsal horn.

Effects of estradiol on astrocyte activation at the spinal cord dorsal horn.

Figure 3.9 displays representative immunostained images demonstrating positive labeling of GFAP for astrocytes in ipsilateral spinal cord dorsal horn in OVX vehicle- and estradiol-treated rats in saline and carrageenan treatment groups, across different time conditions. Cy3, the secondary antibody used to detect GFAP, varies in red fluorescence intensity from panel A to panel J, indicating varied levels of GFAP-expressing astrocyte activation. Figure 3.11 shows positive labeling of GFAP for astrocytes with DAPI-stained nuclei fluoresced blue, displaying approximately consistent cell numbers across panels.

Figure 3.10 quantifies this information by showing mean fluorescence intensity of GFAP-detecting Cy3 in ipsilateral spinal cord dorsal horn of estradiol- and vehicle-treated OVX rats at 1, 5, and 24 hours after Cg or saline administration. Significant main effects of hormone and injection were observed [Hormone: $F(1,36)=323.36$, $p<0.001$; Injection: $F(1,36)=13.94$, $p<0.01$]. Specifically, the mean fluorescence intensity for the vehicle-treated group ($M=0.94$) was significantly greater compared with the estradiol-treated group ($M=0.35$, $p<0.001$). The group that received Cg administration ($M=0.70$) also showed significantly increased fluorescence intensity than the group that received saline ($M=0.58$, $p<0.001$).

Additionally, a significant interaction of hormone and injection was observed [$F(1,36)=160.63$, $p<0.001$]. Specifically, the vehicle-treated group that received saline administration ($M=0.67$) had significantly decreased mean fluorescence intensity compared with the vehicle-treated group that received Cg administration ($M=1.21$) and the estradiol-treated

group that received saline (M=0.50) had significantly increased intensity compared with the estradiol-treated group that received Cg (M=0.20; $p<0.001$). Further, the estradiol-treated group that received saline had significantly decreased intensity compared with the vehicle-treated group that received saline ($p<0.001$) and the estradiol-treated group that received Cg had significantly decreased intensity compared with the vehicle-treated group that received Cg ($p<0.001$).

Effects of estradiol on microglia activation at the spinal cord dorsal horn.

Figure 3.12 displays representative immunostained images demonstrating positive labeling of OX-6 for microglia in ipsilateral spinal cord dorsal horn in OVX vehicle- and estradiol-treated rats in saline and carrageenan treatment groups, across different time conditions. Cy3, the secondary antibody used to detect OX-6, varies in fluorescence intensity from panel A to panel J, indicating varied levels of OX-6-expressing microglia activation.

Figure 3.13 quantifies this information by showing mean fluorescence intensity of OX-6-detecting Cy3 in ipsilateral spinal cord dorsal horn of estradiol- and vehicle-treated OVX rats at 1, 5, and 24 hours after Cg or saline administration. Significant main effects of hormone and time were observed [Hormone: $F(1,36)=70.01$, $p<0.001$; Time: $F(2,36)=7.72$, $p<0.01$]. Specifically, the mean fluorescence intensity for the vehicle-treated group (M=1.78) was significantly greater compared with the estradiol-treated group (M=1.33, $p<0.001$). Also, the following significant differences in fluorescent intensity were found among time conditions: intensity was increased 1 hour post-injection (M=1.57) compared with 5 hours (M=1.42; $p<0.05$) and intensity was increased 24 hours (M=1.68) post-injection compared with 5 hours post-injection ($p<0.001$).

Additionally, a significant interaction of hormone and injection was observed [$F(1,36)=26.54$, $p<0.001$]. Specifically, the vehicle-treated group that received saline administration (M=1.64) had significantly decreased mean fluorescence intensity compared with the vehicle-treated group that received Cg administration (M=1.92) and the estradiol-treated group that received saline (M=1.47) had significantly increased intensity compared with the estradiol-treated group that received Cg (M=1.20; $p<0.001$). Further, the estradiol-treated group that received saline had significantly decreased intensity compared with the vehicle-treated group that received saline ($p<0.001$) and the estradiol-treated group that received Cg had significantly decreased intensity compared with the vehicle-treated group that received Cg ($p<0.001$).

Correlations between ipsilateral PWL and astrocyte activation at the spinal cord dorsal horn in estradiol- and vehicle-treated OVX rats after Cg or saline administration, at the low heat intensity.

Significant correlations were observed between ipsilateral PWL and GFAP-expression of astrocytes at the medium and highest heat intensities. Specifically, PWL correlated negatively with GFAP at the medium heat intensity in the vehicle-treated group [$r=0.67$, $p<0.05$]. At the highest heat intensity, PWL correlated negatively with GFAP across all treatment groups [$r=0.35$, $p<0.05$] and within the vehicle-treated group [$r=0.76$, $p<0.001$; Table 3.5]. Linear regression analyses showed that GFAP did not predict PWL with statistical significance (Figure 3.8).

Correlations between ipsilateral PWL and microglia activation at the spinal cord dorsal horn in estradiol- and vehicle-treated OVX rats after Cg or saline administration, at the low heat intensity.

Ipsilateral PWL correlated significantly with OX-6-expression of microglia across all heat intensities. Specifically, PWL correlated negatively with OX-6 in the estradiol-treated group that was administered Cg at the lowest heat intensity [r=0.59, p<0.05] and at the medium heat intensity [r=0.68, p<0.05; Table 3.5]. Significant positive correlations were observed for PWL with OX-6 at the highest heat intensity in the estradiol-treated group [r=0.43, p<0.05] and in the vehicle-treated group administered saline [r=0.64, p<0.05; Table 3.5]. Linear regression analyses showed that OX-6 did not predict PWL with statistical significance (Figure 3.8).

Correlations between macrophage response at the injury site and glial cell activation at the spinal cord dorsal horn.

Significant positive correlations were observed between CD68-expression of macrophages and GFAP-expression of astrocytes. Specifically, CD68 correlated positively with GFAP across all treatment groups [r=0.58, p<0.001] and within the vehicle-treated group [r=0.78, p<0.001]. Significant negative correlations between CD68 and GFAP were observed within the estradiol-treated group [r=-0.91, p<0.001] and within the estradiol-treated group administered saline [r=-0.68, p<0.05; Table 3.4].

Significant positive correlations were also observed between CD68-expression of macrophages and OX-6-expression of microglia. Specifically, CD68 correlated positively with OX-6 across all treatment groups [r=0.46, p<0.001], within the vehicle-treated group [r=0.51, p<0.001], and within the estradiol-treated group administered Cg [r=0.63, p<0.05]. A

significant negative correlation between CD68 and GFAP was observed within the estradiol-treated group [r=-0.62, $p<0.05$; Table 3.4].

Estradiol's extent of activation between macrophage response at injury site and glial response at spinal cord dorsal horn.

Macrophage activation at injury site compared to astrocyte activation at spinal cord dorsal horn.

Figure 3.14A, C, and E show mean fluorescence intensity (activation) expressed as percent change from control, or vehicle/saline treatment, between CD68-expressing macrophages at the injury site and GFAP-expressing astrocytes at the spinal cord dorsal horn across treatment groups. Significant differences were found in percent change of activation, or extent of cell activation, between the two sites. Specifically, compared to CD68 activation, GFAP activation was greater in the vehicle/saline-treated group [$F(1,22)= 24.82$, $p<.05$], the vehicle/Cg-treated group [$F(1,22)= 81.48$, $p<.05$], and the estradiol/Cg treated group [$F(1,22)= 112.34$, $p<.05$]. Also, GFAP activation was greater in both the vehicle- [$F(1,46)= 26.91$, $p<.05$] and estradiol-treated groups [$F(1,46)= 26.96$, $p<.05$] across injection treatments. This pattern is repeated again in the saline- [$F(1,46)= 11.13$, $p<.05$] and Cg-treated groups [$F(1,46)= 21.09$, $p<.05$] across hormone treatments. Table 3.6 displays corresponding values for CD68 and GFAP activation.

Figure 3.15 shows this data broken down across post-injection behavioral testing time points of 1 hour (A, B, and C), 5 hours (D, E, and F) and 24 hours (G, H, and I). Significant differences were found in percent change of activation between the two sites at the different time

points. Specifically, at 1 hour post-injection, GFAP activation exceeded CD68 activation in the estradiol/saline-treated group [$F(1,6)= 18.28$, $p<.05$], the vehicle/Cg-treated group [$F(1,6)= 22.09$, $p<.05$], and the estradiol/Cg-treated group [$F(1,6)= 17.83$, $p<.05$]. Across injection treatments, GFAP activation was greater in the estradiol-treated group [$F(1,14)= 26.96$, $p<.05$] and across hormone treatments, GFAP activation was greater in both the saline- [$F(1,14)= 6.52$, $p<.05$] and Cg-treated groups [$F(1,14)= 6.72$ $p<.05$]. This pattern of greater GFAP activation was repeated at 5 hours and 24 hours post-injection in the vehicle/saline-treated group ([$F(1,6)= 39.26$, $p<.05$]; [$F(1,6)= 21.64$, $p<.05$], respectively) the estradiol/saline-treated group ([$F(1,6)= 19.74$, $p<.05$]; [$F(1,6)= 6.50$, $p<.05$], respectively), the vehicle/Cg-treated group ([$F(1,6)= 62.42$, $p<.05$]; [$F(1,6)= 98.56$, $p<.05$], respectively), the estradiol/Cg-treated group ([$F(1,6)= 124.47$, $p<.05$]; [$F(1,6)= 76.80$, $p<.05$], respectively), the vehicle-treated group ([$F(1,14)= 51.19$, $p<.05$]; [$F(1,14)= 9.29$, $p<.05$], respectively), the estradiol-treated group ([$F(1,14)= 5.93$, $p<.05$]; [$F(1,14)= 10.13$, $p<.05$], respectively), the saline-treated group (24 hours only: [$F(1,14)= 7.47$, $p<.05$], and the Cg-treated group ([$F(1,14)= 12.30$, $p<.05$]; [$F(1,14)= 10.51$, $p<.05$], respectively).

Macrophage activation at injury site compared to astrocyte activation at spinal cord dorsal horn.

Figure 3.14B, D, and F show mean fluorescence intensity (activation) expressed as percent change from control, or vehicle saline, between CD68-expressing macrophages at the injury site and OX-6-expressing microglia at the spinal cord dorsal horn. Significant differences were found in percent change of activation, or extent of cell activation, between the two sites. Specifically, compared to CD68 activation, OX-6 activation was less in the estradiol/saline-

treated group [F(1,22)= 5.95, p<.05], and vehicle/Cg-treated group [F(1,22)= 11.89, p<.05], but greater in the estradiol/Cg-treated group [F(1,22)= 153.78, p<.05]. Across injection treatments, OX-6 activation was greater in the estradiol-treated group [F(1,46)= 8.25, p<.05], and across hormone treatments, OX-6 activation was greater in the Cg-treated group [F(1,46)= 6.64, p<.05]. Table 3.6 displays corresponding values for CD68 and OX-6 activation.

Figure 3.16 shows this data broken down across post-injection behavioral testing time points of 1 hour (A, B, and C), 5 hours (D, E, and F) and 24 hours (G, H, and I). Significant differences were found in percent change of activation between the two sites at the different time points. Specifically, at 1 hour post-injection, OX-6 activation was greater than CD68 activation in the estradiol/Cg-treated group [F(1,6)= 43.02, p<.05] and the estradiol-treated group [F(1,6)= 8.25, p<.05]. At 5 hours post-injection, OX-6 activation was less than CD68 activation in the estradiol/saline-treated group [F(1,6)= 7.25, p<.05], vehicle/Cg-treated group [F(1,6)= 66.00, p<.05], and the vehicle-treated group [F(1,14)= 4.99, p<.05], but greater in the estradiol/Cg-treated group [F(1,6)= 135.53, p<.05] and the estradiol-treated group [F(1,14)= 7.19, p<.05]. At 24 hours post-injection, OX-6 activation was greater in the vehicle-saline treated group [F(1,6)= 42.92, p<.05], and estradiol/Cg-treated group [F(1,6)= 30.77, p<.05], but less in the estradiol/saline-treated group [F(1,6)= 97.92, p<.05] and vehicle/Cg-treated group [F(1,6)= 18.36, p<.05].

Aim 2: Effects of estradiol and Cg administration on IL-1β cytokine expression in glial cells of the spinal cord dorsal horn.

Effects of estradiol on IL-1β expression in spinal cord dorsal horn.

Figure 3.17 displays representative immunostained images demonstrating positive labeling of the cytokine, IL-1β, in ipsilateral spinal cord dorsal horn in OVX vehicle- and estradiol-treated rats in saline and carrageenan treatment groups, across different time conditions. FITC, the secondary antibody used to detect IL-1β, varies in fluorescence intensity from panel A to panel J, indicating varied levels of IL-1β-expressing cytokine activation.

Figure 3.18 quantifies this information by showing mean fluorescence intensity of IL-1β-detecting FITC in ipsilateral spinal cord dorsal horn of estradiol- and vehicle-treated OVX rats at 1, 5, and 24 hours after Cg or saline administration. Significant main effects of hormone, injection, and time were observed [Hormone: $F(1,36)=1474.82$, $p<0.001$; Injection: $F(1,36)=2759.82$, $p<0.001$; Time: $F(2,36)=43.35$, $p<0.001$]. Specifically, the mean fluorescence intensity for the vehicle-treated group ($M=0.55$) was significantly greater compared with the estradiol-treated group ($M=0.40$, $p<0.001$). The group that received Cg administration ($M=0.58$) also showed significantly increased fluorescence intensity than the group that received saline ($M=0.37$, $p<0.001$). Additionally, significant differences in fluorescent intensity were found among all three time conditions: intensity was increased 1 hour post-injection ($M=0.50$) compared with 5 hours ($M=0.45$) and 24 hours post-injection (24: $M=0.47$, $p<0.001$) and intensity was increased 24 hours post-injection compared with 5 hours post-injection ($p<0.01$).

In addition, a significant interaction of hormone and injection was observed [$F(1,36)=87.55$, $p<0.001$]. Specifically, the vehicle-treated group that received saline

administration (M=0.43) had significantly decreased mean fluorescence intensity compared with the vehicle-treated group that received Cg administration (M=0.68) and the estradiol-treated group that received saline (M=0.31) had significantly decreased intensity compared with the estradiol-treated group that received Cg (M=0.48; $p<0.001$). Further, the estradiol-treated group that received saline had significantly decreased intensity compared with the vehicle-treated group that received saline ($p<0.001$) and the estradiol-treated group that received Cg had significantly decreased intensity compared with the vehicle-treated group that received Cg ($p<0.001$).

A significant interaction was also found between hormone and time [$F(2,36)=8.79$, $p<0.001$]. Post hoc analyses show that in the vehicle-treated group, mean fluorescence intensity was significantly increased 1 hour post-Cg/saline administration (M=0.88) compared with 5 hours (M=0.74) and 24 hours post-injection (M=0.80), and intensity was increased 24 hours post-injection compared with 5 hours post-injection ($p<0.001$). In the estradiol-treated group, a similar pattern was observed where intensity was significantly increased 1 hour post-Cg/saline administration (M=0.70) compared with 5 hours (M=0.61) and 24 hours post-injection (M=0.64), and intensity was increased 24 hours post-injection compared with 5 hours post-injection ($p<0.001$). Further, intensity was significantly increased within each time point in the vehicle-treated group compared with the estradiol-treated group ($p<0.001$).

Effects of estradiol on colocalization of IL-1β expression and astrocyte activation at spinal cord dorsal horn.

In order to analyze the colocalization of IL-1β with glial activation, Pearson's correlation coefficient was calculated to measure the degree of colocalization using an image analysis

software program, Volocity. Figure 3.19 displays representative immunostained images demonstrating positive co-labeling of GFAP with IL-1β, for astrocytes and cytokines (respectively) in ipsilateral spinal cord dorsal horn in OVX vehicle- and estradiol-treated rats in saline and carrageenan treatment groups, across different time conditions. CY3 and FITC, the secondary antibodies used to detect GFAP and IL-1β, vary in their degree of fluorescent colocalization from panel A to panel J, indicating different levels of co-activation of astrocytes and cytokines.

Figure 3.20 quantifies this information by showing the degree of colocalization between Cy3 and FITC (detecting GFAP and IL-1B, respectively) by using Pearson's correlation coefficient (r^2) in ipsilateral spinal cord dorsal horn of estradiol- and vehicle-treated OVX rats at 1, 5, and 24 hours after Cg or saline administration. Significant main effects of hormone and injection were observed [Hormone: $F(1,36)=101.31$, $p<0.001$; Injection: $F(1,36)=16.70$, $p<0.001$]. Specifically, the correlation coefficient for the vehicle-treated group ($r^2=0.54$) was significantly greater compared with the estradiol-treated group ($r^2=0.43$, $p<0.001$). The group that received Cg administration ($r^2=0.51$) also showed significantly increased colocalization between GFAP and IL-1B than the group that received saline ($r^2=0.46$, $p<0.001$).

Additionally, a significant interaction of hormone and injection was observed [$F(1,36)=16.70$, $p<0.001$]. Specifically, the vehicle-treated group that received saline administration ($r^2=0.50$) had significantly decreased mean fluorescence intensity compared with the vehicle-treated group that received Cg administration ($r^2=0.59$, $p<0.001$). Also, the estradiol-treated group that received saline ($r^2=0.43$) had significantly decreased intensity compared with the vehicle-treated group that received saline ($p<0.001$) and the estradiol-treated group that

received Cg (r^2=0.43) had significantly decreased intensity compared with the vehicle-treated group that received Cg ($p<0.001$).

Effects of estradiol on colocalization of IL-1β expression and microglia activation at spinal cord dorsal horn.

Figure 3.21 displays representative immunostained images demonstrating positive co-labeling of OX-6 with IL-1β, for microglia and cytokines (respectively) in ipsilateral spinal cord dorsal horn in OVX vehicle- and estradiol-treated rats in saline and carrageenan treatment groups, across different time conditions. CY3 and FITC, the secondary antibodies used to detect OX-6 and IL-1β, vary in their degree of fluorescent colocalization from panel A to panel J, indicating different levels of co-activation of microglia and cytokines.

Figure 3.22 quantifies this information by showing the degree of colocalization between Cy3 and FITC (detecting OX-6 and IL-1B, respectively) by using Pearson's correlation coefficient (r^2) in ipsilateral spinal cord dorsal horn of estradiol- and vehicle-treated OVX rats at 1, 5, and 24 hours after Cg or saline administration. Significant main effects of hormone and injection were observed [Hormone: $F(1,36)=456.92$, $p<0.001$; Injection: $F(1,36)=18.41$, $p<0.01$]. Specifically, the correlation coefficient for the vehicle-treated group (r^2=0.90) was significantly greater compared with the estradiol-treated group (r^2=0.70 $p<0.001$). The group that received Cg administration (r^2=0.82) also showed significantly increased colocalization than the group that received saline (r^2=0.78, $p<0.001$).

Additionally, a significant interaction of hormone and injection was observed [$F(1,36)=103.09$, $p<0.001$]. Specifically, the vehicle-treated group that received saline administration (r^2=0.83) had a significantly decreased correlation coefficient compared with the

vehicle-treated group that received Cg administration (r^2=0.97) and the estradiol-treated group that received saline (r^2=0.72) had significantly increased intensity compared with the estradiol-treated group that received Cg (r^2=0.67; p<0.001). Further, the estradiol-treated group that received saline had significantly decreased intensity compared with the vehicle-treated group that received saline (p<0.001) and the estradiol-treated group that received Cg had significantly decreased intensity compared with the vehicle-treated group that received Cg (p<0.001).

Correlations between ipsilateral behavioral responses (PWL) and IL-1β expression.

Significant negative correlations were observed between ipsilateral PWL and IL-1β expression in the spinal cord dorsal horn. PWL correlated negatively with IL-1β across all treatment groups at the lowest [*r*=-0.29, p<0.05] and highest heat intensities [*r*=-0.55, p<0.05]. Also, the medium [*r*=-0.67, p<0.05] and highest heat intensities [*r*=-0.72, p<0.001] showed negative correlations between PWL and IL-1β in the vehicle group, while the highest heat intensity alone mimicked this correlation in the estradiol-treated group [*r*=-0.41, p<0.05; Table 3.5]. Although linear regression analyses failed to show a statistically significant relationship between PWL and IL-1β, the linear relationships were negative for both vehicle- (β=-28.26) and estradiol-treated groups (β=-51.9; Figure 3.8).

Correlations between PWL and the colocalization of IL-1β expression and glial activation at the spinal cord dorsal horn in estradiol- and vehicle-treated OVX rats after Cg or saline administration.

A significant negative correlation was observed between ipsilateral PWL and the colocalization of GFAP-expressing astrocytes and IL-1β in the spinal cord dorsal horn, at the

medium heat intensity in the vehicle group. The colocalization of OX-6-expressing microglia and IL-1β correlated significantly with PWL across all heat intensities. Positive correlations were observed in the vehicle-treated group administered Cg at the low [r=0.75, p<0.05] and highest heat intensities [r=0.67, p<0.05]. At the highest heat intensity, positive correlations were also observed in the overall estradiol-treated group [r=0.45, p<0.05] and the estradiol-treated group administered saline [r=0.70, p<0.05]. Negative correlations were observed in the vehicle-treated groups at the medium [r=-0.43, p<0.05] and highest heat intensities [r=-0.46, p<0.05; Table 3.5]. Linear regression analyses results show that colocalization of glial activity did not significantly predict PWL (Figure 3.8).

Aim 3: Effects of estradiol and Cg administration on levels of intracellular markers in spinal cord tissue associated with inflammatory responses in glial cells.

Effects of estradiol on protein levels of GFAP in spinal cord tissue.

Figure 3.23 shows the western blot analysis of GFAP protein levels in the spinal cords of OVX vehicle- and estradiol-treated rats in saline and carrageenan treatment groups, across different time conditions. Although the main effect of time failed to reach statistical significance, [F(2,31)=3.28, p=0.051], protein levels were lower at 5 hours (M=105.8) and 24 hours (M=101.2) after injection when compared to 1 hour (M=151.0) after injection, across hormone treatment groups. No significant changes in protein level were observed across hormone or injection conditions.

Effects of estradiol on protein levels of OX-6 in spinal cord tissue.

Figure 3.24 shows the western blot analysis of OX-6 protein levels in the spinal cords of OVX vehicle- and estradiol-treated rats in saline and carrageenan treatment groups, across different time conditions. A significant main effect of time was observed [$F=(1,24)=93.10$, $p<0.01$], where protein levels were decreased at 5 hours (M=115.6) after injection when compared to 24 hours (M=170.0) after injection. Although a statistically significant interaction effect of hormone and time was not found [$F(1,24)=4.17$, $p=0.052$], protein levels were decreased in the estradiol-treated group (M=107.3) when compared to the vehicle group (M=123.9) at 5 hours after injection. No significant changes in protein level were found between saline- and Cg-injected groups.

Effects of estradiol on protein levels of pKa in spinal cord tissue.

Figure 3.25 shows the western blot analysis of pKA protein levels in the spinal cords of OVX vehicle- and estradiol-treated rats in saline and carrageenan treatment groups, across different time conditions. Although the main effect of time failed to reach statistical significance [$F(2,31)=2.92$, $p=0.069$], protein levels were higher at 24 hours (M=123.8) when compared with 1 hour (M=95.9) and 5 hours (M=111.7) after injection across hormone treatment groups.

Effects of estradiol on levels of pERK in spinal cord tissue.

Figure 3.26 shows the western blot analysis of pERK protein levels in the spinal cords of OVX vehicle- and estradiol-treated rats in saline and carrageenan treatment groups, across different time conditions. No significant changes in protein level were found across hormone, injection, and time conditions.

Effects of estradiol on levels of tERK in spinal cord tissue.

Figure 3.27 shows the western blot analysis of tERK protein levels in the spinal cords of OVX vehicle- and estradiol-treated rats in saline and carrageenan treatment groups, across different time conditions. No significant changes in protein level were found across hormone, injection, and time conditions.

Effects of estradiol on levels of stat 3 (79) in spinal cord tissue.

Figure 3.28 shows the western blot analysis of stat 3 (79) protein levels in the spinal cords of OVX vehicle- and estradiol-treated rats in saline and carrageenan treatment groups, across different time conditions. A significant main effect of delay was observed [$F(2,31)=5.30$, $p<0.05$), where protein levels were increased at 1 hour ($M=106.0$) post-injection when compared to 5 hours ($M=69.0$) and 24 hours ($M=62.0$) post-injection.

Effects of estradiol on levels of nNOS in spinal cord tissue.

Figure 3.29 shows the western blot analysis of nNOS protein levels in the spinal cords of OVX vehicle- and estradiol-treated rats in saline and carrageenan treatment groups, across different time conditions. No significant changes in protein level were found across hormone, injection, and time conditions.

Correlation of intracellular markers with nociceptive behavioral responses (PWL).

Significant positive correlations were observed between ipsilateral PWL and pKA protein levels across all treatment groups at the lowest [$r=0.35$, $p<0.05$] and highest heat intensities [$r=0.34$, $p<0.05$] across all treatment groups. In the vehicle group, significant positive

correlations were found at the medium heat [r=0.52, p<0.05] and high heat [r=0.63, p<0.05], and an additional positive correlation was found between the two variables in the vehicle-treated group administered saline injection at the medium heat [r=0.75, p<0.05]. Protein levels of pERK showed a significant negative correlation with PWL in the estradiol-treated group administered Cg injection [r=-0.75, p<0.05]. Also, Stat 3 (79) protein levels showed a significant negative correlation with PWL in the vehicle-treated group administered saline injection [r=-0.82, p<0.05]. Levels of tERK and nNOS proteins did not correlate significantly with PWL (Table 3.7).

Linear regression analyses showed that pKA protein levels explained a significant proportion of variance in PWL in the vehicle-treated group [R^2 = .30, F(1, 22) = 9.45, p < 0.01] in the form of a positive linear relationship (β=0.29). In the estradiol-treated group, levels of pERK protein explained a significant proportion of variance in PWL [R^2 = .40, F(1, 22) = 11.27, p < 0.01] through a negative linear relationship (β=-38.05). Although stat 3 (79) protein levels did not correlate significantly with levels of intracellular markers, the linear relationships are negative in both vehicle- (β=-0.211) and estradiol-treated groups (β=-0.08; Figure 3.30)

Correlation of GFAP-expressing astrocyte activation with levels of intracellular markers.

A significant negative correlation were observed between GFAP and pERK in the vehicle group [r =-0.53; p<0.05; Table 3.7]. Linear regression analyses showed that GFAP did not successfully predict levels of pKA, pERK, tERK, stat 3 (79), or nNOS intracellular markers with statistical significance. However, the linear relationship between stat 3 (79) protein levels and

GFAP was observed to be significantly different between the vehicle- (β=-0.32) and estradiol-treated (β=0.30) groups [$F(1, 39) = 9.45$, $p < 0.05$; Figure 3.31].

The correlation of OX6-expressing astrocyte activation with levels of intracellular markers.

A significant negative correlation was observed between OX-6 and pERK across all treatment groups (r =-0.53). Significant positive correlations were observed between OX-6 and tERK in the vehicle group (r =0.60) and across all treatments(r =0.49). nNOS also correlated positively with OX-6 in the estradiol-treated group administered saline (r =0.80). Linear regression analyses showed that while OX-6 did not successfully predict levels of pKA, pERK, tERK, stat 3 (79), or nNOS intracellular markers with statistical significance, protein levels of nNOS formed negative positive relationships when correlated with both vehicle- (β=1362.00) and estradiol-treated groups (β=546.20; Figure 3.32).

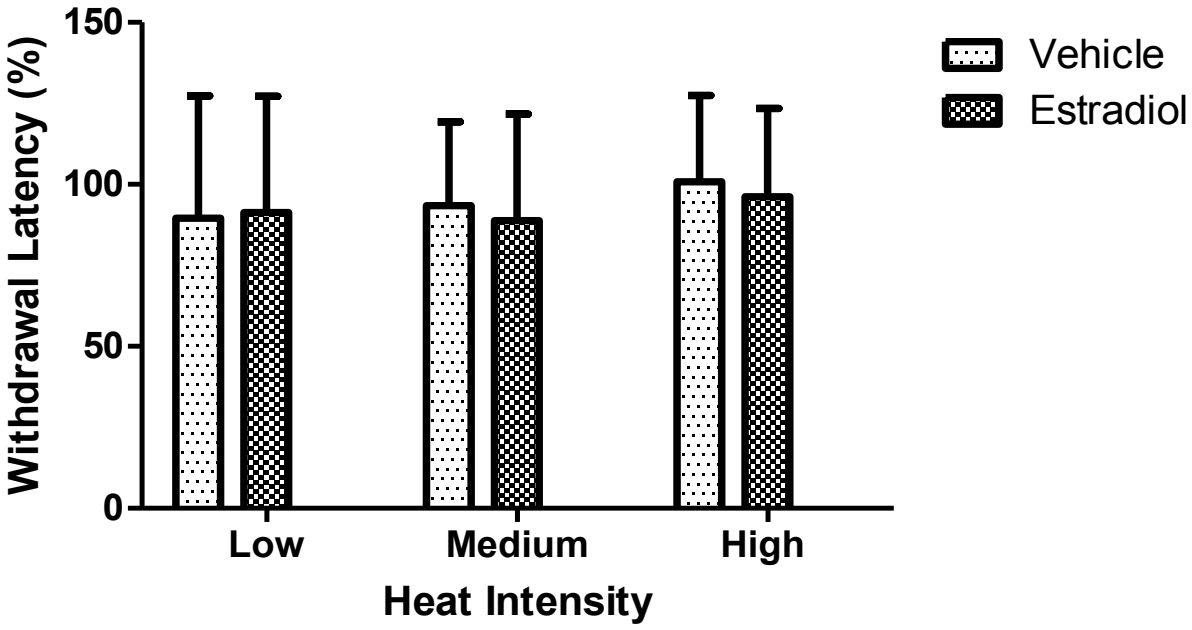

Figure 3.1. Baseline paw withdrawal latencies (PWL) of ovariectomized (OVX) vehicle- and estradiol-treated rats across low (4.5 mV), medium (4.9 mV), and high (5.3 mV) heat intensities. (*) Represents statistically significant difference. Error bars represent standard deviation. n=10 per group, $p<0.05$.

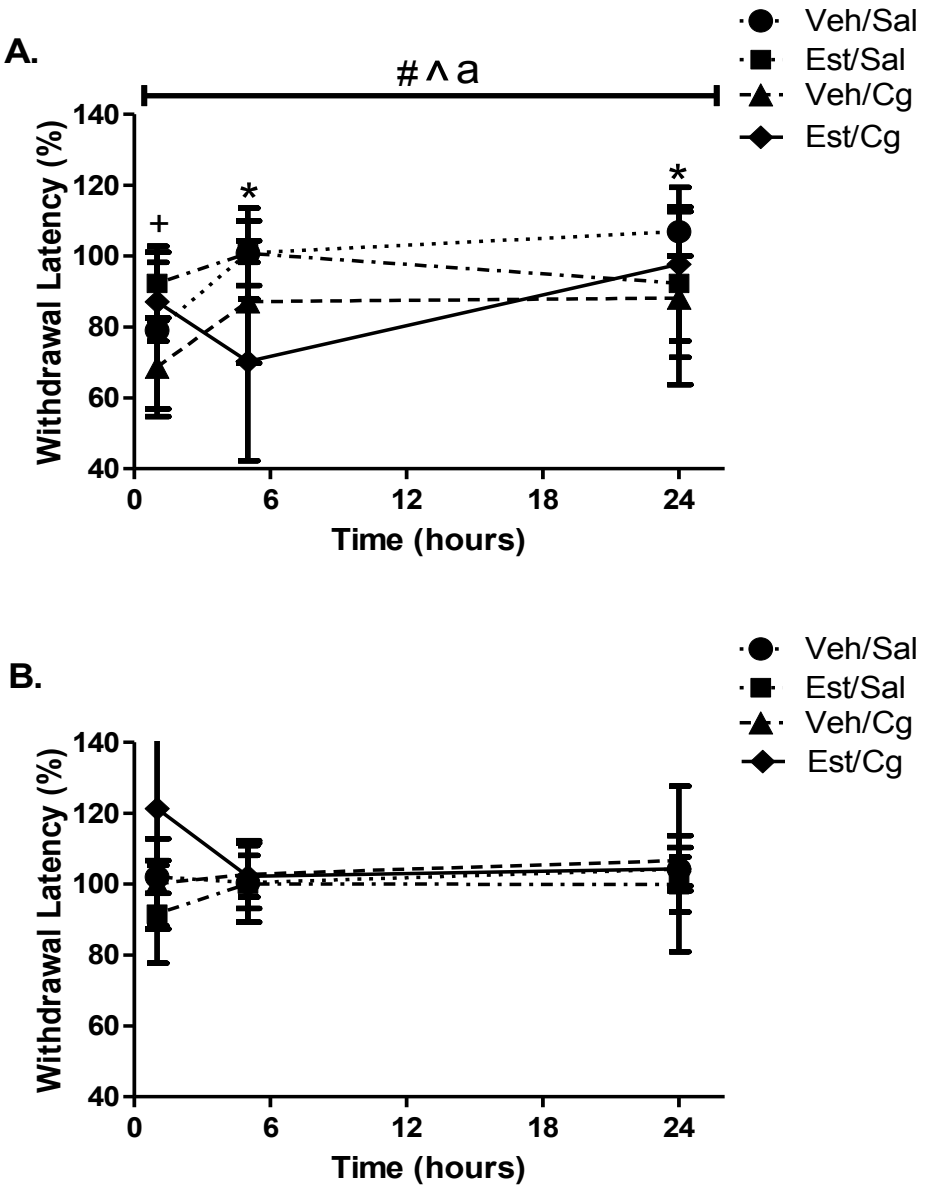

Figure 3.2. A (ipsilateral paw) and B (contralateral paw) show paw withdrawal latencies (PWL) of ovariectomized (OVX) vehicle- and estradiol-treated rats in saline and carrageenan treatment groups, across different time conditions at the low intensity heat channel (4.5 mV). Treatment groups include Veh/Sal (vehicle saline), Est/Sal (estrogen/saline), Veh/Cg (vehicle/carrageenan), and Est/Cg (estrogen/carrageenan). (*) Represents statistically significant difference between time condition; (+) represents statistically significant difference between treatment groups; (&) represents main effect of hormone; (#) represents main effect of time; (^) represents main effect of injection; (a) represents interaction effect of hormone*time; (b) represents interaction effect of time*injection; (c) represents interaction effect of hormone*injection; (d) represents interaction effect of hormone*time*injection. Error bars represent standard deviation. n =10 per group, $p<0.05$.

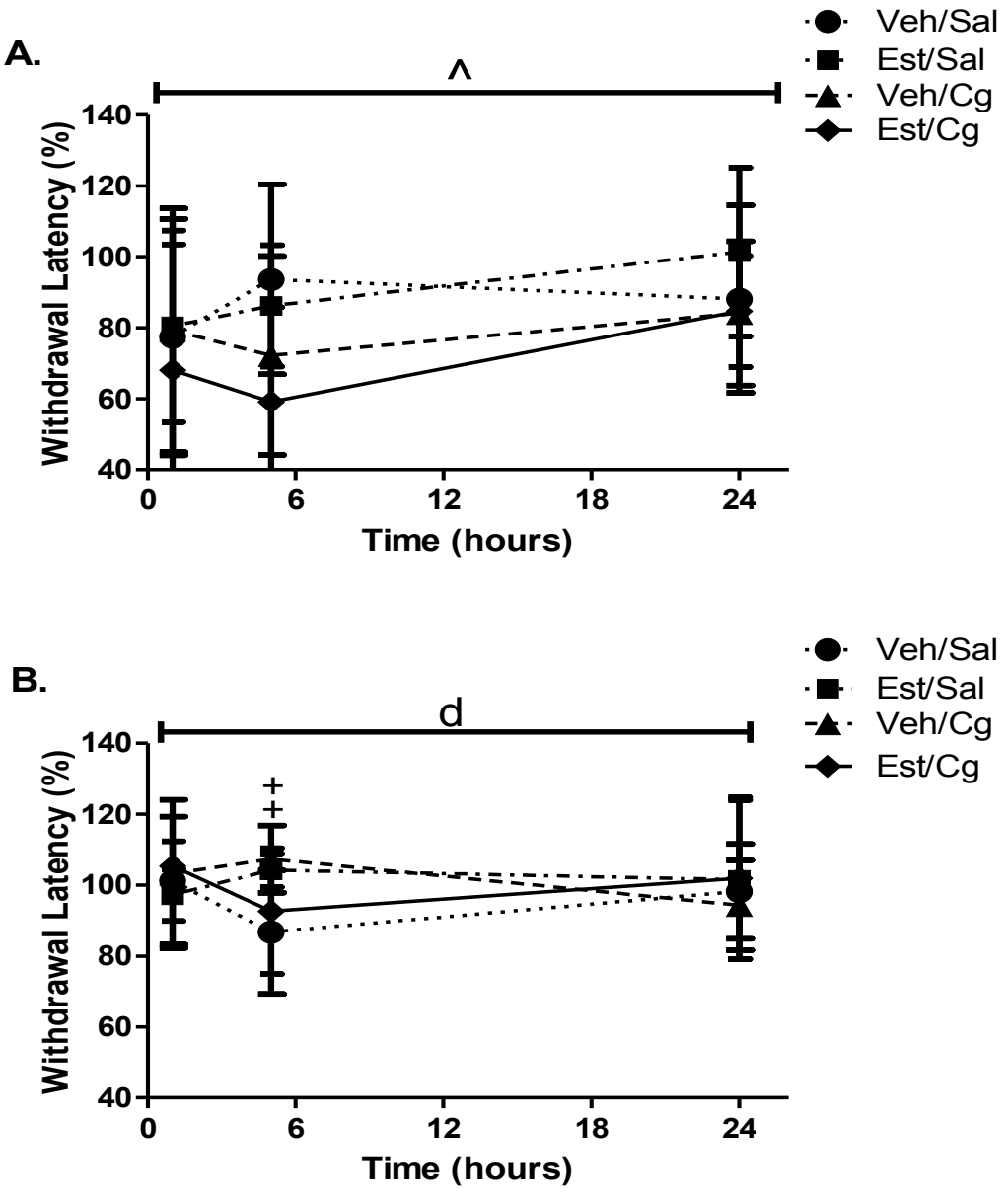

Figure 3.3. A(ipsilateral paw) and B (contralateral paw) show paw withdrawal latencies (PWL) of ovariectomized (OVX) vehicle- and estradiol-treated rats in saline and carrageenan treatment groups, across different time conditions at the medium intensity heat channel (4.9 mV). Treatment groups include Veh/Sal (vehicle saline), Est/Sal (estrogen/saline), Veh/Cg (vehicle/carrageenan), and Est/Cg (estrogen/carrageenan).(*) Represents statistically significant difference between time condition; (+) represents statistically significant difference between treatment groups; (&) represents main effect of hormone; (#) represents main effect of time; (^) represents main effect of injection; (a) represents interaction effect of hormone*time; (b) represents interaction effect of time*injection; (c) represents interaction effect of hormone*injection; (d) represents interaction effect of hormone*time*injection. Error bars represent standard deviation. n =10 per group, $p<0.05$.

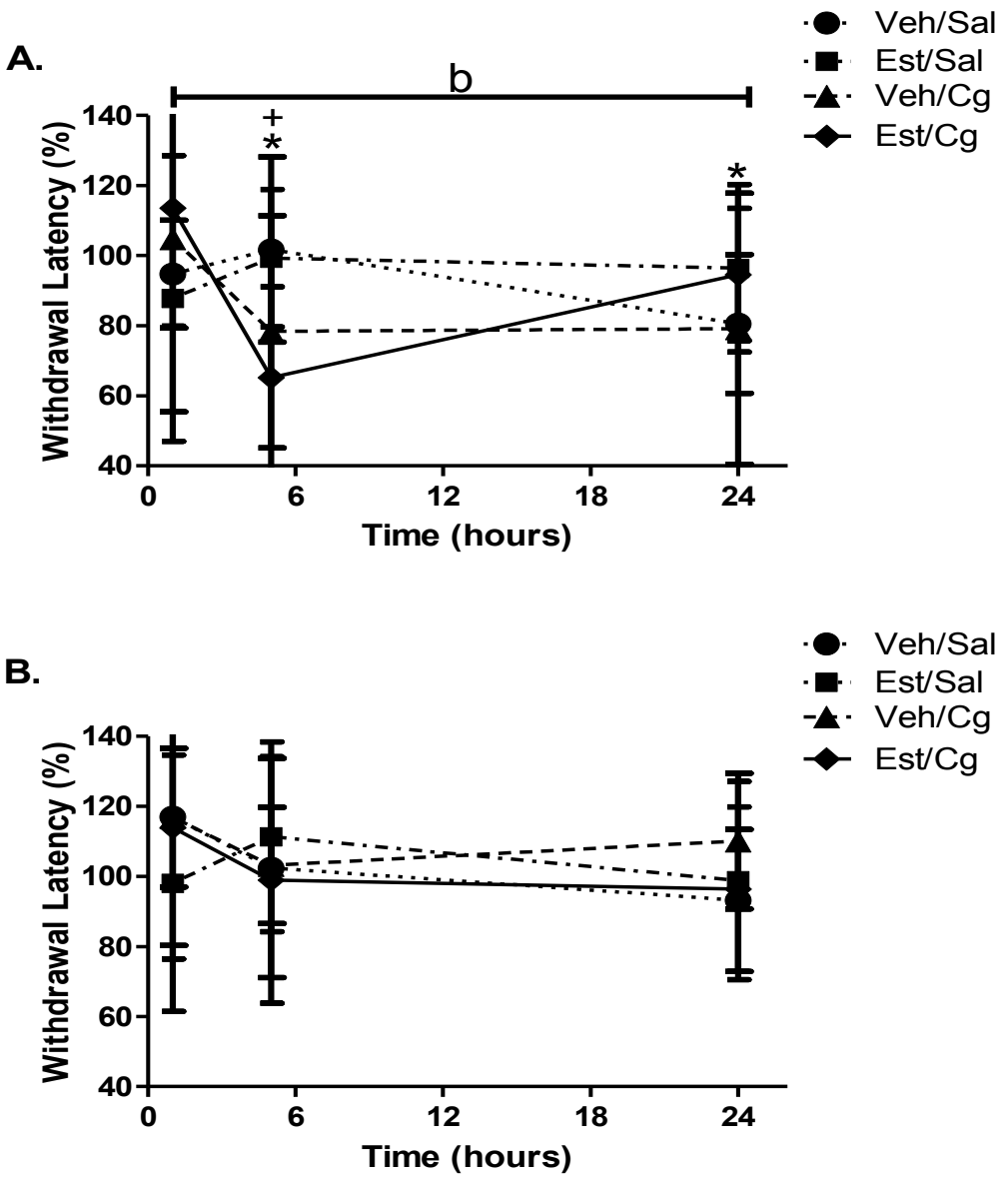

Figure 3.4. A(ipsilateral paw) and B (contralateral paw) show paw withdrawal latencies (PWL) of ovariectomized (OVX) vehicle- and estradiol-treated rats in saline and carrageenan treatment groups, across different time conditions at the high intensity heat channel (5.3 mV). Treatment groups include Veh/Sal (vehicle saline), Est/Sal (estrogen/saline), Veh/Cg (vehicle/carrageenan), and Est/Cg (estrogen/carrageenan).(*) Represents statistically significant difference between time condition; (+) represents statistically significant difference between treatment groups; (&) represents main effect of hormone; (#) represents main effect of time; (^) represents main effect of injection; (a) represents interaction effect of hormone*time; (b) represents interaction effect of time*injection; (c) represents interaction effect of hormone*injection; (d) represents interaction effect of hormone*time*injection. Error bars represent standard deviation. n =10 per group, $p<0.05$.

Table 3.1. Mean PWL expressed as percentage change from baseline across treatment group and time condition in ipsilateral and contralateral paws.

	Group	Low*	Medium*	High*	**Heat Intensity*
Ipsi PWL	**Veh Sal**	95.4±10.3	77.3± 33.3	94.8± 15.4	
1 HR	**Est Sal**	100.0±0.0	80.4± 27.0	87.8±40.8	
	Veh Cg	68.7±7.8	79.3± 34.3	104.8±49.4	
	Est Cg	100.0±0.0	68.1± 35.4	113.6±33.7	
5 HR	**Veh Sal**	95.4±9.8	93.6±26.8	101.7±26.4	
	Est Sal	104.4±5.9	86.1± 17.1	99.2±19.6	
	Veh Cg	106.0±8.1	72.2± 28.0	78.3± 33.1	
	Est Cg	70.2±7.8	59.2± 26.6	65.2±25.9	
24HR	**Veh Sal**	106.9±7.9	88.1±26.4	80.5±19.8	
	Est Sal	100.8±9.4	101.3± 23.8	96.4±23.9	
	Veh Cg	104.4±7.5	84.1±20.3	79.1± 38.6	
	Est Cg	97.7±5.6	84.6± 15.6	94.6±18.9	
Contra PWL	**Veh Sal**	102.1±4.6	101.3±18.0	116.9±36.7	
1 HR	**Est Sal**	91.5±13.8	97.2± 7.3	98.1± 36.6	
	Veh Cg	100.1±12.7	103.2± 20.9	116.8± 19.8	
	Est Cg	121.3±32.9	105.4± 7.0	113.9±37.5	
5 HR	**Veh Sal**	100.4± 11.2	86.8±17.4	102.4±31.3	
	Est Sal	100.1±10.8	104.2±4.8	111.3±27.1	
	Veh Cg	102.7±9.6	107.3± 9.4	103.2±16.6	
	Est Cg	102.2± 5.9	92.7±17.8	99.0±35.1	
24 HR	**Veh Sal**	104.2± 6.1	98.2±13.4	93.1±20.3	
	Est Sal	99.9± 7.8	101.3± 22.4	98.8±28.3	
	Veh Cg	106.6±7.0	94.3±12.7	109.0±19.4	
	Est Cg	104.3± 23.3	102.0± 22.8	96.4±23.5	

Legend. Treatment groups are designated as follows: Veh Sal= vehicle saline; Est Sal= estradiol saline; Veh Cg= vehicle carrageenan; Est Cg= estradiol carrageenan. Data represents mean PWL expressed as percentage change from baseline ± standard deviation from the mean across treatment group and time condition in ipsilateral and contralateral paws, taken at low (4.5 mV), medium (4.9 mV), and high (5.3 mV) heat intensities. *n*=10 per group.

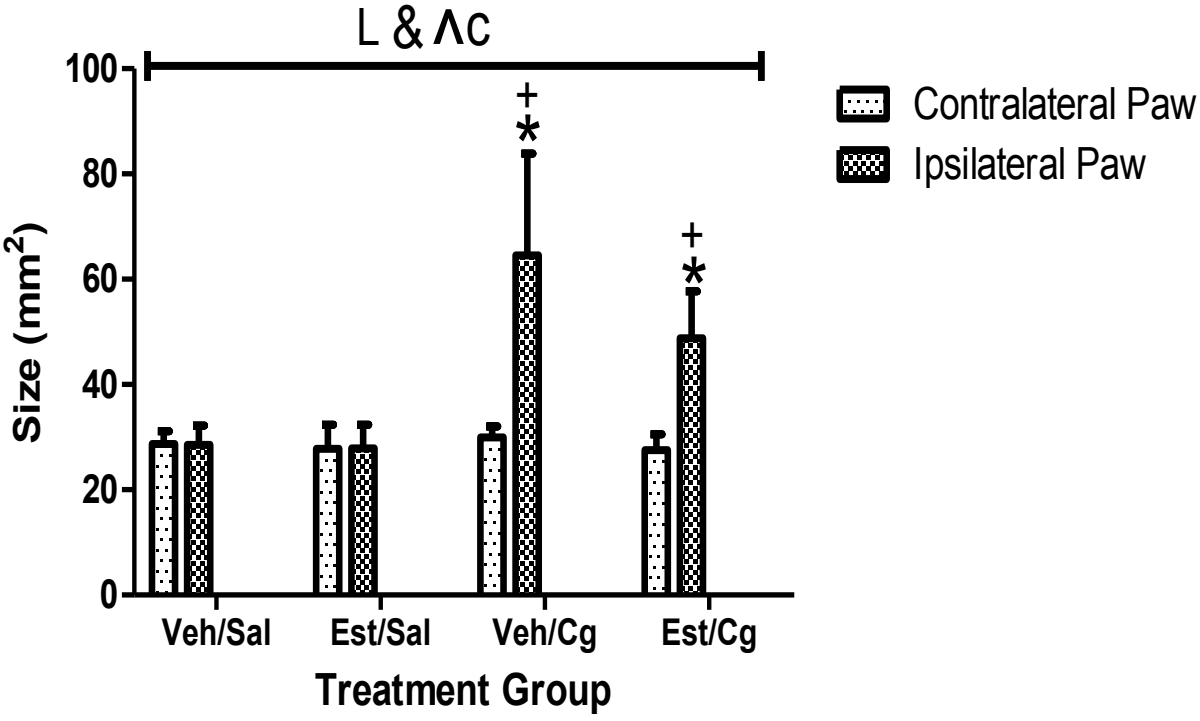

Figure 3.5. Paw size of ovariectomized (OVX) vehicle- and estradiol-treated rats in saline and carrageenan treatment groups. Treatment groups include Veh/Sal (vehicle saline), Est/Sal (estrogen/saline), Veh/Cg (vehicle/carrageenan), and Est/Cg (estrogen/carrageenan). (*) Represents statistically significant difference from the contralateral paw; (+) represents statistically significant difference between treatment groups; (&) represents main effect of hormone; (^) represents main effect of injection; (L) represents main effect of location of injection; (c) represents interaction effect of hormone*injection. Error bars represent standard deviation. n =10 per group, $p<0.05$.

Table 3.2. Mean paw size across treatment group and time condition in ipsilateral and contralateral paws.

	Group	1HR	5HR	24HR
	Overall	42.9±14.7	48.8±27.3	35.6±9.5
	Estradiol	40.7±10.3	41.6±18.5	32.8±9.7
	Vehicle	45.2±19.7	56.0±35.4	38.4±9.7
Ipsilateral	**Veh Sal**	30.0±0.0	25.5±6.4	30.0±0.0
Paw Size	**Est Sal**	31.9±2.7	26.3±2.5	25.5±6.4
	Veh Cg	60.4±15.4	86.5±2.1	46.8±0.0
	Est Cg	49.5±1.1	57.0±8.5	40.0±5.7
	Overall	30.4±1.2	26.8±3.2	28.5±3.6
	Estradiol	31.3±0.3	25.3±0.9	26.4±4.7
	Vehicle	29.5±1.0	28.4±4.0	30.0±0.0
Contralateral	**Veh Sal**	30.0±0.0	26.0±2.8	30.0±0.0
Paw Size	**Est Sal**	31.5±0.0	25.3±1.1	26.4±7.8
	Veh Cg	29.0±1.4	30.9±4.0	30.0±0.0
	Est Cg	31.0±0.0	25.3±1.1	26.3±2.5

Legend. Treatment groups are designated as follows: Veh Sal= vehicle saline; Est Sal= estradiol saline; Veh Cg= vehicle carrageenan; Est Cg= estradiol carrageenan. Data represents mean paw size ± standard deviation from the mean across treatment group and time conditions in ipsilateral and contralateral. *n*=10 per group.

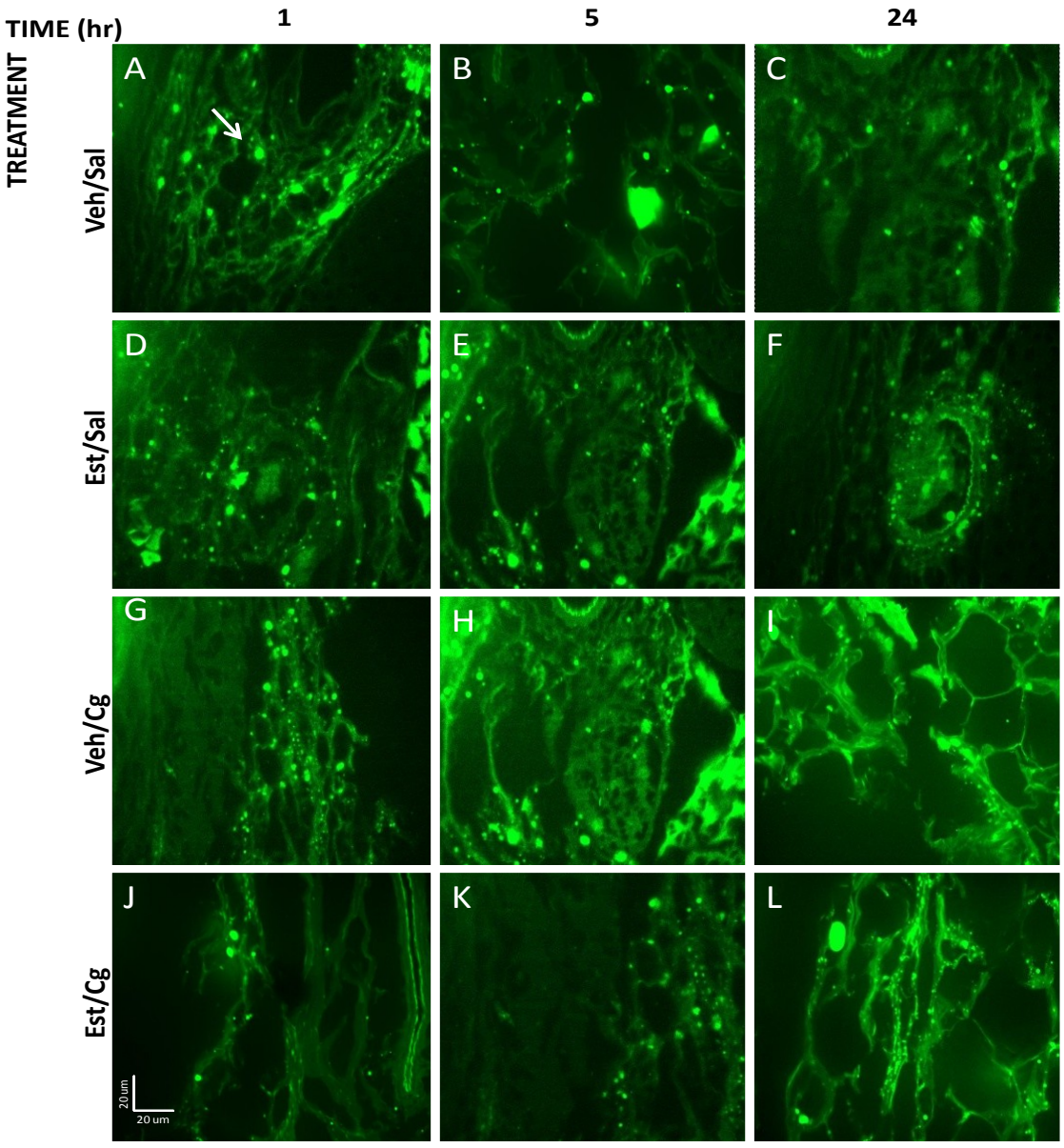

Figure 3.6. Representative immunostained images demonstrating positive labeling of CD68 for macrophages in ipsilateral, plantar-region hindpaw tissue in ovariectomized (OVX) vehicle- and estradiol-treated rats in saline and carrageenan treatment groups, across different time conditions. The scale bar in J is 20 um and applies to all panels.

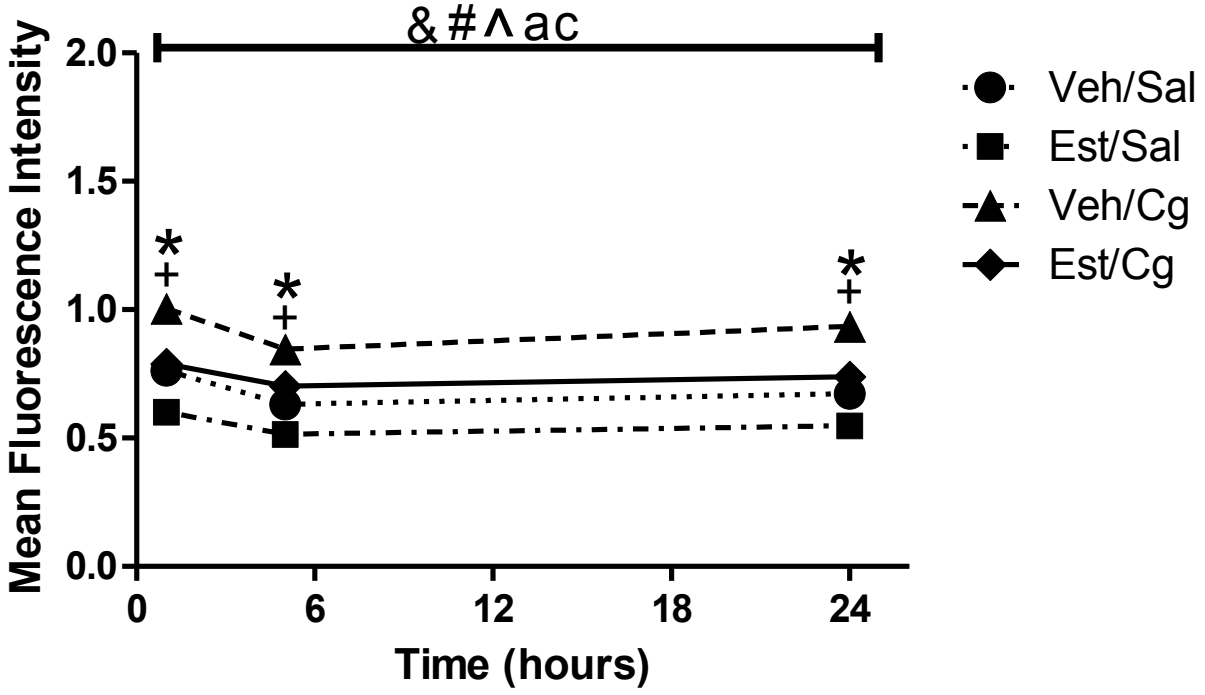

Figure 3.7. Mean fluorescence intensity of CD68-expressing macrophages in ipsilateral, plantar-region hindpaw tissue of ovariectomized (OVX) vehicle- and estradiol-treated rats in saline and carrageenan treatment groups, across different time conditions.
(*) Represents statistically significant difference between time condition; (+) represents statistically significant difference between treatment groups; (&) represents main effect of hormone; (#) represents main effect of time; (^) represents main effect of injection; (a) represents interaction effect of hormone*time; (b) represents interaction effect of time*injection; (c) represents interaction effect of hormone*injection; (d) represents interaction effect of hormone*time*injection. Error bars represent standard deviation. n= 4 per group, $p<0.05$.

Table 3.3. Summary of correlations between ipsilateral paw size and CD68 expression of macrophages at the injury site.

	Group	CD68
	Overall	**0.40***
	Estradiol	**0.45***
	Vehicle	0.38
Ipsilateral	**Veh Sal**	0.08
Paw Size	**Est Sal**	0.34
	Veh Cg	-0.16
	Est Cg	-0.28

Legend. Treatment groups are designated as follows: Veh Sal= vehicle saline; Est Sal= estradiol saline; Veh Cg= vehicle carrageenan; Est Cg= estradiol carrageenan. Data represents correlation coefficients for specified analysis. Significant correlation coefficients are designated by (*) for $p<.05$ and (**) for $p<0.001$. *n*=4 per group.

Table 3.4. Summary of correlations between macrophage activation at the injury site and glial activation at the spinal cord dorsal horn.

Group	GFAP	OX-6
Overall	**0.58****	**0.46****
Estradiol	**-0.91****	**-0.62***
Vehicle	**0.78****	**0.51***
Veh Sal	-0.04	0.08
Est Sal	**-0.63***	0.29
Veh Cg	-0.06	0.34
Est Cg	-0.21	**0.63***

Legend. Treatment groups are designated as follows: Veh Sal = vehicle saline; Est Sal = estradiol saline; Veh Cg = vehicle carrageenan; Est Cg = estradiol carrageenan. Data represents correlation coefficients for specified analysis. Significant correlation coefficients are designated by (*) for $p<.05$ and (**) for $p<.0001$. *n*=4 per group.

Table 3.5. Summary of correlations between ipsilateral PWL and protein levels analyzed via immunofluorescence.

	Group	GFAP	OX-6	GFAP/IL-1B	OX-6/IL-1B	IL-1B	CD68
	Overall	-0.08	-0.11	-0.12	-0.05	**-0.29***	**-0.33***
	Estradiol	0.40	0.34	0.30	0.28	-0.36	-0.38
LOW	**Vehicle**	-0.19	-0.29	-0.19	-0.01	-0.24	-0.30
HEAT	**Veh Sal**	0.05	-0.35	-0.05	0.12	-0.26	0.05
	Est Sal	-0.15	0.35	0.31	0.19	0.35	0.34
	Veh Cg	0.00	-0.15	-0.05	**0.75***	-0.06	-0.34
	Est Cg	0.31	**-0.59***	0.11	-0.08	0.04	-0.04
	Overall	-0.07	0.01	-0.07	0.01	-0.28	**-0.31***
	Estradiol	0.28	0.07	0.22	0.06	-0.21	-0.26
MEDIUM	**Vehicle**	**-0.67***	-0.30	**-0.53***	**-0.43***	**-0.67***	**-0.68***
HEAT	**Veh Sal**	-0.27	0.03	0.16	0.56	-0.45	-0.55
	Est Sal	-0.17	-0.47	-0.35	-0.25	0.00	0.05
	Veh Cg	-0.26	0.04	-0.21	0.51	0.12	-0.13
	Est Cg	0.23	**-0.68***	-0.19	-0.40	0.34	0.27
	Overall	**-0.35***	0.01	-0.24	-0.20	**-0.55****	**-0.57****
	Estradiol	0.35	**0.43***	0.16	**0.45***	**-0.41***	**-0.43***
HIGH	**Vehicle**	**-0.76****	-0.05	-0.38	**-0.46***	**-0.72****	**-0.73****
HEAT	**Veh Sal**	-0.44	**0.64***	0.54	**0.68***	-0.46	-0.27
	Est Sal	-0.20	0.46	0.40	**0.70***	-0.39	-0.29
	Veh Cg	-0.35	0.21	-0.11	-0.02	-0.13	-0.47
	Est Cg	0.42	-0.45	-0.22	-0.29	-0.12	-0.11

Legend. Treatment groups are designated as follows: Veh Sal = vehicle saline; Est Sal = estradiol saline; Veh Cg = vehicle carrageenan; Est Cg = estradiol carrageenan. Data represents correlation coefficients for specified analysis. Significant correlation coefficients are designated by (*) for $p<.05$ and (**) for $p<.0001$. n=4 per group.

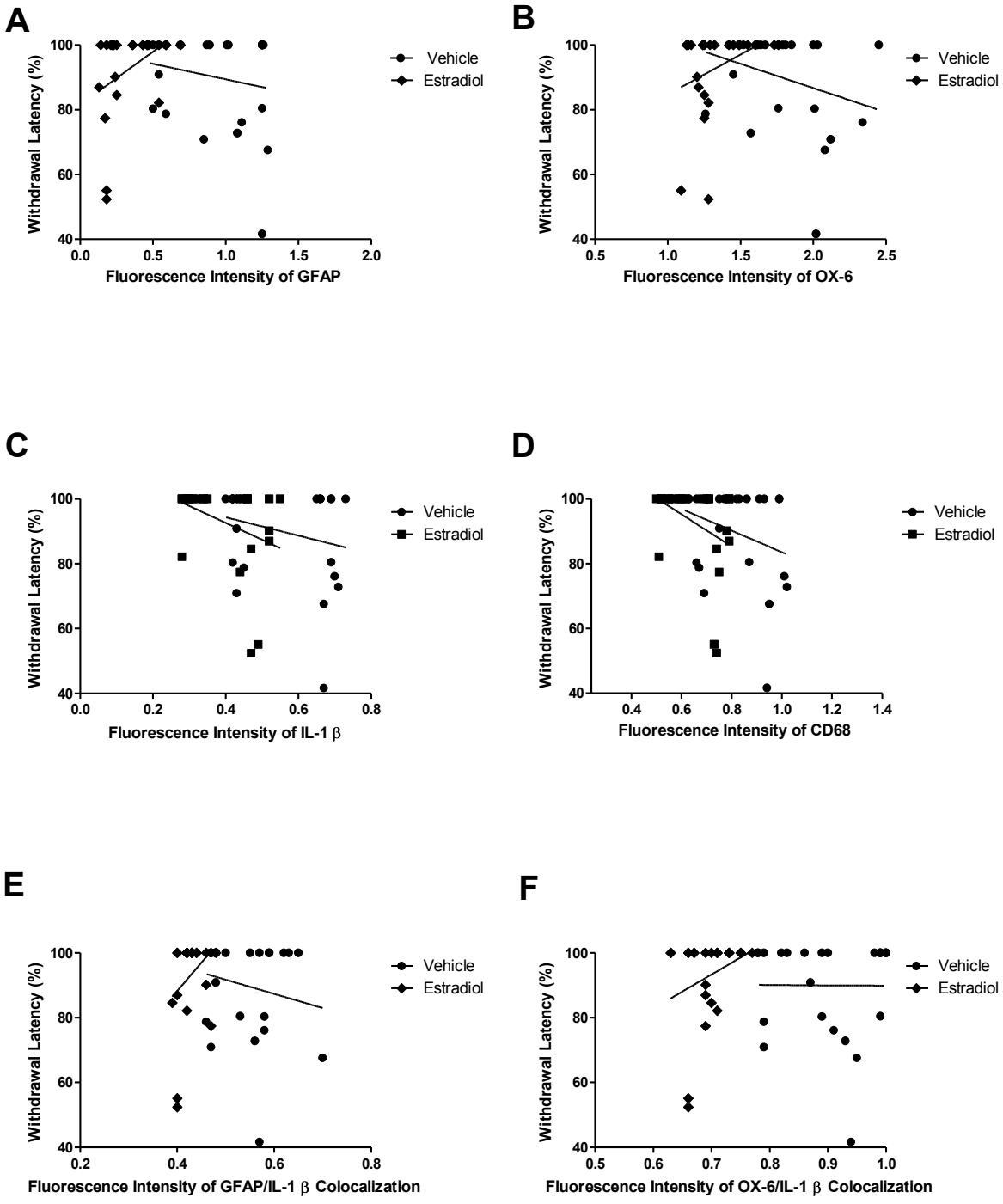

Figure 3.8. **Linear Regression analysis of paw withdrawal latency and A) GFAP; B) OX-6; C) IL-1β; D) CD68; E) GFAP/IL-1β; F)OX-6/ IL-1β**, $p<0.05$.

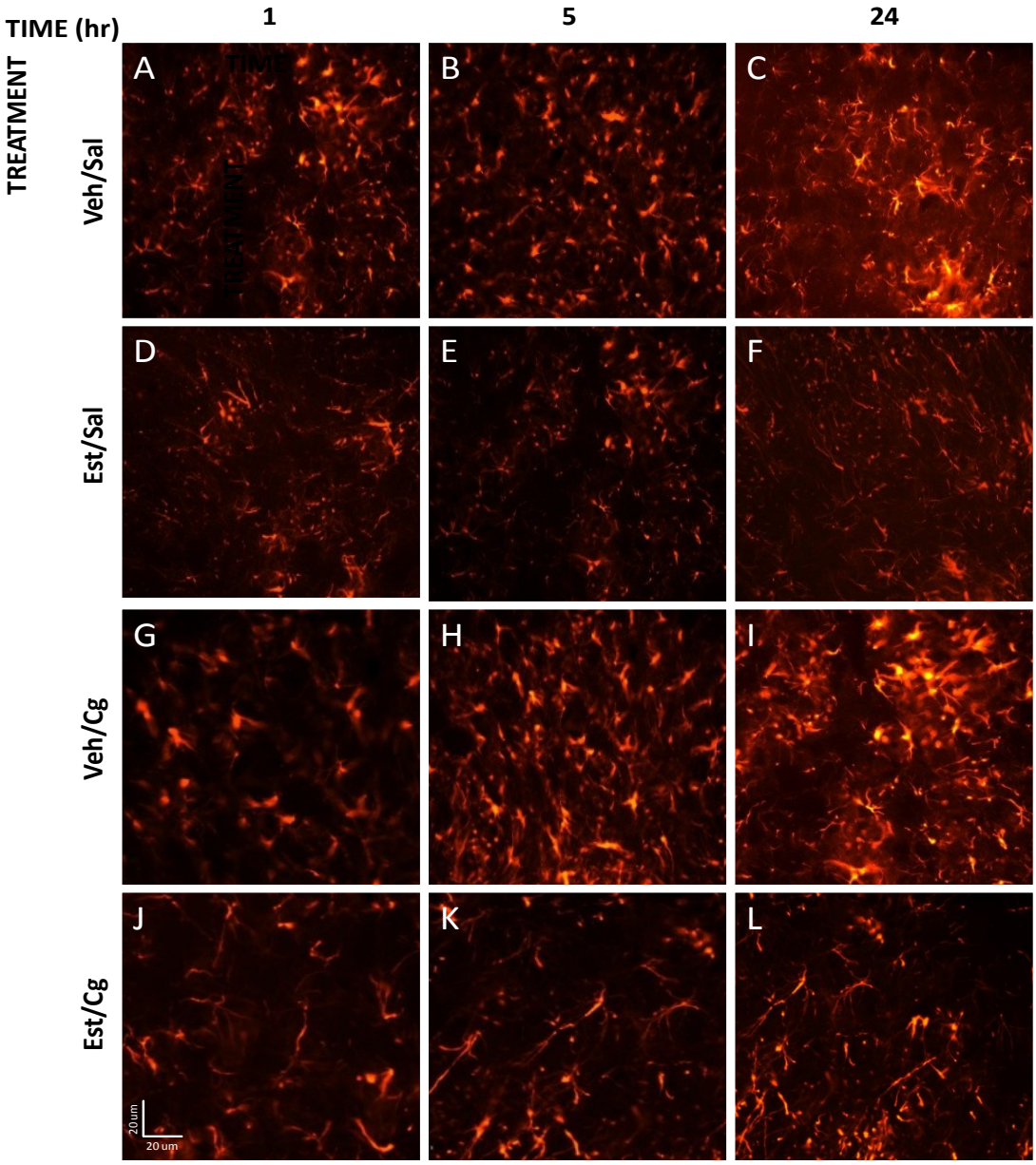

Figure 3.9. Representative immunostained images demonstrating positive labeling of GFAP for astrocytes in ipsilateral dorsal horn of ovariectomized (OVX) vehicle- and estradiol-treated rats in saline and carrageenan treatment groups, across different time conditions. The scale bar in J is 20 um and applies to all panels.

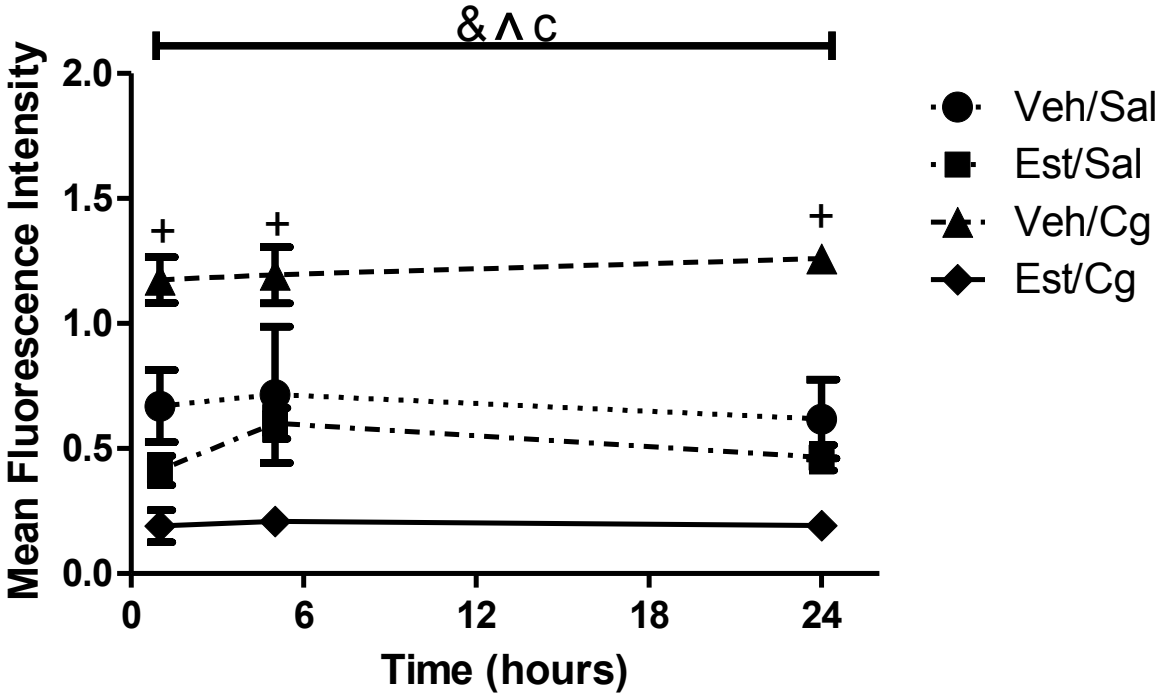

Figure 3.10. Mean fluorescence intensity of GFAP-expressing astrocytes in spinal cord dorsal horn of ovariectomized (OVX) vehicle- and estradiol-treated rats in saline and carrageenan treatment groups, across different time conditions.
(*) Represents statistically significant difference between time condition; (+) represents statistically significant difference between treatment groups; (&) represents main effect of hormone; (#) represents main effect of time; (^) represents main effect of injection; (a) represents interaction effect of hormone*time; (b) represents interaction effect of time*injection; (c) represents interaction effect of hormone*injection; (d) represents interaction effect of hormone*time*injection. Error bars represent standard deviation. n= 4 per group, $p<0.05$.

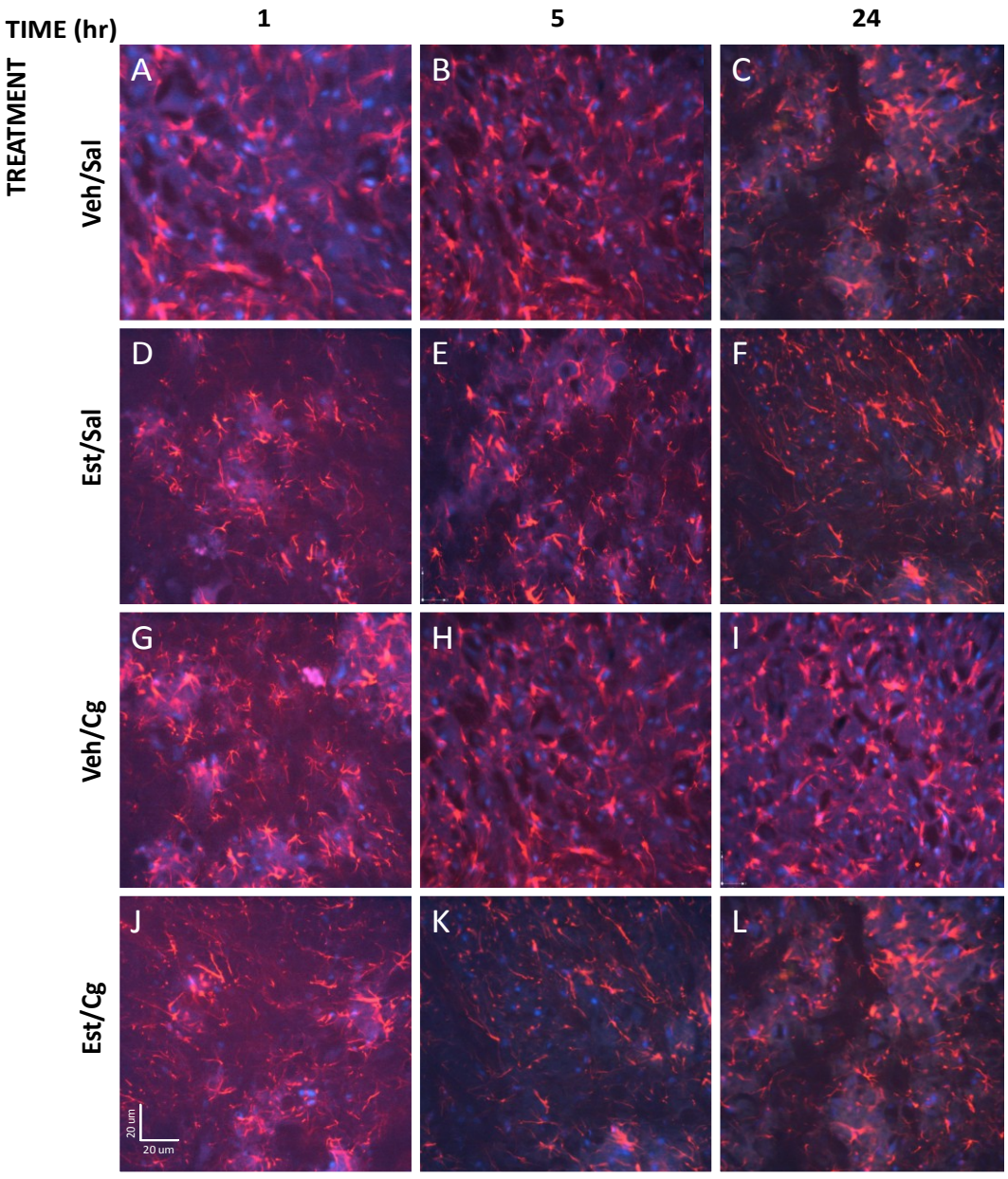

Figure 3.11. Representative immunostained images demonstrating positive labeling of GFAP for astrocytes with DAPI-stained nuclei in ipsilateral dorsal horn of ovariectomized (OVX) vehicle- and estradiol-treated rats in saline and carrageenan treatment groups, across different time conditions. The scale bar in J is 20 um and applies to all panels.

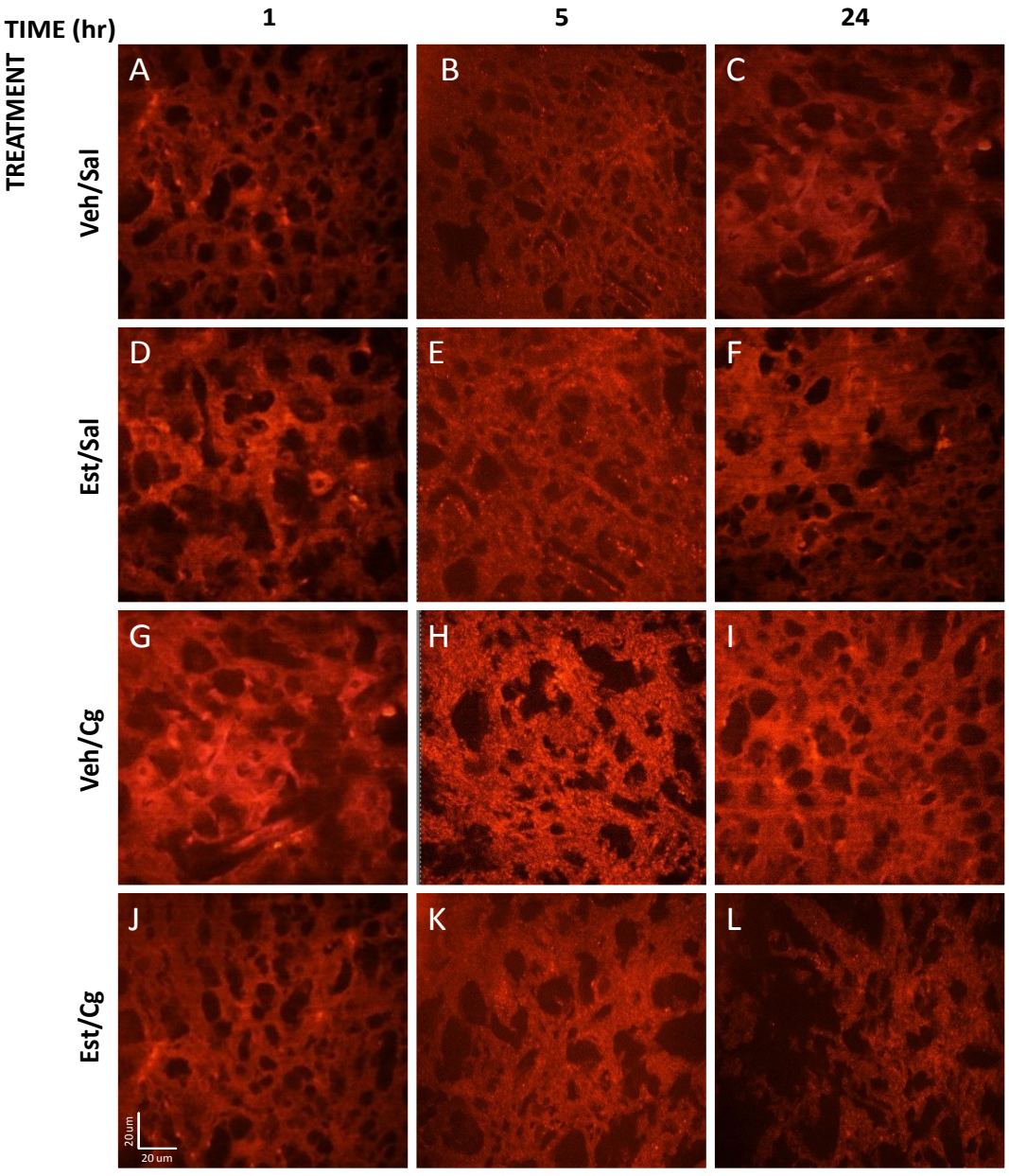

Figure 3.12. Representative immunostained images demonstrating positive labeling of OX-6 for microglia in ipsilateral dorsal horn of ovariectomized (OVX) vehicle- and estradiol-treated rats in saline and carrageenan treatment groups, across different time conditions. The scale bar in J is 50 um and applies to all panels.

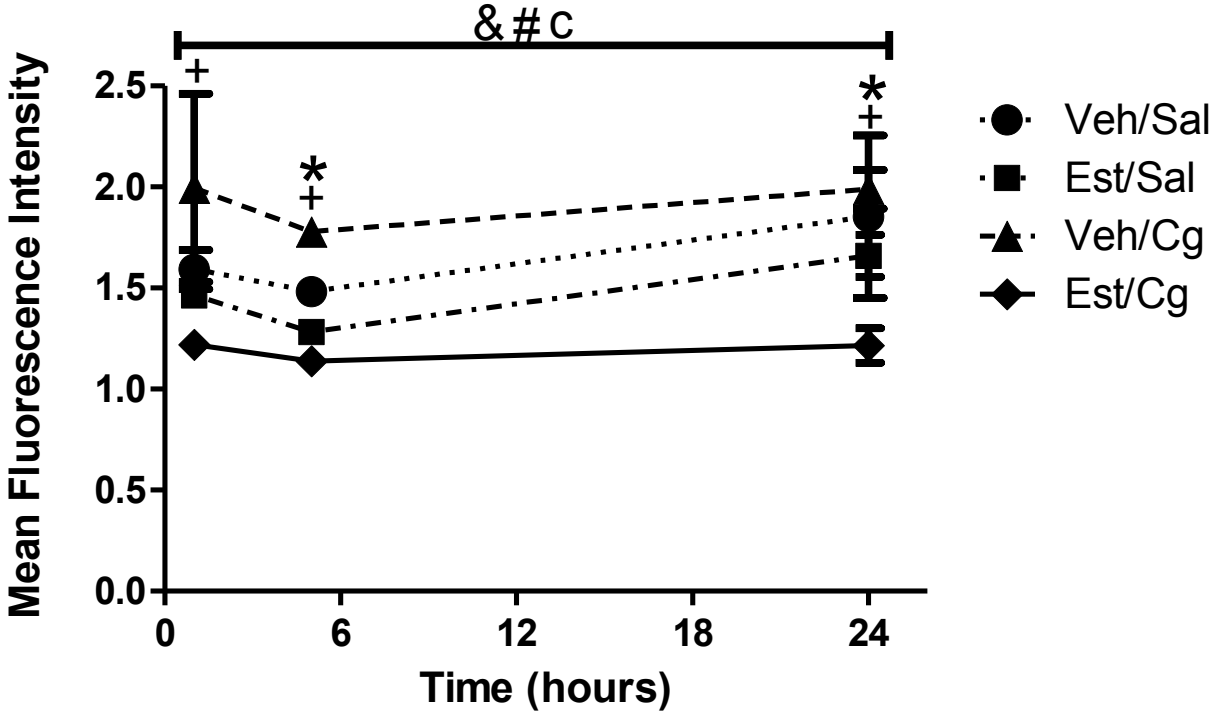

Figure 3.13. Mean fluorescence intensity of OX-6-expressing microglia in spinal cord dorsal horn of ovariectomized (OVX) vehicle- and estradiol-treated rats in saline and carrageenan treatment groups, across different time conditions.
(*) Represents statistically significant difference between time condition; (+) represents statistically significant difference between treatment groups; (&) represents main effect of hormone; (#) represents main effect of time; (^) represents main effect of injection; (a) represents interaction effect of hormone*time; (b) represents interaction effect of time*injection; (c) represents interaction effect of hormone*injection; (d) represents interaction effect of hormone*time*injection. Error bars represent standard deviation. *n*=4 per group, $p<0.05$.

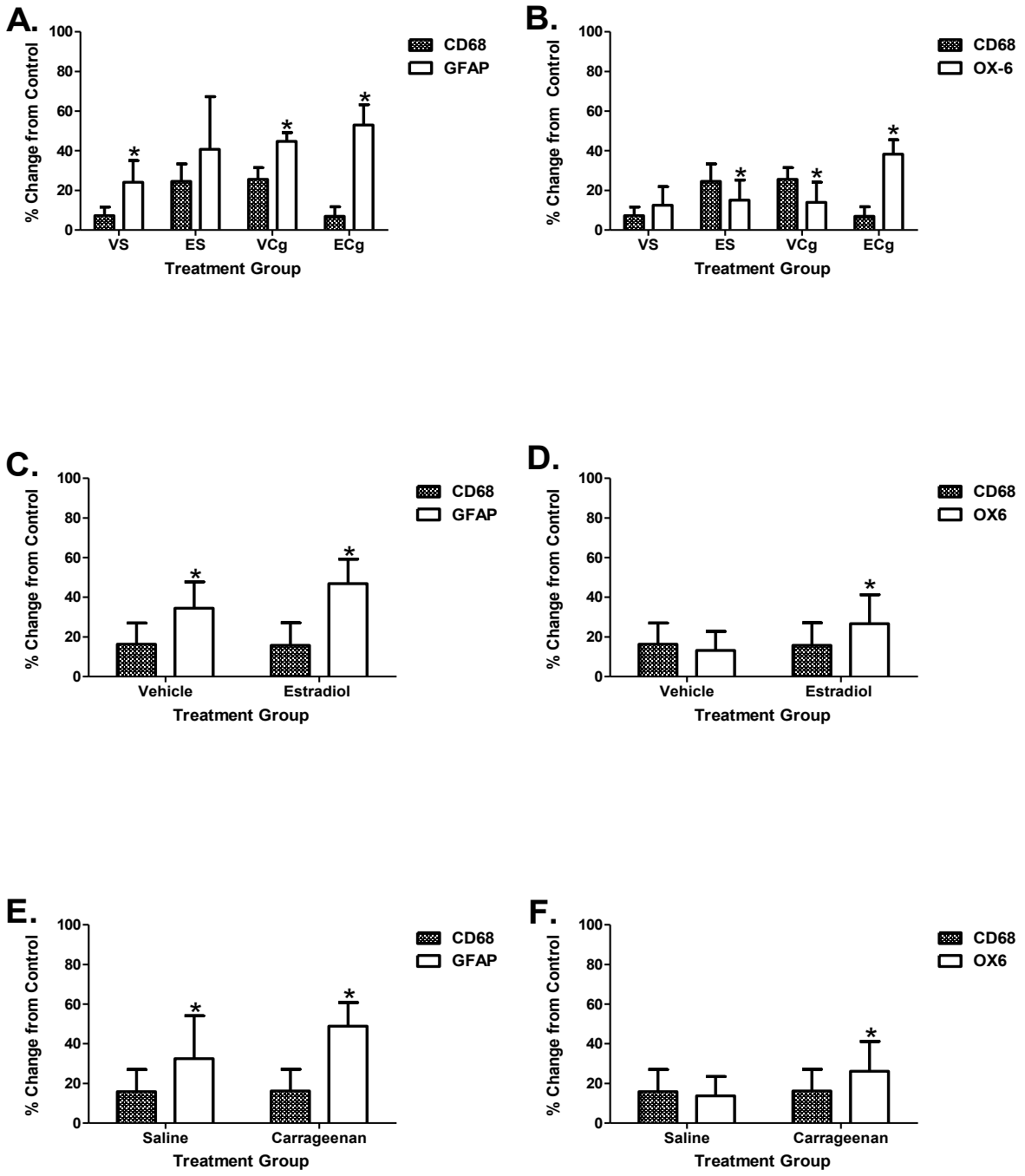

Figure 3.14. Comparison of mean fluorescence intensity (activation) expressed as percent change from control (vehicle/saline) between CD68-expressing macrophages at the injury site and GFAP-expressing astrocytes (A, C, and E) and OX-6 expressing microglia (D, E, and F) at the spinal cord dorsal horn across treatment groups. (*) Represents statistically significant difference of percent change between CD68 and GFAP/OX-6. Error bars represent standard deviation. n=4 per group, $p<.05$.

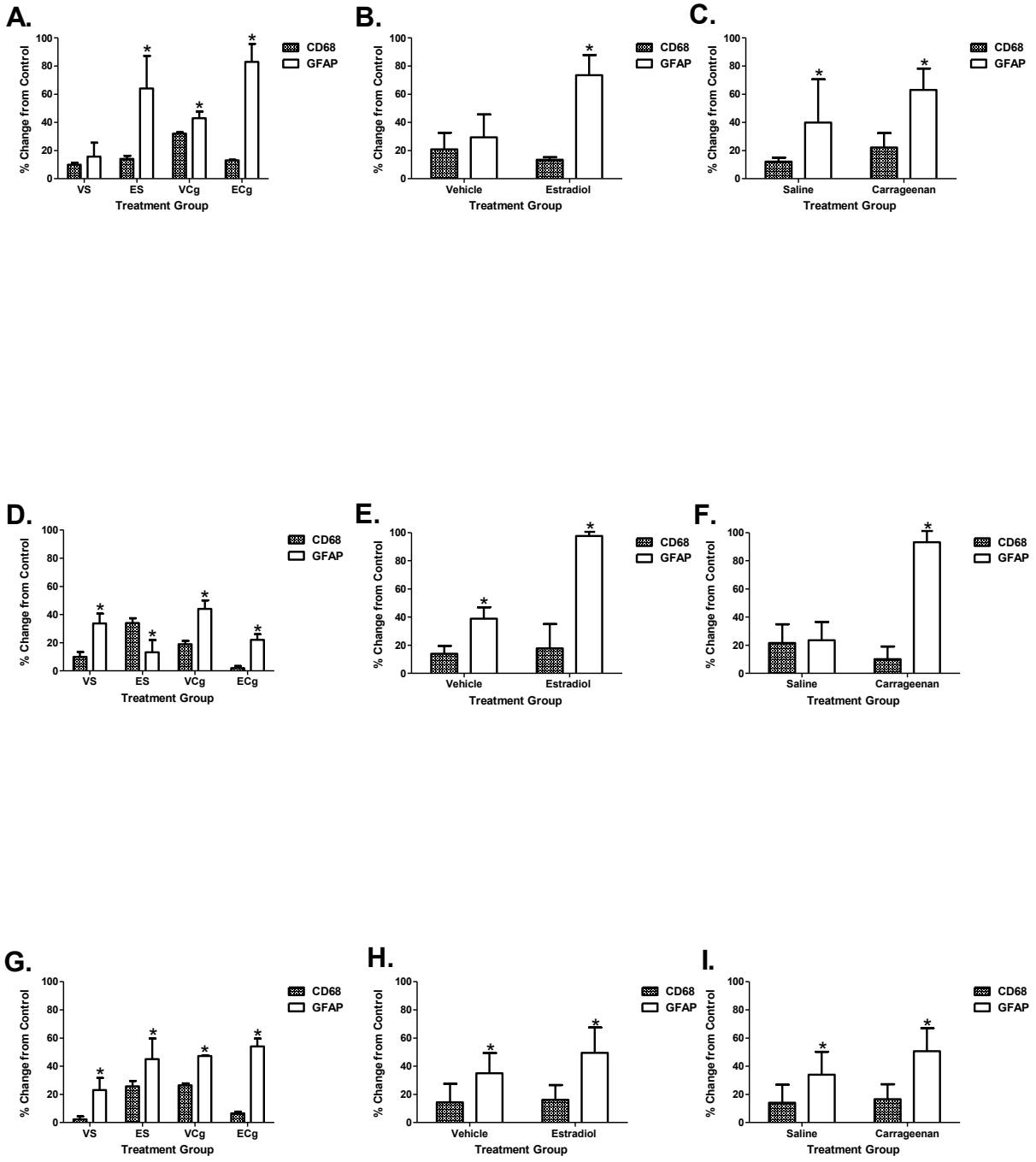

Figure 3.15. Comparison of mean fluorescence intensity (activation) expressed as percent change from control (vehicle/saline) between CD68-expressing macrophages at the injury site and GFAP-expressing astrocytes at the spinal cord dorsal horn across treatment groups at 1 hour (A, B, and C), 5 hours (D, E, and F) and 24 hours (G, H, and I) after injection. (*) Represents statistically significant difference of percent change between CD68 and GFAP. Error bars represent standard deviation. *n*=4 per group, p<.05.

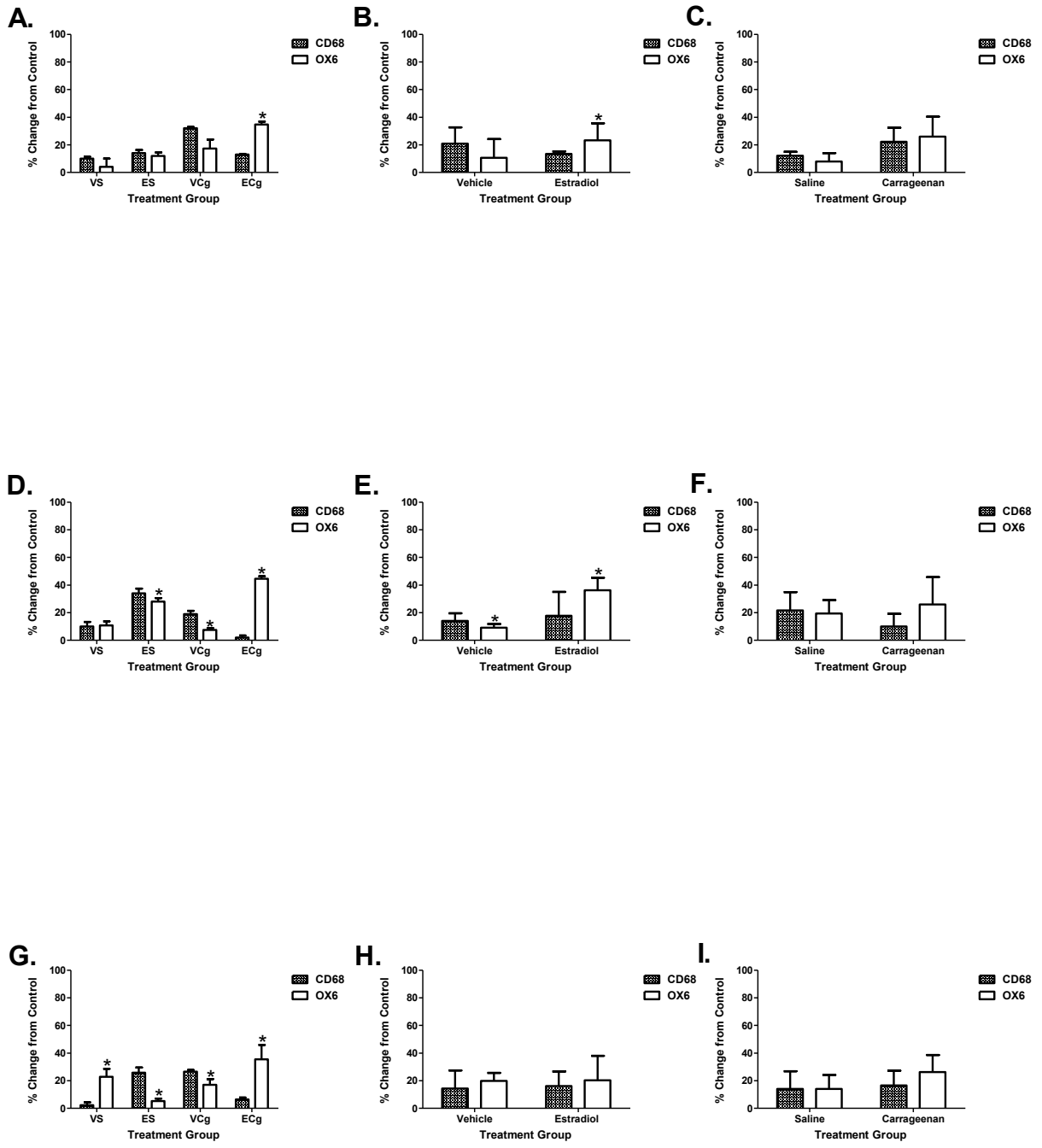

Figure 3.16. Comparison of mean fluorescence intensity (activation) expressed as percent change from control (vehicle/saline) between CD68-expressing macrophages at the injury site and OX-6-expressing microglia at the spinal cord dorsal horn across treatment groups at 1 hour (A, B, and C), 5 hours (D, E, and F) and 24 hours (G, H, and I) after injection. (*) Represents statistically significant difference of percent change between CD68 and GFAP. Error bars represent standard deviation. *n*=4 per group, p<.05.

Table. 3.6. Percent change from control (Vehicle Saline) of mean fluorescence intensity (activation) between CD68-expressing macrophages at the injury site and GFAP-expressing astrocytes and OX-6 expressing microglia at the spinal cord across treatment groups.

Group	CD68	GFAP	OX-6
Vehicle	16.4±10.6	34.5±13.3	13.2±9.6
Estradiol	15.8±11.4	46.9±12.3	26.7±14.7
Saline	15.9±11.1	32.5±21.6	13.8±9.7
Carrageenan	16.3±10.9	48.9±12.0	26.1±15.1
Veh Sal	7.3±4.3	24.2±10.9	12.5±9.4
Est Sal	24.6±8.9	40.8±26.5	15.1±10.2
Veh Cg	25.6±5.9	44.8±4.4	13.9±10.1
Est Cg	7.0±4.8	53.0±10.2	38.3±7.3

Legend. Treatment groups are designated as follows: Veh Sal = vehicle saline; Est Sal = estradiol saline; Veh Cg = vehicle carrageenan; Est Cg = estradiol carrageenan. Data represents percent change from control (Vehicle Saline) of mean fluorescence intensity (activation) ± standard deviation from the mean between CD68-expressing macrophages at the injury site and GFAP-expressing astrocytes and OX-6 expressing microglia at the spinal cord across treatment groups. n=4 per group.

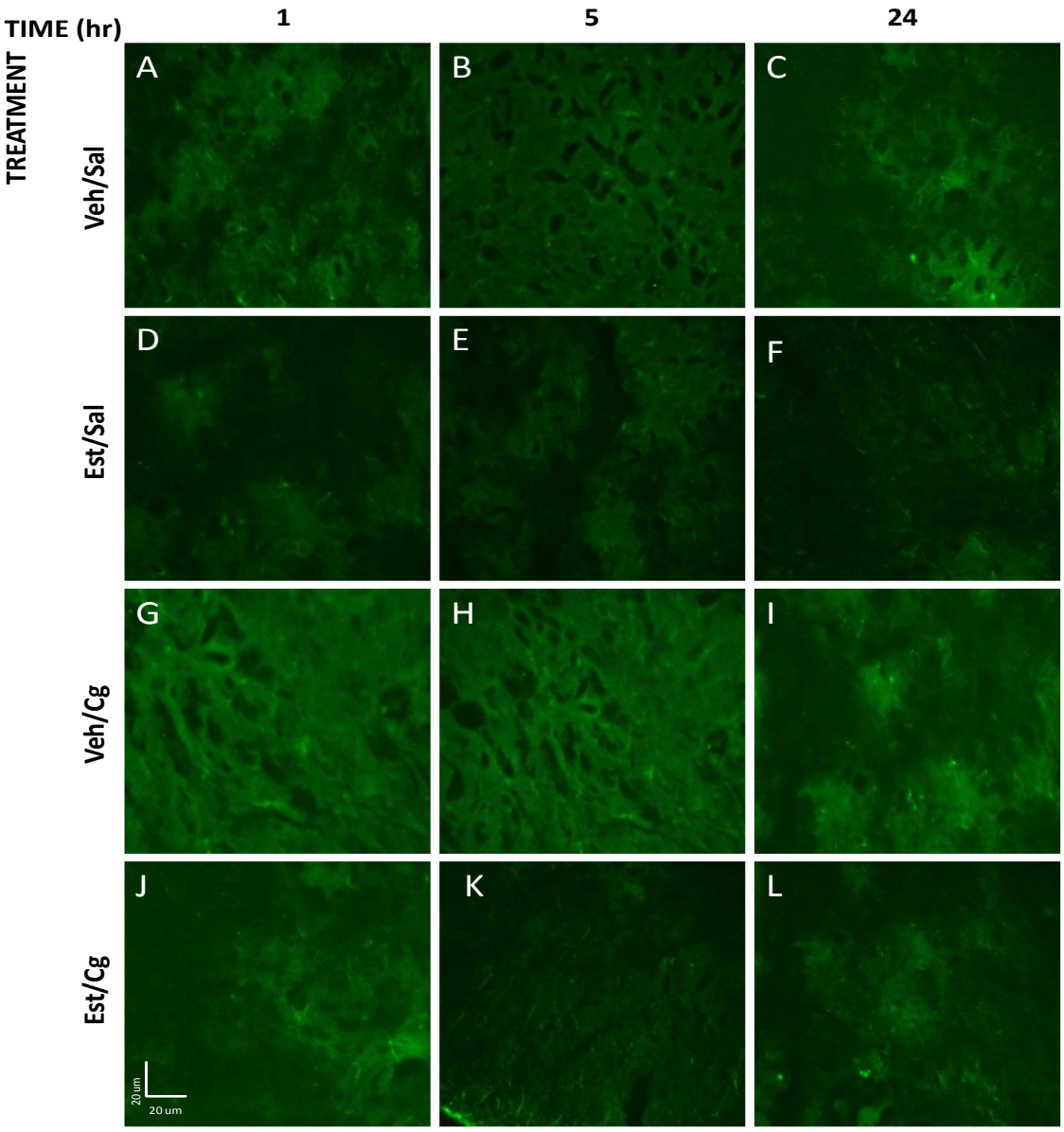

Figure 3.17. Representative immunostained images demonstrating positive labeling of IL-1B for cytokines in ipsilateral dorsal horn of ovariectomized (OVX) vehicle- and estradiol-treated rats in saline and carrageenan treatment groups, across different time conditions. The scale bar in J is 20 um and applies to all panels.

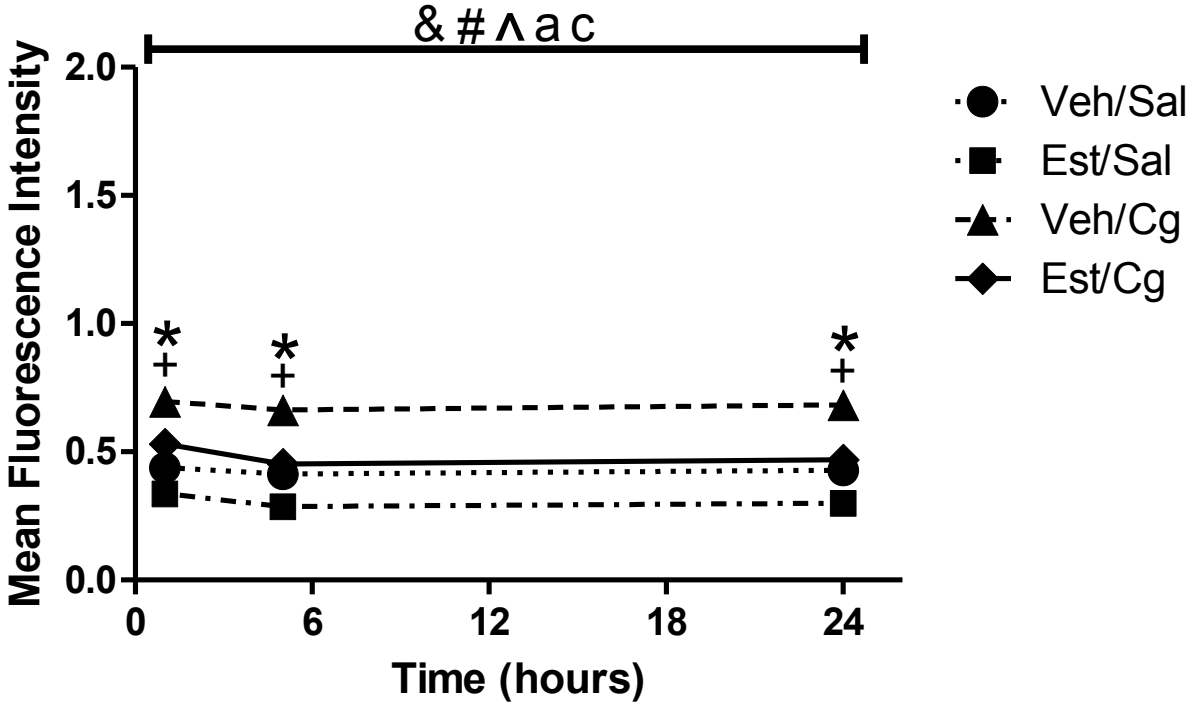

Figure 3.18. Mean fluorescence intensity of Il-1β-expressing cytokines in spinal cord dorsal horn of ovariectomized (OVX) vehicle- and estradiol-treated rats in saline and carrageenan treatment groups, across different time conditions.
(*) Represents statistically significant difference between time condition; (+) represents statistically significant difference between treatment groups; (&) represents main effect of hormone; (#) represents main effect of time; (^) represents main effect of injection; (a) represents interaction effect of hormone*time; (b) represents interaction effect of time*injection; (c) represents interaction effect of hormone*injection; (d) represents interaction effect of hormone*time*injection. Error bars represent standard deviation. Error bars represent standard deviation. *n* 4 per group, $p<0.05$.

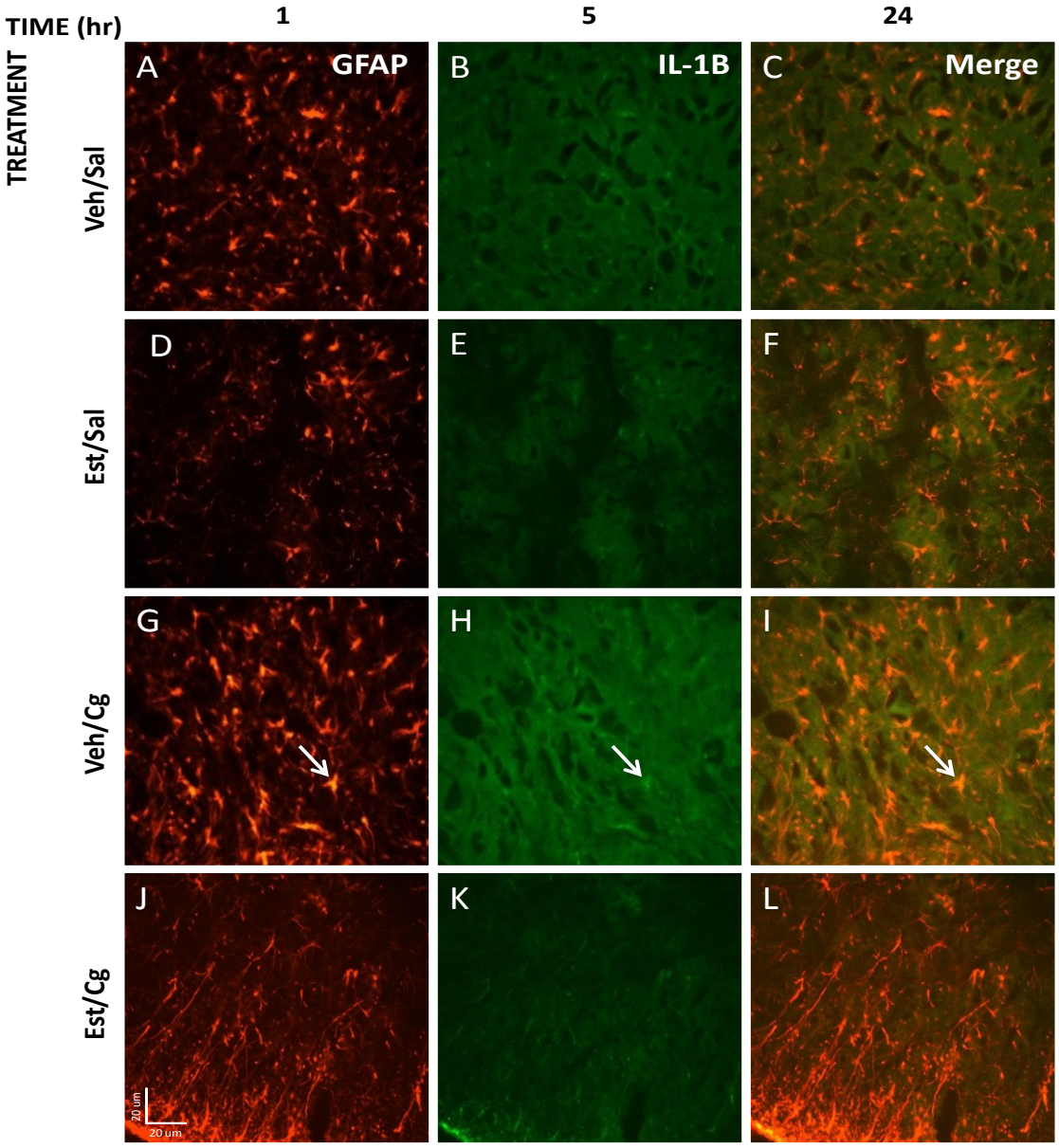

Figure 3.19. Representative immunostained images demonstrating positive co-labeling of GFAP with IL-1B for astrocytes and cytokines in ipsilateral dorsal horn of ovariectomized (OVX) vehicle- and estradiol-treated rats in saline and carrageenan treatment groups, across different time conditions. Arrows indicate representation of colocalization of GFAP with IL-1B (panel G-I). The scale bar in J is 20 um and applies to all panels.

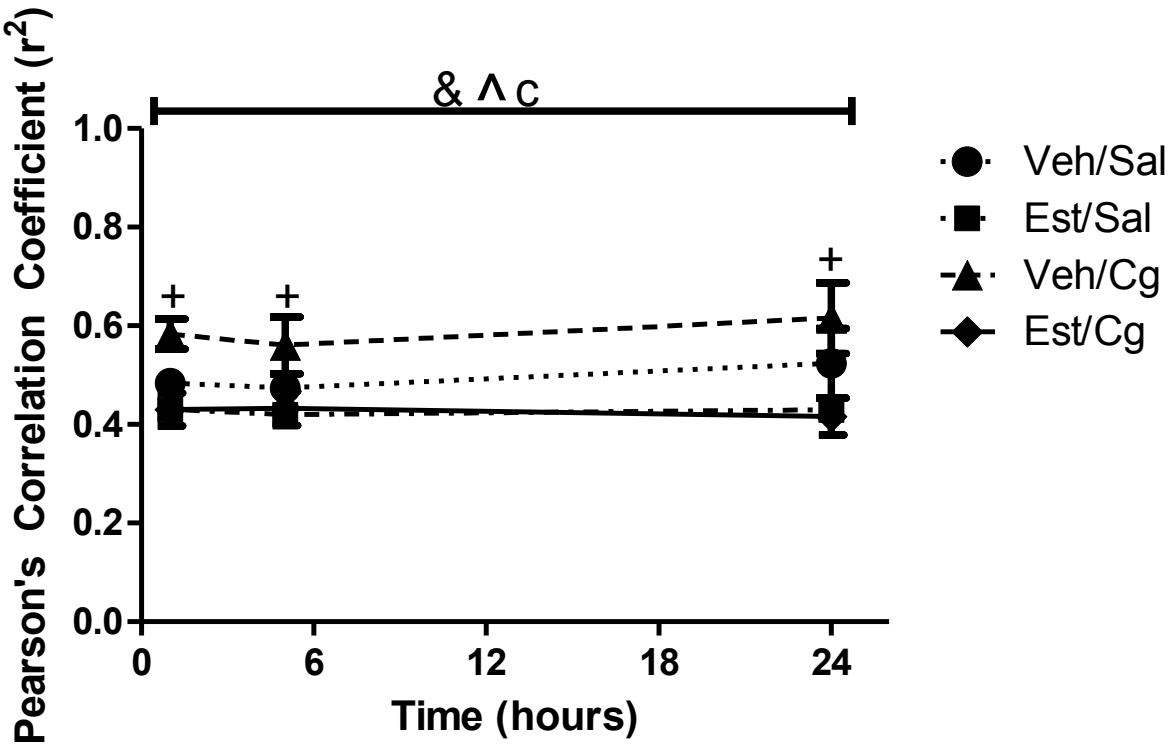

Figure 3.20. Pearson's correlation coefficient (r^2) of GFAP with IL-1B expressing colocalization of astrocytes with cytokines in spinal cord dorsal horn of ovariectomized (OVX) vehicle- and estradiol-treated rats in saline and carrageenan treatment groups, across different time conditions.

(*) Represents statistically significant difference between time condition; (+) represents statistically significant difference between treatment groups; (&) represents main effect of hormone; (#) represents main effect of time; (^) represents main effect of injection; (a) represents interaction effect of hormone*time; (b) represents interaction effect of time*injection; (c) represents interaction effect of hormone*injection; (d) represents interaction effect of hormone*time*injection. Error bars represent standard deviation. *n*= 4 per group $p<0.05$.

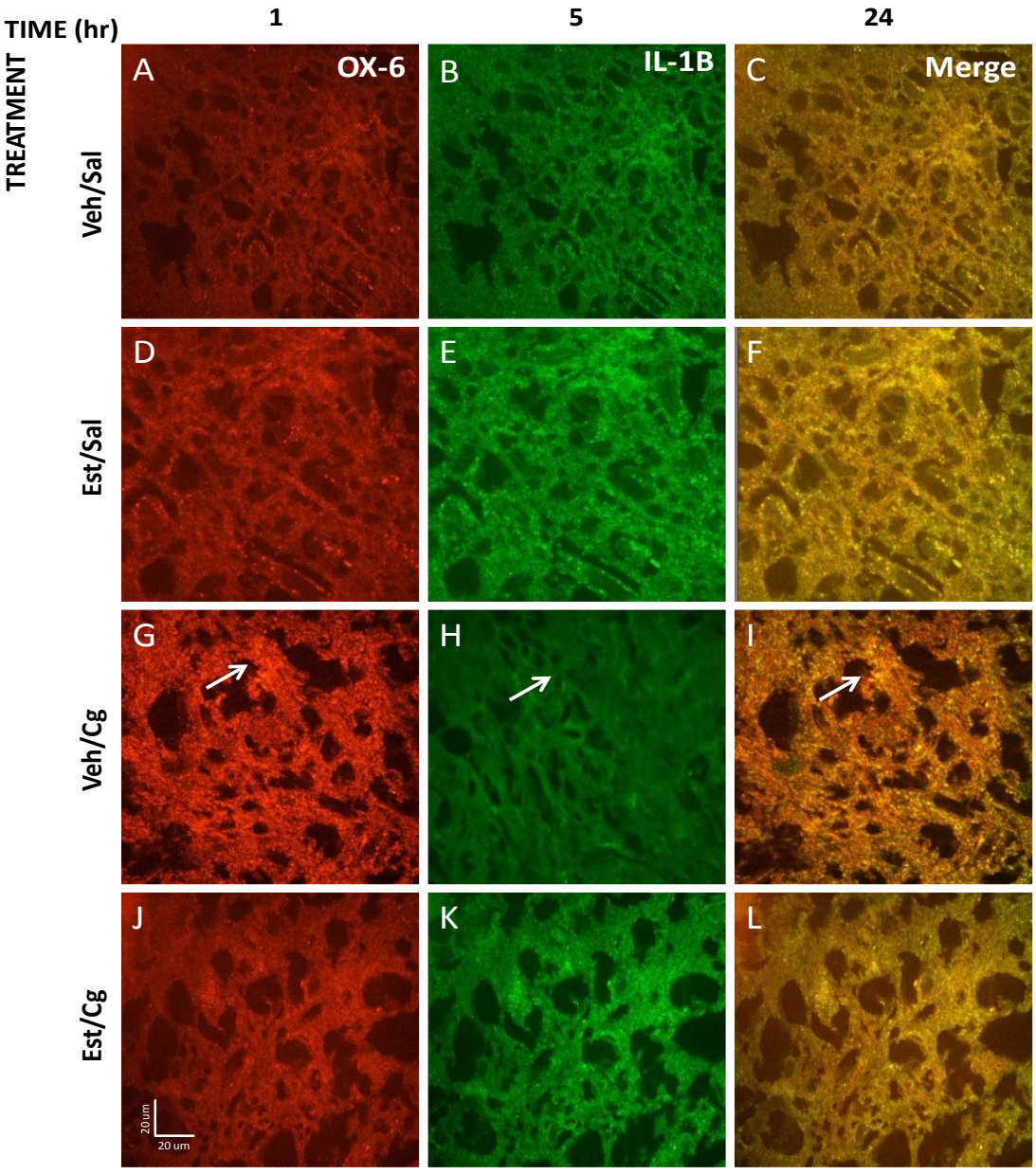

Figure 3.21. Representative immunostained images demonstrating positive co-labeling of OX-6 with IL-1B for microglia and cytokines in ipsilateral dorsal horn of ovariectomized (OVX) vehicle- and estradiol-treated rats in saline and carrageenan treatment groups, across different time conditions. Arrows indicate representation of colocalization of OX-6 with IL-1B (panel G-I). The scale bar in J is 20 um and applies to all panels.

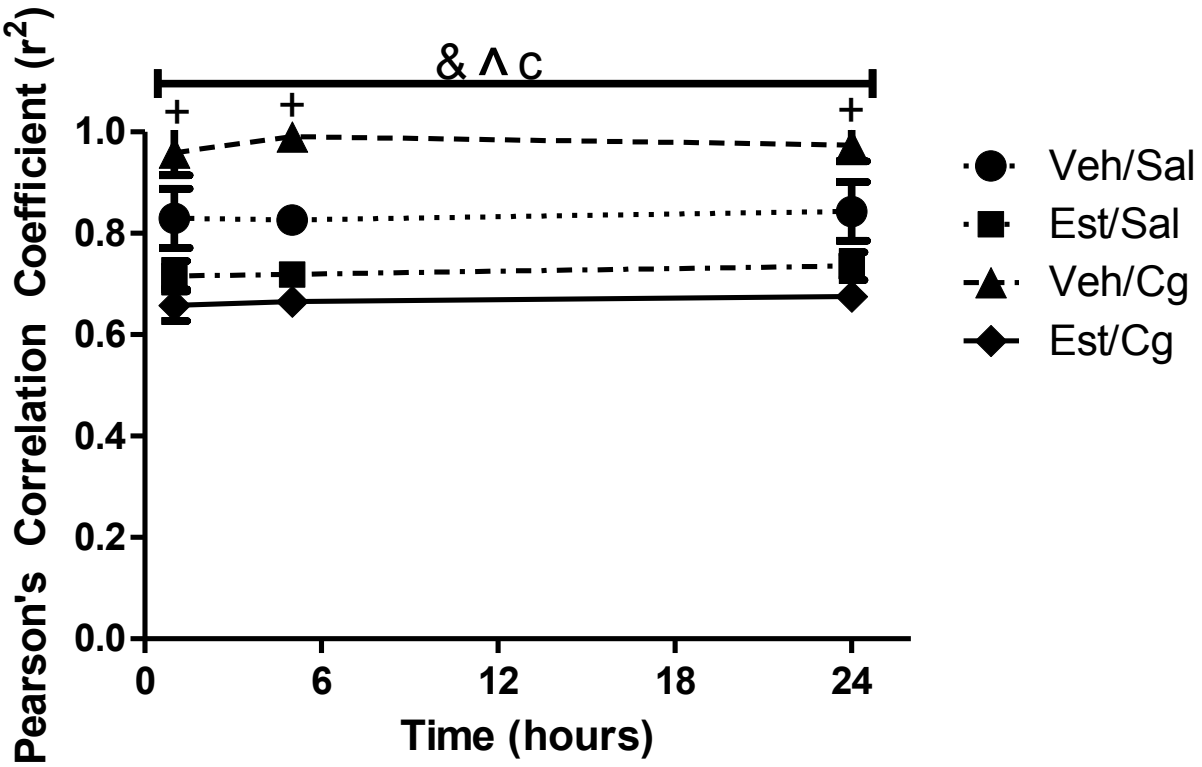

Figure 3.22. Pearson's correlation coefficient (r^2) of OX-6 with IL-1B expressing colocalization of microglia with cytokines in spinal cord dorsal horn of ovariectomized (OVX) vehicle- and estradiol-treated rats in saline and carrageenan treatment groups, across different time conditions.

(*) Represents statistically significant difference between time condition; (+) represents statistically significant difference between treatment groups; (&) represents main effect of hormone; (#) represents main effect of time; (^) represents main effect of injection; (a) represents interaction effect of hormone*time; (b) represents interaction effect of time*injection; (c) represents interaction effect of hormone*injection; (d) represents interaction effect of hormone*time*injection. Error bars represent standard deviation. n=4 per group $p<0.05$.

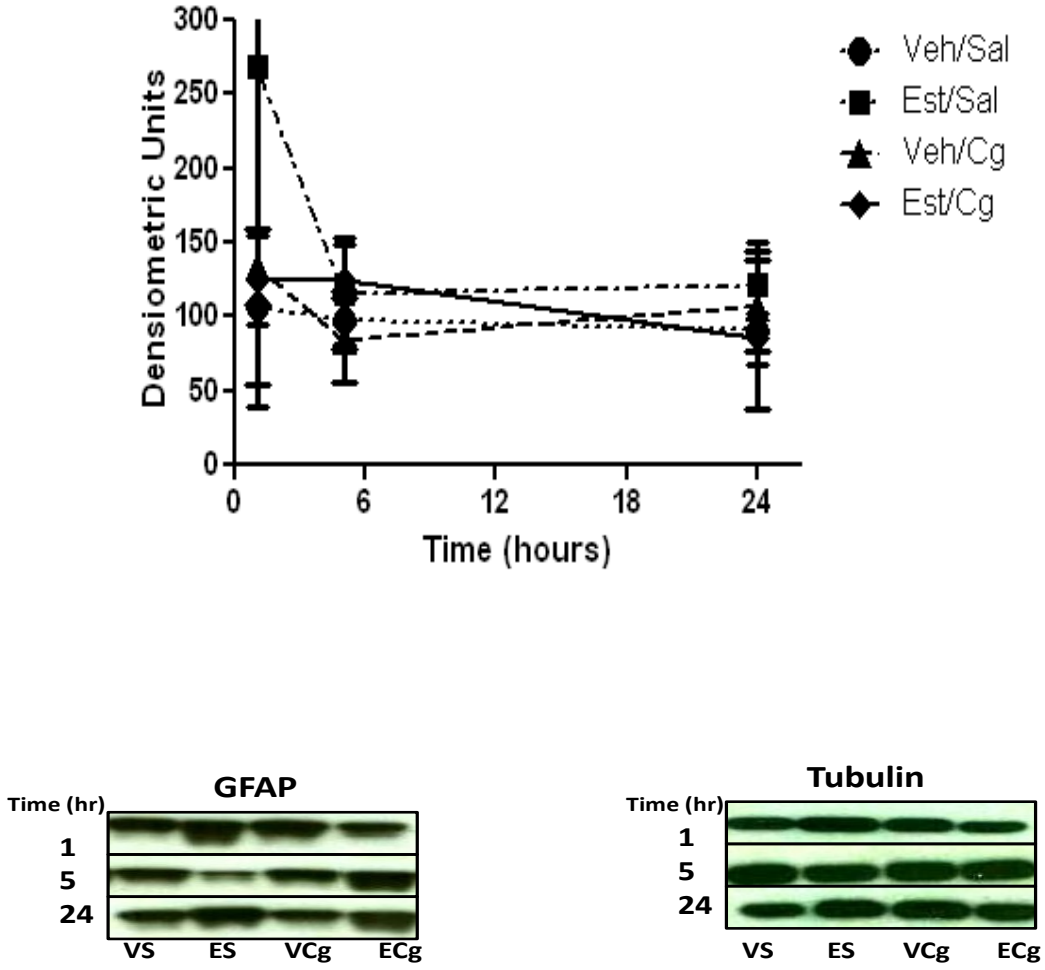

Figure 3.23. Western blot analysis of GFAP in ovariectomized (OVX) vehicle- and estradiol-treated rats in saline and carrageenan treatment groups, across different time conditions.

Data presented as mean protein levels normalized to tubulin. (*) Represents statistically significant difference between time condition; (+) represents statistically significant difference between treatment groups; (&) represents main effect of hormone; (#) represents main effect of time; (^) represents main effect of injection; (a) represents interaction effect of hormone*time; (b) represents interaction effect of time*injection; (c) represents interaction effect of hormone*injection; (d) represents interaction effect of hormone*time*injection. Error bars represent standard deviation. n=4 per group, $p<0.05$.

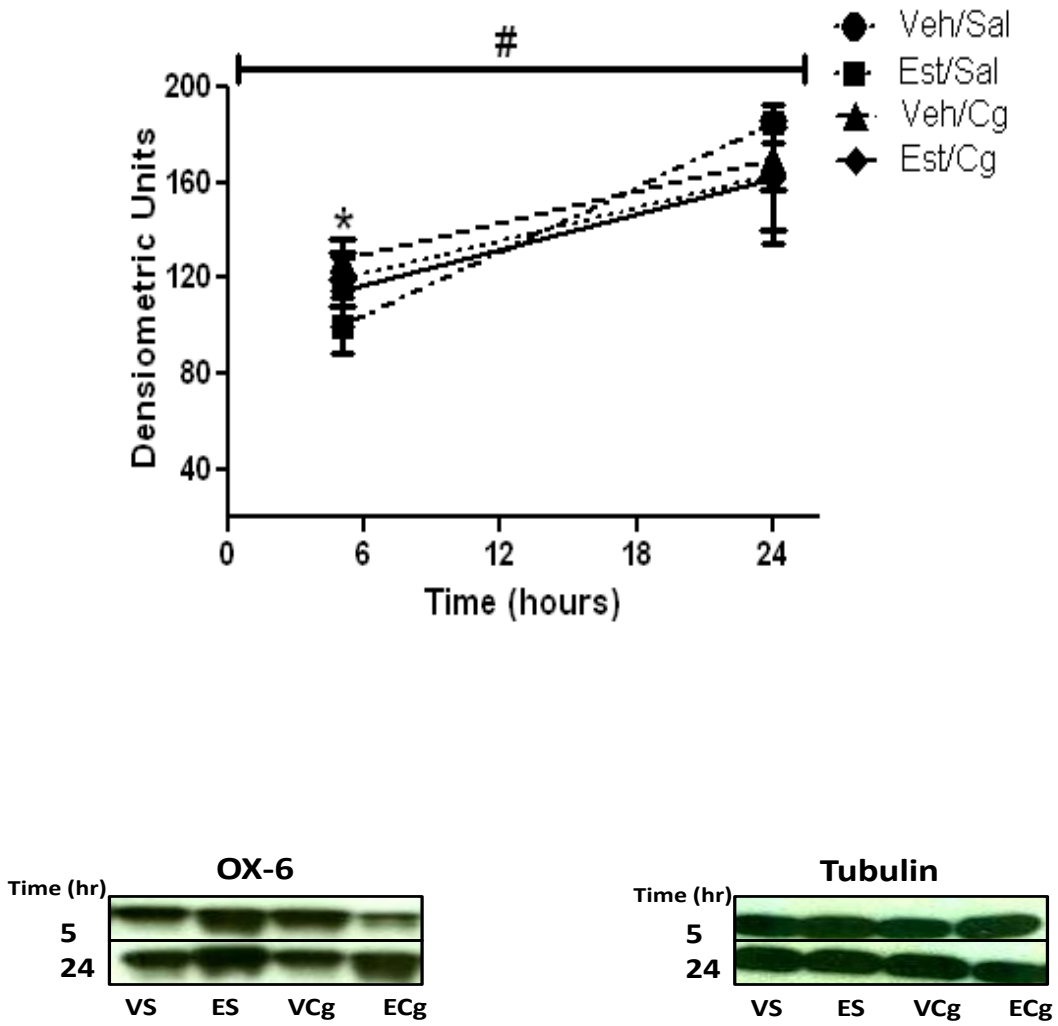

Figure 3.24. Western blot analysis of OX-6 in ovariectomized (OVX) vehicle- and estradiol-treated rats in saline and carrageenan treatment groups, across different time conditions. Data presented as mean protein levels normalized to tubulin. (*) Represents statistically significant difference between time condition; (+) represents statistically significant difference between treatment groups; (&) represents main effect of hormone; (#) represents main effect of time; (^) represents main effect of injection; (a) represents interaction effect of hormone*time; (b) represents interaction effect of time*injection; (c) represents interaction effect of hormone*injection; (d) represents interaction effect of hormone*time*injection. Error bars represent standard deviation. *n*=4 per group, $p<0.05$.

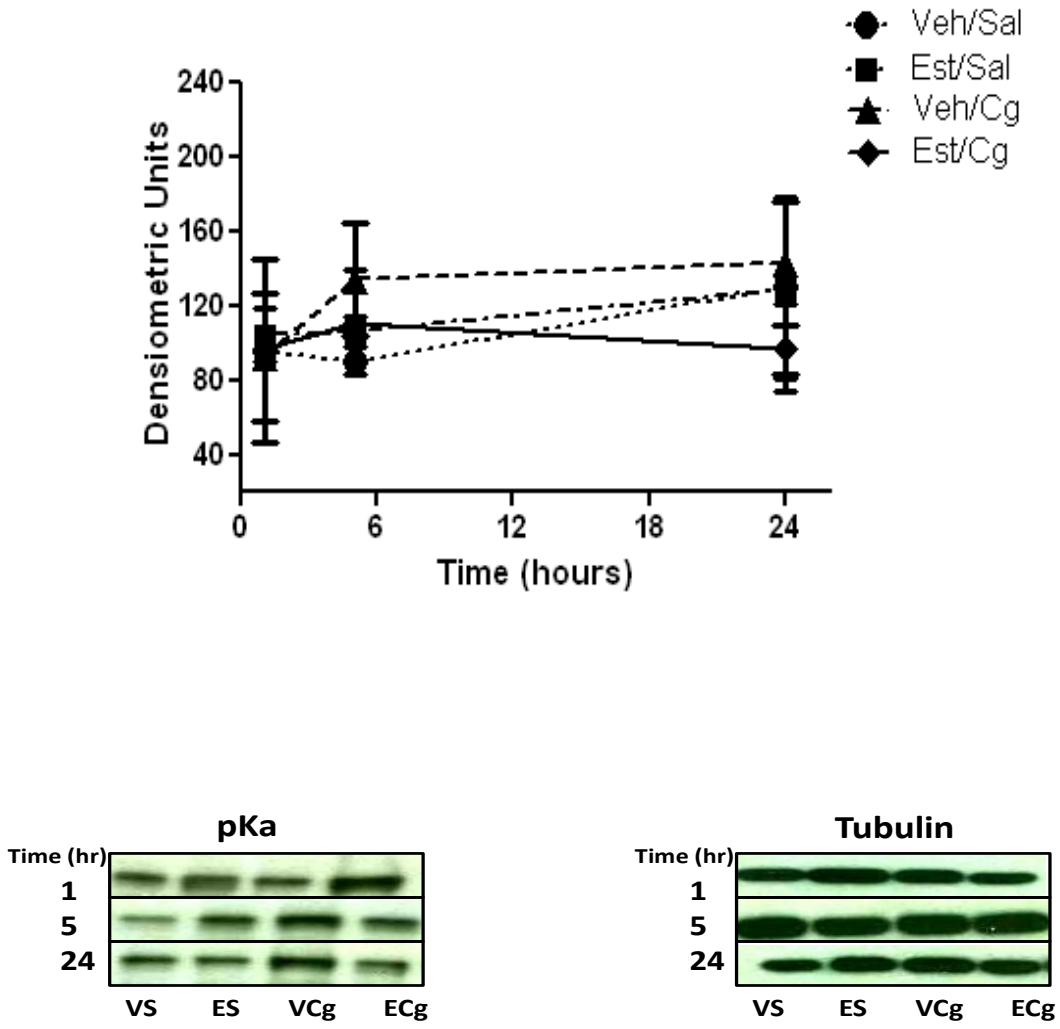

Figure 3.25. Western blot analysis of pKa in ovariectomized (OVX) vehicle- and estradiol-treated rats in saline and carrageenan treatment groups, across different time conditions. Data presented as mean protein levels normalized to tubulin. (*) Represents statistically significant difference between time condition; (+) represents statistically significant difference between treatment groups; (&) represents main effect of hormone; (#) represents main effect of time; (^) represents main effect of injection; (a) represents interaction effect of hormone*time; (b) represents interaction effect of time*injection; (c) represents interaction effect of hormone*injection; (d) represents interaction effect of hormone*time*injection. Error bars represent standard deviation. n =4 per group, $p<0.05$.

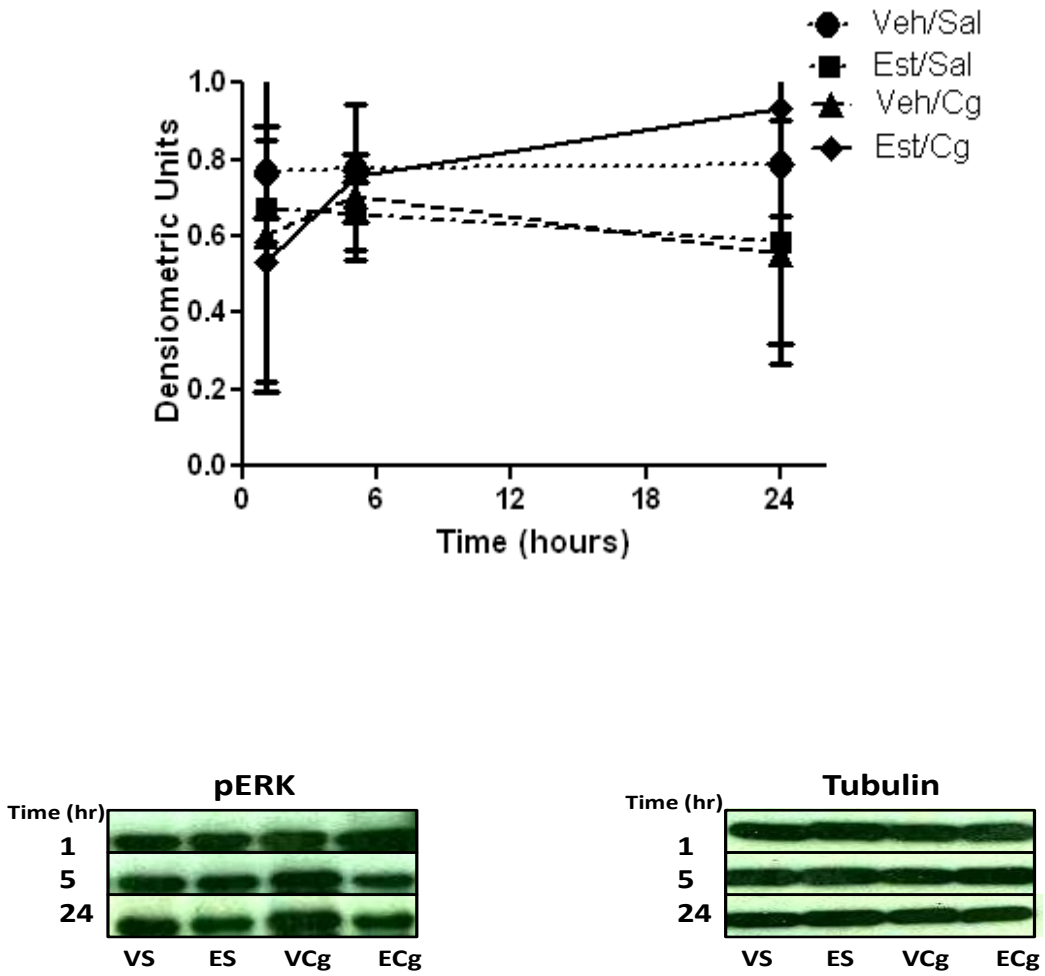

Figure 3.26. Western blot analysis of pERK in ovariectomized (OVX) vehicle- and estradiol-treated rats in saline and carrageenan treatment groups, across different time conditions.

Data presented as mean protein levels normalized to tubulin. (*) Represents statistically significant difference between time condition; (+) represents statistically significant difference between treatment groups; (&) represents main effect of hormone; (#) represents main effect of time; (^) represents main effect of injection; (a) represents interaction effect of hormone*time; (b) represents interaction effect of time*injection; (c) represents interaction effect of hormone*injection; (d) represents interaction effect of hormone*time*injection. Error bars represent standard deviation. n=4 per group $p<0.05$.

.

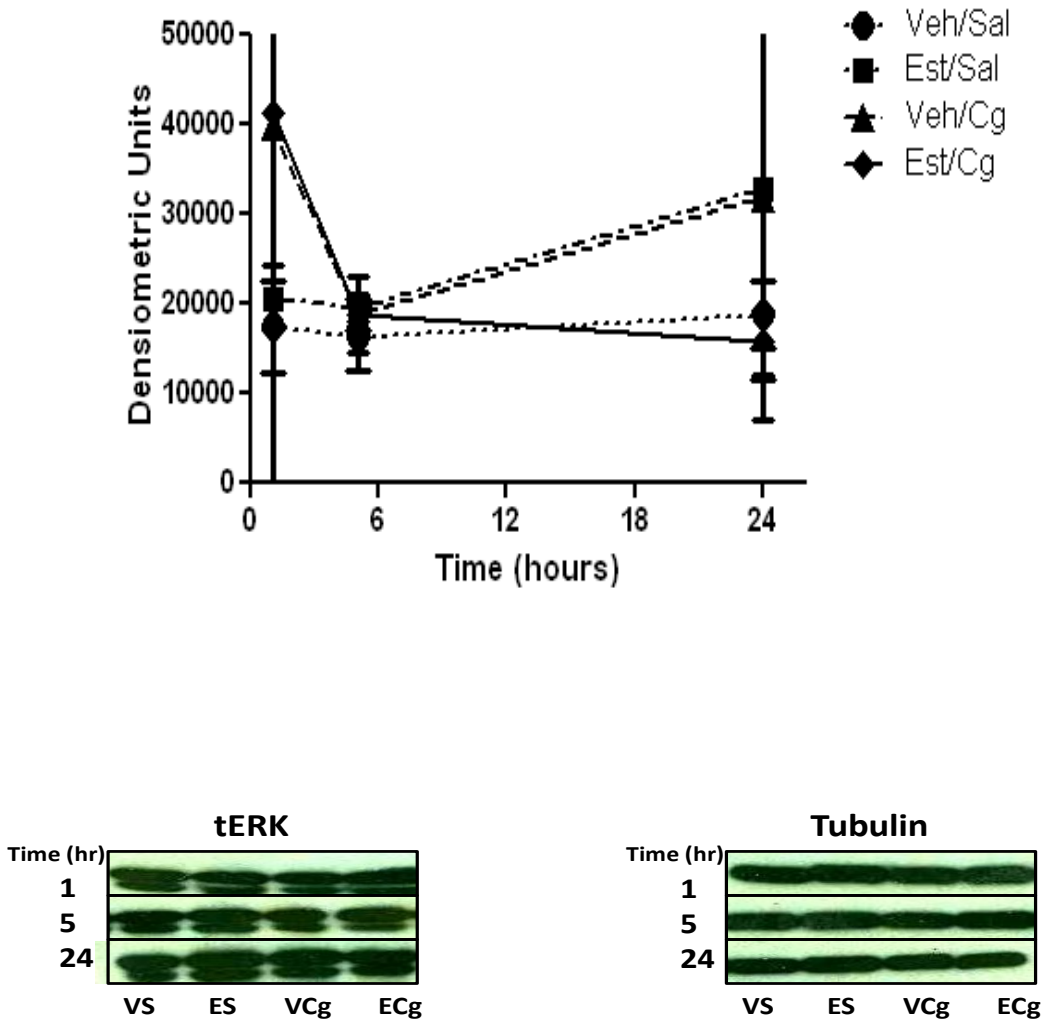

Figure 3.27. Western blot analysis of tERK in ovariectomized (OVX) vehicle- and estradiol-treated rats in saline and carrageenan treatment groups, across different time conditions. Data presented as mean protein levels normalized to tubulin. (*) Represents statistically significant difference between time condition; (+) represents statistically significant difference between treatment groups; (&) represents main effect of hormone; (#) represents main effect of time; (^) represents main effect of injection; (a) represents interaction effect of hormone*time; (b) represents interaction effect of time*injection; (c) represents interaction effect of hormone*injection; (d) represents interaction effect of hormone*time*injection. Error bars represent standard deviation. n=4 per group $p<0.05$.

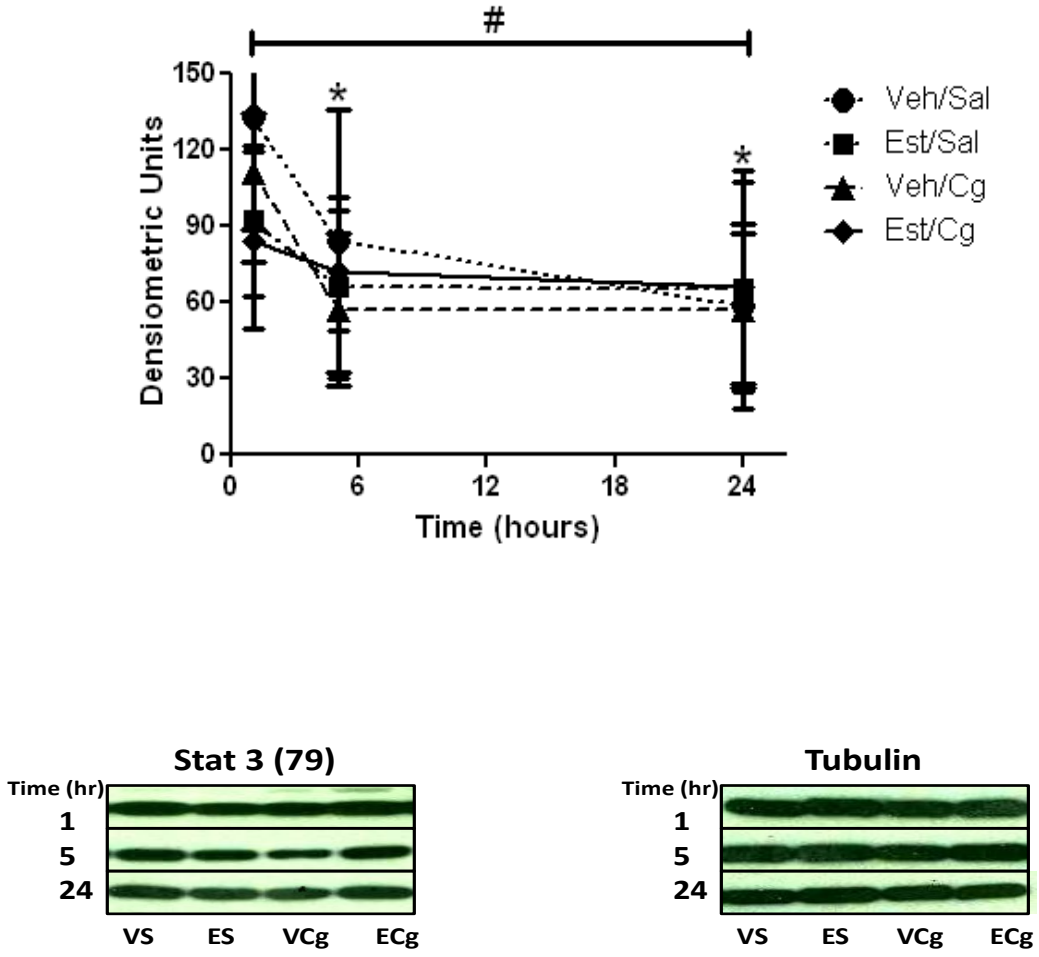

Figure 3.28. Western blot analysis of Stat 3 (79) in ovariectomized (OVX) vehicle- and estradiol-treated rats in saline and carrageenan treatment groups, across different time conditions. Data presented as mean protein levels normalized to tubulin. (*) Represents statistically significant difference between time condition; (+) represents statistically significant difference between treatment groups; (&) represents main effect of hormone; (#) represents main effect of time; (^) represents main effect of injection; (a) represents interaction effect of hormone*time; (b) represents interaction effect of time*injection; (c) represents interaction effect of hormone*injection; (d) represents interaction effect of hormone*time*injection. Error bars represent standard deviation. *n*=4 per group, $p<0.05$.

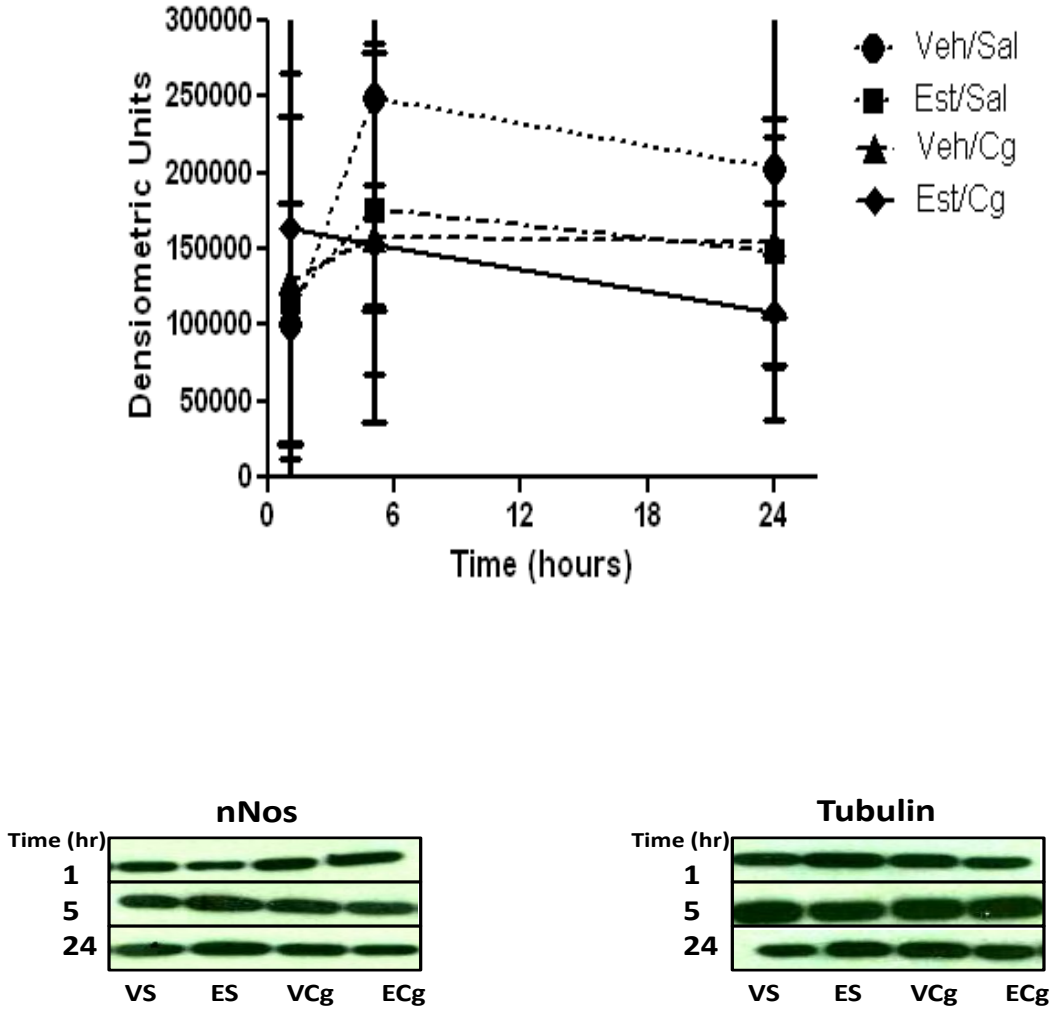

Figure 3.29. Western blot analysis of nNos in ovariectomized (OVX) vehicle- and estradiol-treated rats in saline and carrageenan treatment groups, across different time conditions. Data presented as mean protein levels normalized to tubulin. (*) Represents statistically significant difference between time condition; (+) represents statistically significant difference between treatment groups; (&) represents main effect of hormone; (#) represents main effect of time; (^) represents main effect of injection; (a) represents interaction effect of hormone*time; (b) represents interaction effect of time*injection; (c) represents interaction effect of hormone*injection; (d) represents interaction effect of hormone*time*injection. Error bars represent standard deviation. n=4 per group, $p<0.05$.

Table 3.7. Summary of correlations between ipsilateral PWL and protein levels analyzed via western blots.

	Group	pKA	pERK	Stat 3 (79)	tERK	nNOS
	Overall	**0.35***	-0.23	-0.22	0.07	0.22
	Estradiol	0.30	-0.13	0.05	0.04	0.01
LOW	**Vehicle**	0.41	-0.32	0.33	-0.05	-0.19
HEAT	**Veh Sal**	0.22	0.58	-0.07	-0.64	0.40
	Est Sal	0.32	-0.53	-0.56	0.56	0.62
	Veh Cg	0.63	-0.17	-0.41	0.07	0.24
	Est Cg	0.16	**-0.75***	0.46	0.39	0.51
	Overall	0.30	-0.04	-0.20	-0.11	-0.01
	Estradiol	-0.06	-0.21	0.06	0.14	0.15
MEDIUM	**Vehicle**	**0.52***	-0.26	0.22	-0.13	-0.14
HEAT	**Veh Sal**	**0.75***	0.19	**-0.82***	-0.22	0.16
	Est Sal	0.40	0.30	0.33	-0.42	0.03
	Veh Cg	0.33	-0.02	-0.25	0.02	0.17
	Est Cg	0.34	-0.16	0.49	-0.19	0.35
	Overall	**0.34***	0.18	-0.22	-0.22	-0.23
	Estradiol	0.12	-0.06	-0.23	-0.04	0.24
HIGH	**Vehicle**	**0.63***	-0.36	0.04	0.16	-0.39
HEAT	**Veh Sal**	0.63	0.36	-0.55	-0.31	0.17
	Est Sal	-0.22	0.29	0.58	-0.32	0.28
	Veh Cg	0.23	0.01	-0.45	-0.08	0.10
	Est Cg	0.15	0.17	-0.01	-0.21	0.07

Legend. Treatment groups are designated as follows: Veh Sal = vehicle saline; Est Sal = estradiol saline; Veh Cg = vehicle carrageenan; Est Cg = estradiol carrageenan. Data represents correlation coefficients for specified analysis. Significant correlation coefficients are designated by (*) for $p<.05$ and (**) for $p<.0001$. *n*=9-11 per group.

Table 3.8. Summary of correlations between glial activation markers and protein levels analyzed via western blots.

	Group	pKA	pERK	Stat 3 (79)	tERK	nNOS
	Overall	-0.11	-0.24	-0.14	0.06	0.01
	Estradiol	0.18	-0.03	-0.04	-0.01	-0.10
	Vehicle	-0.34	**-0.53***	0.35	0.15	0.10
GFAP	**Veh Sal**	-0.32	0.15	0.55	-0.19	-0.45
	Est Sal	-0.44	-0.52	-0.19	0.41	0.30
	Veh Cg	0.50	-0.18	-0.30	0.03	0.19
	Est Cg	0.15	-0.61	0.75	0.24	0.34
	Overall	-0.23	**-0.56***	0.08	**0.49***	0.10
	Estradiol	-0.23	-0.49	0.25	0.45	0.43
	Vehicle	-0.15	-0.47	-0.09	**0.60***	0.00
OX-6	**Veh Sal**	-0.45	-0.64	0.57	0.62	-0.55
	Est Sal	-0.62	-0.39	-0.36	0.31	**0.80***
	Veh Cg	-0.33	-0.31	0.43	0.45	0.18
	Est Cg	0.11	-0.57	0.17	0.59	-0.40

Legend. Treatment groups are designated as follows: Veh Sal = vehicle saline; Est Sal = estradiol saline; Veh Cg = vehicle carrageenan; Est Cg = estradiol carrageenan. Data represents correlation coefficients for specified analysis. Significant correlation coefficients are designated by (*) for $p<.05$ and (**) for $p<.0001$. n=9-11 per group.

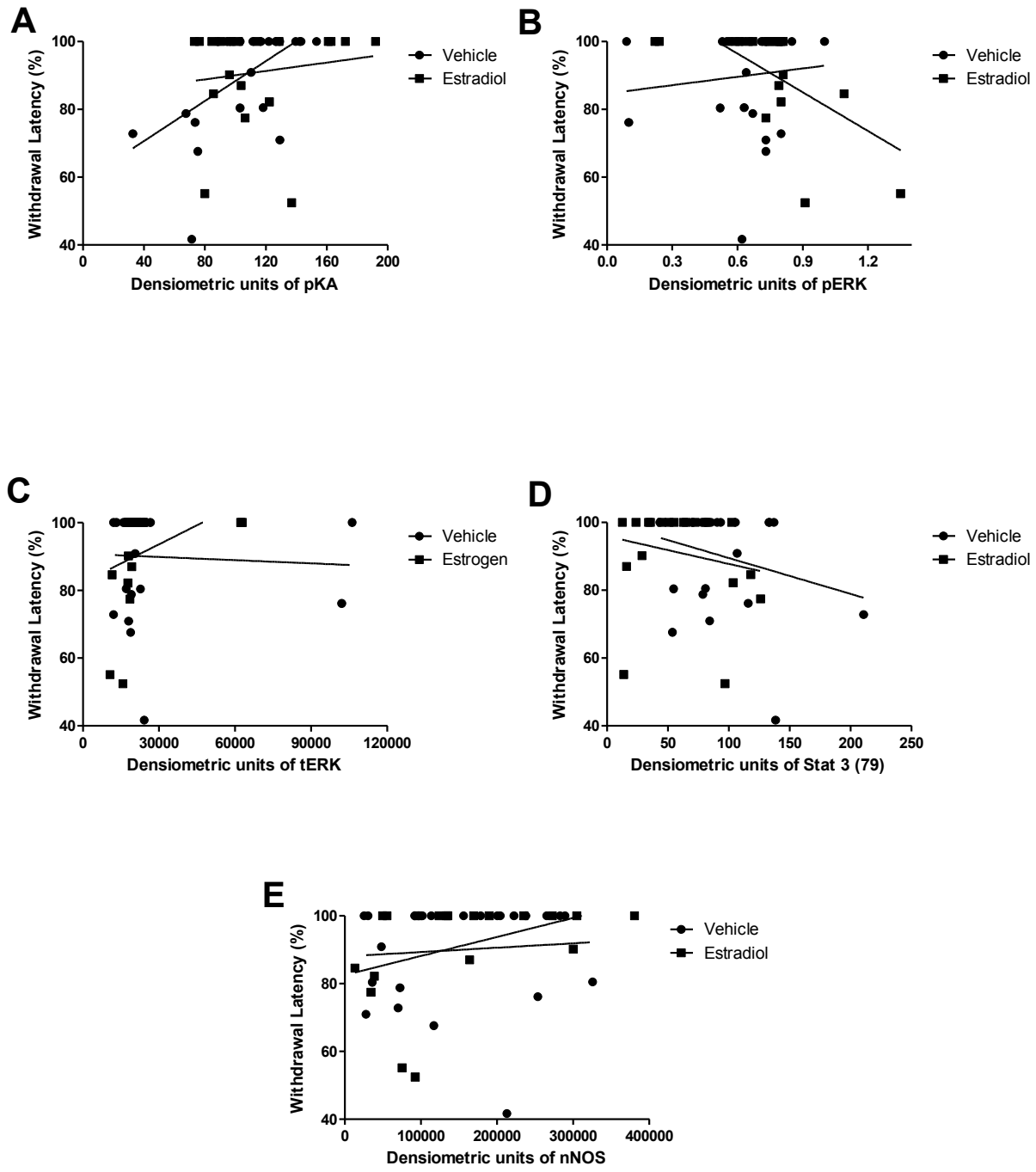

Figure 3.30. **Linear Regression analysis of paw withdrawal latency and A) pKA; B) pERK; C) tERK; D) Stat; E) nNOS**, $p<0.05$.

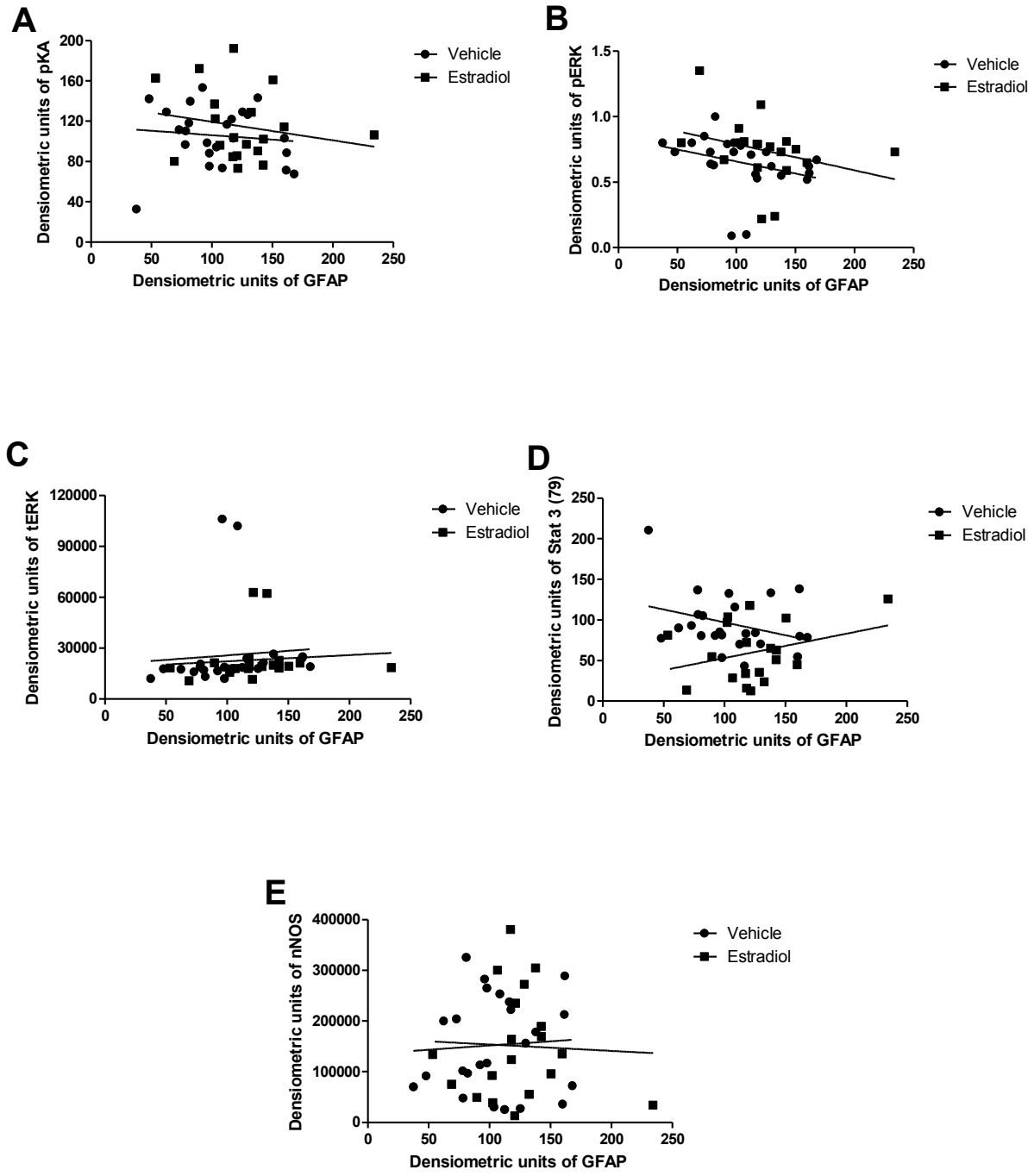

Figure 3.31. **Linear Regression analysis of GFAP and A) pKA; B) pERK; C) tERK; D) Stat; E) nNOS**, $p<0.05$.

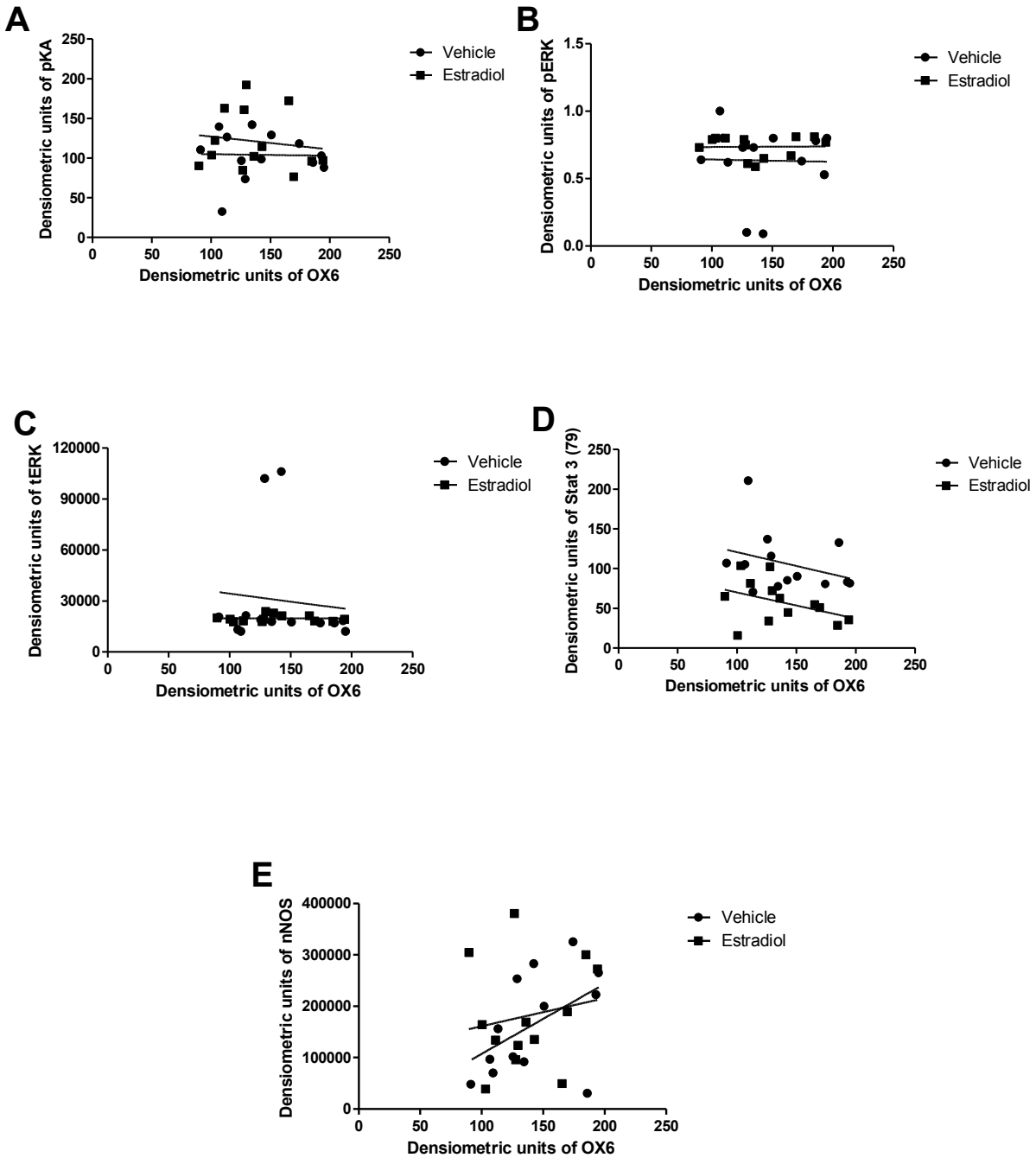

Figure 3.32. **Linear Regression analysis of OX-6 and A) pKA; B) pERK; C) tERK; D) Stat; E) nNOS**, $p<0.05$.

Chapter 4. Discussion

Estradiol exerts its anti-hyperalgesic effect by concomitantly reducing macrophage activation at the injury site and dampening glial cell activation in the dorsal horn, with overall greater activity in the dorsal horn.

Inflammation, dynamically mediated by the nervous, immune, and endocrine systems, is the common denominator in numerous neurodegenerative illnesses that cripple the once healthy and active lifestyles of adults who live past their prime. Postmenopausal women, in particular, are prime targets for chronic inflammatory diseases like diabetic neuropathy and rheumatoid arthritis, which are critically associated with an endogenous decrease in estrogen. A growing body of research investigating the effects of hormones on the inflammatory response desperately seeks to answer fundamental questions regarding the safety and efficacy of hormone replacement therapy. Recent studies have implicated the exogenous administration of estradiol in both anti-inflammatory (Berg et al., 2002; Uemura et al., 2005; Rogers et al., 2001) and pro-inflammatory roles (Martin & Behbehani, 2006; Ceccarelli, et al., 2003b). Understanding the specific mechanisms underlying estradiol's diverse neuroimmune effects on inflammation is essential to making progress in hormone replacement therapy research.

As such, we have investigated the degree to which estradiol's attenuation of behavioral responses to inflammation occurs through immune cell response at the injury site compared with glial cell responses at the spinal cord dorsal horn. Our findings show that estradiol treatment interacted significantly with time to attenuate behavioral responses to inflammation. Estradiol mimicked this anti-inflammatory activity in paw edema effects after Cg/saline administration. Immunofluorescent analyses reveal that estradiol treatment markedly dampens activation of macrophages at the injury site and glial cell activation at the spinal cord dorsal horn in response

to inflammation. Significant correlations of immunofluorescent activity with behavioral responses were also found across all heat intensities. Taken together, these findings suggest that estradiol decreases behavioral responses to inflammation by concomitantly reducing immune cell response at the injury site and dampening glial cell response at the spinal cord.

Our data show that prior to inflammatory insult, estradiol does not significantly affect behavioral responses to inflammation. While this finding contradicts a recent study that found that estradiol's anti-inflammatory action may extend to nociception without inflammatory insult (Li et al., 2009), other studies support the finding that estradiol does not significantly affect baseline responses to nociception (Wang et al., 2006; Loyd et al., 2008). This discrepancy may be attributed to variability in nociceptive behavioral measurement models or hormone treatment paradigms. Estradiol was found to significantly decrease inflammatory responses 1 hour after Cg/saline injection when compared to 5 and 24 hours after injection, at the lowest heat intensity in the ipsilateral paw. This finding suggests that estradiol may exert its anti-hyperalgesic effect soon after inflammatory insult, but not after a prolonged delay such as 5 or 24 hours. Previous studies have observed significant time effects of estradiol's anti-inflammatory activity in NSAID treatment in carrageenan-induced hyperalgesia, especially 5 hours after injection (Hunter et al., 2011). Responses to inflammation at various time points need to be further investigated in different pain measurement assays in order to better understand estradiol's time course of action.

A lack of significant effects in the contralateral paw suggests that estradiol acts peripherally to attenuate pain responses. Significant main effects of injection and time across heat intensities and a significant injection-time interaction in the ipsilateral paw indicate that Cg successfully induced an inflammatory state and behavioral responses to nociception changed significantly across time at the highest heat intensity. Paw size analyses support estradiol's anti-

inflammatory activity, showing that estradiol significantly decreased paw edema expansion in response to Cg-induced inflammation. These data suggest that estradiol appears to decrease the release of inflammatory mediators at the injury site, which in turn diminishes the cascade of inflammatory responses in the primary sensory neuron, followed by the dorsal horn of the spinal cord.

Many studies have highlighted estradiol's significant role in modulating immune system function by exerting specific effects on immune cells that express estrogen receptors, such as macrophages (Straub, 2007). As the first line of defense against pathogens, macrophages directly influence subsequent immune responses such as the release of a wide range of inflammatory mediators like cytokines and NO (Serbina et al., 2008). To explore estradiol's impact on immune cell responses at the injury site, we analyzed tissue-resident macrophage activity. Results of immunofluorescent analyses of CD68-expressing macrophage activation corroborate estradiol's important role in regulating immune responses to inflammation. Specifically, our data show that estradiol interacted with time and injection treatment to decrease macrophage activation post Cg and saline injection. Since a reduction of macrophage activity was found in saline-injected rats in addition to Cg-injected rats, estradiol may act to reduce pain in response to physical trauma as well as to inflammation. Correlational analyses reveal that a significant negative relationship was observed between CD68 expression and PWL across all treatment groups, where a decrease in macrophage activity was accompanied by an increase in PWL, which indicates a lessening of pain behavior. These findings suggest that immune activity at the injury site is one critical target of estradiol's anti-hyperalgesic mechanism.

Some studies present data that contradict this anti-inflammatory role of estradiol in the immune system, showing instead a pro-inflammatory role for estradiol in mediating immune cell

responses. For example, 17β-estradiol (E2) has been shown to enhance the expression of inflammatory mediators by LPS-activated tissue resident macrophages through estrogen receptor alpha (ERα) signaling (Soucy et al., 2005). Also, researchers have shown that chronic E2 administration in OVX mice significantly enhances both cytokine (IL-1β, IL-6, and TNF-α) and inducible NO synthase (iNOS) mRNA release in thioglycolate (TGC)-elicited macrophages (Calippe et al., 2010). However, many more studies support estradiol's anti-inflammatory actions in various pain models (Carlsten et al., 1992; Tarkowski, 1997; Shiraj et al., 1995; Hayashi et al., 1998). This discrepancy can be explained by the incredibly complex nature of estradiol's anti-nociceptive effects that is influenced by several different variables, such as model of nociceptive behavioral measurement, vacillating levels of endogenous estrogen, dose and type of estradiol administration, and time course of hormone treatment relative to noxious exposure.

Pain has traditionally been viewed as the result of a series of neuronal events in which peripheral nerves relay pain messages to nociceptive neurons, which then release a cascade of inflammatory mediators like substance P and excitatory amino acids to further excite pain-transmission neurons (Watkins, 2001). However, this does not even begin to paint a complete picture of pain because it does not take into account the incredibly dynamic modulation of signals that arise in prolonged inflammatory states or in neuropathic pain. For example, injury can result in perceived pain that emerges not only from the injured tissue, but also from surrounding healthy tissues: a phenomenon that cannot simply be explained by the diffusion of inflammatory mediators. Moreover, a significant suppression or exacerbation of pain can occur at various levels of synaptic communication, especially in pathological pain states (Campbell & Meyer, 2006).

Glial activation in the spinal cord dorsal horn is linked to the development of pathological pain states in various pain syndromes, such as diabetic neuropathy and rheumatoid arthritis, which are marked by inflammation (Scholz & Woolf, 2007). In order to elucidate estradiol's anti-inflammatory effects at the level of the spinal cord dorsal horn, we examined glial activity across treatment groups. Immunofluorescent analyses of GFAP-expressing astrocyte activation and OX-6-expressing microglia revealed significant effects of estradiol's anti-hyperalgesic activity in the dorsal horn of the spinal cord. Significant interactions of hormone and injection show that estradiol decreased inflammatory responses in the dorsal horn by dampening microglia and astroglia activation in Cg- and saline-treated rats. Corresponding immunofluorescent images illustrate this dampening effect by showing decreased activation of glial processes in estradiol-treated conditions when compared with the vehicle-treated group. Glial cell activation is characterized by the expression of surface antigens, the production of neuroimmune modulators, and consequent changes in morphology, such as an increase in intermediate filaments like glial fibrillary acidic protein (GFAP) in astrocytes (Wieseler-Frank et al., 2005).

While linear regression analyses did not significantly predict any relationships of glial cell activation with nociceptive behavioral responses, correlation (Pearson's r) analyses yielded several significant relationships. GFAP showed negative correlations with PWL in the vehicle-treated groups at both the medium and highest heat intensities, and also across treatments at the highest heat. This finding is consistent with estradiol's anti-inflammatory role because it means as PWL decreased, which signifies an increase in pain response, astrocyte activation increased. The lack of significant correlations between GFAP and PWL in the estradiol-treated groups suggests that estradiol functioned to dampen astrocyte activation and block the stereotypical glial inflammatory response that is seen in the vehicle-treated group. At the lowest and medium heat

intensities, OX-6 showed significant negative correlations with PWL in the estradiol-treated group administered Cg. This finding of increased PWL associated with decreased microglial activation supports a key role of microglia in the inflammatory response that can be correlated with behavior.

Interestingly, positive correlations between OX-6 and PWL were found in both the estradiol and vehicle/saline groups at the highest heat intensity, indicating that as PWL decreased, microglial activation decreased. Although microglial activation has largely been linked to pro-inflammatory events, this unanticipated anti-inflammatory activity of microglia can be explained by the notion that just as estradiol acts in both anti- and pro-inflammatory roles, microglia can also tailor its function to more neuroprotective activities. In other words, microglial activation is not synonymous with pro-inflammatory activity as suggested by some studies (Scholz & Woolf, 2007; Wieseler-Frank et al., 2005); in fact, glial cells are the nervous system's immunocompetent cells, performing phagocytosis and other daily functions that keep cells healthy and toxicity-free (Milligan & Watkins, 2009). Consequently, microglia cells may assume anti-inflammatory roles to protect nearby tissue from damage by decreasing levels of pro-inflammatory mediators (Turrin & Rivest, 2006).

This finding actually corroborates estradiol's dual effect on inflammation, because glial cells express estrogen receptors and it is possible that estradiol exerts its neuroprotective effects through glial cells themselves. Specifically, estradiol's actions are mediated through estrogen receptors (i.e., ERα and ERβ) which are part of the nuclear receptor super-family (Milligan & Watkins, 2009). Since these receptors are primarily involved in ligand-regulated transcription, it has been classically thought that estrogen receptors function only to mediate actions in the brain via genomic or long-term transcriptional effects (Fiocchetti et al., 2012). New studies, however,

show that estrogen receptors are also involved in mediating rapid, membrane-initiated effects of estradiol in the brain. These effects are thought to be independent of estrogen receptor transcriptional activities and have been implicated in estradiol-mediated neuroprotection (Fiocchetti et al., 2012). Investigating these complex receptor effects will further our understanding of estradiol's mechanisms.

To specifically investigate to what extent estradiol's anti-inflammatory activity occurs at the injury site compared with the spinal cord dorsal horn, percent change of activation (compared to vehicle/saline treatment) was examined in the comparison of CD68 and GFAP activation and CD68 and OX-6 activation. Across all treatment groups, except for vehicle- and saline-only treatments, GFAP-expressing astrocyte activation at the dorsal horn exceeded CD68-expressing macrophage activation at the injury site, especially 5 and 24 hours post-injection. OX-6-expressing microglia activation was also greater than CD68-expressing macrophage activation in the estradiol- and estradiol/Cg-treated groups. However, CD68 activation was greater in the estradiol/saline- and vehicle/Cg-treated groups. Again, most significant differences were found at 5 and 24 hours post-injection. Taken together, this data suggests that overall, estradiol-mediated hyperalgesic activity is greater at the dorsal horn than at the injury site. Additionally, the differences in extent of activity by astrocytes and microglia may suggest varying patterns of recruitment and activation by estradiol as part of its mechanism.

It is useful to compare the series of events that lead to pro-inflammatory roles and anti-inflammatory roles for glial cells. Pro-inflammatory activities are as follows. Chronic inflammation, characterized by a persistent noxious input, causes lasting central sensitization. This results in transcriptional changes in dorsal horn neurons that increase synaptic sensitivity (Milligan & Watkins, 2009). Astrocytes respond with increased Ca^{2+} signaling, leading to the

release of glutamate (Glu), ATP that binds to $P2X_4$, tumour-necrosis factor- (TNF), interleukin 1 (IL-1), IL-6, nitric oxide (NO) and prostaglandin E_2 (PGE_2). These pro-inflammatory mediators are also released from activated microglia. Matrix metalloproteinase 9 (MMP9) stimulates pro-IL-1 cleavage and microglial activation, while MMP2 stimulates pro-IL-1 cleavage and maintains astrocyte activation. The activation of p38 mitogen-activated protein kinase (p38 MAPK) occurs in both microglia and astrocytes on IL-1 signalling. Astrocytes and microglia also express the chemokine receptors CX3CR1 (not shown) and CCR2, and when they bind, the glial cells become activated (Milligan & Watkins, 2009). After nerve damage, heat shock proteins (HSPs) are secreted and can bind to Toll-like receptors (TLRs) expressed on both astrocytes and microglia, resulting in further activity (Figure 4.1A).

Glial cells can exert neuroprotective effects by releasing anti-inflammatory cytokines such as IL-10 and IL-4 and they also express cannabinoid receptors (CB_1 and CB_2). CB_1 and CB_2 have demonstrated anti-inflammatory functions and inhibition of microglial toxicity through the suppression of chemotactic responses and MAPK signal transduction, resulting in inflammatory cytokine inhibition. Also, the glutamate transporters, glutamate transporter 1 (GLT1) and glutamate–aspartate transporter (GLAST), can begin to reuptake glutamate normally. ATP activation of microglial $P2RX_7$ purinoreceptors leads to release of TNF, which protects neurons from the neurotoxic effects of excess glutamate (Figure 4.1B). Another neuroprotective function is that the spread of tissue degeneration is prevented after direct injury when activated astrocytes remove the dying neurons and tissue debris (Milligan & Watkins, 2009). In non-activated cells (not shown), nuclear factor-B (NF-B) is kept in the cytosol by inhibitor of b (IB), which binds to particular regions to prevent exposure of the nuclear-localization signal. When stimulated by pro-inflammatory cytokines, IB proteins are phosphorylated, which results in their ubiquitin-

dependent degradation. This results in the translocation of NF-B to the nucleus, which then binds to target genes that cause further activation for pro-inflammatory cytokines (Milligan & Watkins, 2009). The varying roles of glial cells in pro- and anti-inflammatory activity need to be researched further to thoroughly evaluate glia as potential targets for drug or hormone replacement therapy.

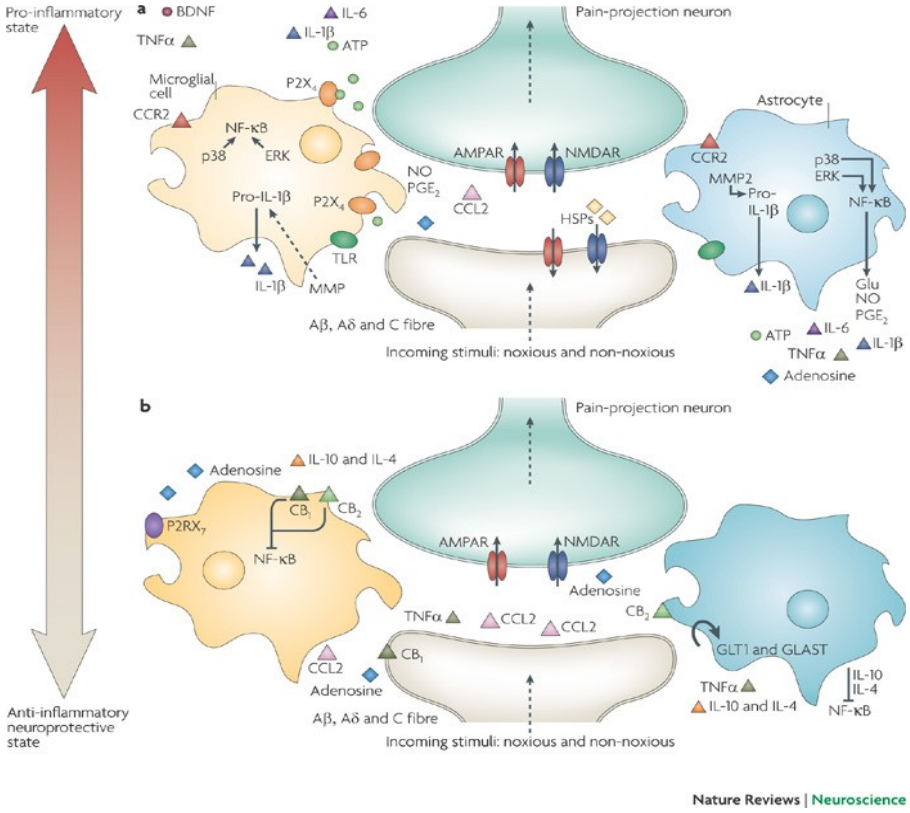

Figure 4.1. A. Pro-inflammatory roles for glia. Chronic inflammation, characterized by the persistence of a noxious input, causes lasting central sensitization, resulting in transcriptional changes in dorsal horn neurons that increase synaptic sensitivity. Astrocytes respond with increased Ca^{2+} signaling, leading to a series of pro-inflammatory events that involve mediators like glutamate (Glu), ATP that binds to $P2X_4$, tumour-necrosis factor- (TNF), interleukin 1 (IL-1), IL-6, nitric oxide (NO) and prostaglandin E_2 (PGE_2). These pro-inflammatory mediators are also released from activated microglia. **B. Anti-inflammatory roles for glia.** Glial cells can exert neuroprotective effects by releasing anti-inflammatory cytokines such as IL-10 and IL-4 and they also express cannabinoid receptors (CB_1 and CB_2). CB_1 and CB_2 have demonstrated anti-inflammatory functions and inhibition of microglial toxicity through the suppression of chemotactic responses and MAPK signal transduction, resulting in inflammatory cytokine inhibition. Also, the glutamate transporters, glutamate transporter 1 (GLT1) and glutamate–aspartate transporter (GLAST), can begin to reuptake glutamate normally. ATP activation of microglial $P2RX_7$ purinoreceptors leads to release of TNF, which protects neurons from the neurotoxic effects of excess glutamate.
From: Watkins & Milligan (2009), NATURE REVIEWS NEUROSCIENCE. Vol 10, 23-36

Estradiol's dampening of glial cell activation results in decreased colocalization of glial cell activation with IL-1β cytokine expression in the spinal cord dorsal horn.

Glia cannot relay pain information from the spinal cord to the brain across synaptic connections because they do not have axons; instead, cells like microglia and astrocytes regulate pain processing by releasing chemicals that augment neuronal excitability and pain signaling. Once microglia become activated, they generate and release a cascade of inflammatory mediators that activate other microglia, nearby astrocytes, and neurons. Activated glia continue to release these mediators, recruiting even more glia, and directly influence neuron-neuron communication because of their proximity to neuronal cell bodies and their expression of different neurotransmitter receptors sensitive to glutamate, ATP and substance P (Haydon, 2001).

IL-1β, a key pro-inflammatory cytokine, is one such mediator that critically influences the development of varied pain states by directly influencing glial modulation of dorsal horn neurons (Vallejo et al., 2010). If estradiol exerts its anti-inflammatory effects by dampening glial cell responses in the dorsal horn, then cytokine responses should decrease accordingly. Our data show immunofluorescent analyses of IL-1β colocalization with GFAP-expressing astrocytes and OX-6-expressing microglia that provide supporting evidence for this claim. Specifically, we observed a strong co-activation of inflammation-induced IL-1β upregulation and glial cell activation that was considerably diminished by estradiol treatment. Significant interactions of hormone and injection on both activated astrocyte and microglia colocalizations with IL-1β substantiate estradiol's anti-inflammatory activity at the level of the dorsal horn.

While linear regression analyses did not significantly predict any relationships of glial/ IL-1β colocalizations with nociceptive behavioral responses, simple correlations between the two

variables yielded significant relationships, particularly in microglia/ IL-1β colocalization. Negative correlations were observed in the vehicle-treated groups at both medium and highest heat intensities. This finding is consistent with our expectations and previous studies, as both glial and cytokine activity should increase with decreased PWL (Vallejo, 2009).

Although astrocytes and microglia are both central mediators of the nervous system's immune response, their patterns of activation in response to inflammation are different. Recent research suggests that microglia activation is involved primarily during the development of a pain state while astrocyte activation is induced soon after and serves to prolong the painful state by promoting the enhanced release of signaling proteins like IL-1β (Raghavendra et al., 2004). By binding to particular receptor sites along an astrocyte's membrane, IL-1β stimulates activation of the cell, which triggers a positive feedback cycle of continued inflammatory mediator release and more glial recruitment. Pro-inflammatory cytokines like TNFα and IL-1β released from glia function to enhance neuronal excitability and synaptic potency by increasing AMPA and NMDA receptor conductivity and expression on neuronal surfaces (Stelwagen & Malenka, 2006). In particular, IL-1β has been demonstrated to increase intracellular Ca^{2+} flow via NMDA receptors in nociceptive neurons of the spinal cord by inducing the phosphorylation of NMDA receptor subunit NR-1, which results in its activation. This activation leads to a significant rise of NO and PGE_2 release, which in turn multiplies the excitability of pain-projection neurons (Zhang et al., 2008).

For example, peripheral nerve injury is immediately followed by a marked increase of intracellular Ca^{2+} which results in the activation of p38 MAPK and ERK proteins in microglia. Previously mentioned pro-inflammatory cytokines like TNFα and IL-1β can also activate these MAPKs, which in turn trigger the activation of a myriad of transcription factors, such as nuclear

factor κB (NF- κB), that potentiate the additional release of pro-inflammatory mediators (Scholz & Woolf, 2007). Additionally, TNFα, although produced in the periphery, crosses the blood-brain barrier and activates microglia to further secrete inflammatory mediators (Sierra et al., 2007). These cumulative pain processing events all contribute to the pathological activation of glia that is the characteristic trademark of many neurodegenerative disorders marked by chronic inflammation.

Intracellular markers show significant correlations with PWL and glial activity in estradiol- and vehicle-treated OVX rats after Cg or saline administration.

The remarkably dynamic effect that glial cells exert on neuronal responses in pain processing makes them key players in the investigation of estradiol's complex anti-inflammatory activity. Many studies have implicated stereotypical immune signals like TNFα and IL-1β in the mediation of glial-neuronal cross-talk in pathological pain development (Watkins et al., 2009; Marchand et al., 2005), but the intracellular mechanisms behind this essential communication have yet to be clearly delineated. To investigate the effects of pro-inflammatory glial responses on intracellular marker levels in this study, spinal cord protein levels were measured through Western blots and correlated. While protein levels of GFAP, OX-6, tERK, pERK, pKA, and nNOS, did not vary significantly among treatment groups, significant differences were found in STAT3 (79) across time conditions, where protein levels were greater at 1 hour post-injection compared with 5 and 24 hours. This significant main effect of time in STAT3 levels supports previous studies in which researchers demonstrated that STAT3 is activated in a time-dependent manner relative to the time of the peripheral nerve injury (Schwaiger et al., 2000; Qiu et al., 2005; Bareyre et al., 2011). Although it failed to reach statistical significance, a similar time

difference was echoed in GFAP (p=0.051), where protein levels were also observed to be the greatest at 1 hour post-injection.

The investigation of relationships between intracellular markers and PWL shows some significant positive and negative correlations. Protein levels of pKA correlated positively across all treatment groups as well as within the vehicle-treated group and the vehicle/saline group, while pERK levels correlated negatively with PWL in the estradiol-treated group administered Cg injection. Linear regression analyses significantly corroborate these findings by showing that pKA positively predicts PWL in the vehicle-treated group and pERK negatively predicts PWL in the estradiol-treated group across injection and time conditions. This finding indicates that an upregulation of pKA is linked to an increase in PWL, or lessened pain response, while an upregulation of pERK is linked to a decrease in PWL, or increased pain response.

The positive correlation with pKA and PWL is inconsistent with studies described earlier. Researchers determined that pKA signaling, associated strong with cAMP signaling, is involved in inflammatory mediator-induced hyperalgesic behavior (Aley and Levine, 1999; Malmberg et al., 1997) and increased nociceptor firing (Cui and Nicol, 1995; Zhang et al., 2002). pERK levels, on the other hand, were negatively correlated with PWL in the estradiol/Cg group and this finding is consistent with our expectations. pERK, part of the MAPK family, has also been identified as a significant contributer to nociceptor sensitization and pathological pain states (Aley et al., 2001). STAT3 (79) correlated negatively with PWL in the vehicle-treated group administered saline injection. Even though a linear regression analysis did not significantly reproduce this finding, the linear relationships between protein levels of STAT3 and PWL in both vehicle- and estradiol-treated groups had negative slopes. Given what is known about STAT3's pro-inflammatory role in peripheral nerve injury (Schwaiger et al., 2000; Qiu et al.,

2005; Bareyre et al., 2011), this suggests that STAT3 levels may also be associated with a decrease in PWL. Correlations between intracellular marker levels and glial cell yielded a few statistically significant relationships. First, GFAP correlated negatively with pERK in the absence of estradiol; this result was unexpected because both astrocyte activation and pERK expression are associated with pro-inflammatory events (Watkins & Milligan, 2009). Second, OX-6 correlated negatively with pERK across all treatment groups, positively with tERK across all groups and in the absence of estradiol, and positively with nNOS in the presence of estradiol without inflammation. Possible reasons for these inconsistent findings will be discussed in the next section.

Chapter 5. Conclusions

The experiments put forth in this thesis were conducted in order to elucidate the complex neuroimmune underpinnings of estradiol's anti-inflammatory behavior. Studies performed earlier in this lab have shown that estradiol has anti-hyperalgesic effects on nociceptive behavioral responses and cytokine production in rats (Shivers; personal communication, 2009). Our results corroborate these findings and go on to indicate that the dampening of glial cell activation is a key mechanism through which estradiol exerts these anti-hyperalgesic effects. In response to inflammation, both astrocytes and microglia showed dramatic increases in activation, colocalized with increased Il-1β cytokine activity, which was considerably dampened in the presence of estradiol. Additionally, estradiol treatment significantly reduced macrophage activity at the injury site. Comparison of estradiol-mediated injury site and dorsal horn activity revealed overall greater activity at the dorsal horn, especially in astrocytes. Correlation of intracellular markers with glial cell activity and behavioral responses supported the significant roles of the MAPK/ERK and JAK/STAT pathways in inflammatory responses. Taken together, our results show that one key mechanism of estradiol's anti-hyperalgesic activity is the dampening of glial cell activation, by which downstream pro-inflammatory signaling events are reduced. When added to the current literature, our research can shed more light on estradiol's complex neuroimmune role in inflammation.

In Aim 1, we revealed that glial cells are powerful vehicles of neuroimmune mediation for estradiol's anti-inflammatory activity. However, contrary to our expectations, linear regression analyses did not significantly predict any relationships between glial cell activation and nociceptive behavioral responses(PWL). While there was some hormone effect seen in PWL responses at the lowest heat intensity, estradiol's effects were not observed at the medium

or highest heat intensities. One explanation for this result is glass temperature as an unforeseen variable. Specifically, the glass surface in the Hargreaves' machine that the animals are placed on for testing can possibly change the heating of the hindpaw because of its ability to act as a heat sink (Hirata et al., 1990). In this manner, it is plausible that some of estradiol's anti-inflammatory effects on nociceptive behavioral responses may have been masked by inconsistent glass temperature on the testing apparatus. Future studies should employ nociceptive behavioral testing models that minimize such intervening variables. Also, it would be useful and interesting to investigate if there are any differences in estradiol-mediated anti-hyperalgesia among different nociceptive behavioral measurement models. Furthermore, employing a variety of behavioral testing models such as the tail-flick and paw-withdrawal tests can account for varying types of pain responses.

Significantly decreased paw size and macrophage activity at the injury site in the presence of estradiol serve as robust indicators of estradiol's local anti-inflammatory activity, but overall dorsal horn glial activation exceeded injury site macrophage activation. Taken together, the results of Aim 1 support many studies that demonstrate estradiol's anti-hyperalgesic effects in different pain models (Hunter et al., 2011; Carlsten et al., 1992; Tarkowski, 1997; Shiraj et al., 1995; Hayashi et al., 1998) and implicate glia as novel targets of pain processing ((Beggs & Salter, 2007; Jergova & Cizkova, 2007; Watkins & Maier, 2003). Most importantly, these results indicate that estradiol carries out its anti-inflammatory activity concomitantly through the reduction of both macrophage activity at the injury site and glial cell activity at the dorsal horn, with greater activation effects at the dorsal horn.

Since this study, in addition to previous research, has shown that microglia and astrocytes display some differences in response to inflammation (Arevallo, 2011), future studies should

examine potential differences in patterns of activation between the two types of glial cells. Astrocytes in particular are juxtaposed with neuronal synapses that they receive signals from and can in turn modify functionally. An example of this is selective glutamate reuptake by astrocytes, whereby activated astrocytes may take up less than the usual amount of glutamate found near excitatory synapses. This results in glutamate-potentiated excitatory neurotransmission and neurotoxicity via NMDA receptors, by which hyperalgesia is established in the spinal cord dorsal horn (Watkins et al., 2001). In this manner, estradiol treatment that causes decreased astrocyte activation may lead to decreased glutamate concentrations at the synapse and reduced NMDA receptor activity, resulting in anti-hyperalgesia. Previous studies examining estradiol's modulation of NMDA activity in rat DRG neurons found that the presence of estradiol resulted in increased densities of NMDAR currents (McRoberts at al., 2007). Further studies elucidating estradiol's regulation of NMDA receptor activity can shed light on a potentially significant mechanism of estradiol's effect on inflammation.

In Aim 2, we explored estradiol's anti-hyperalgesic effects on the next stage of the inflammatory process by examining glial cell-response mediated cytokine activity. Marked increases in IL-1β activity alone, colocalization of GFAP-expressing astrocytes with IL-1β, and OX-6-expressing microglia with IL-1β in response to inflammation were all significantly reduced by the presence of estradiol. These results corroborate findings that highlight estradiol's influential role in inhibiting cytokine production (Pavlov et al., 2003; Shivers; personal communication, 2009). Moreover, previous studies have shown IL-1β to increase the flow of intracellular Ca^{2+} via NMDA receptors in pain-processing neurons of the spinal cord (Viviani, 2003) and it is well known that glia rely heavily on Ca^{2+} signaling to communicate with neurons (Watkins et al., 2001).

In Aim 3, we investigated potential relationships between glial activation and intracellular marker expression to determine the role of signaling pathways in estradiol's anti-inflammatory activity. Contrary to what we expected, Western blot measurements of GFAP and OX-6 protein levels did not reflect the significant effects seen in immunhistochemical analyses. Additionally, GFAP and OX-6 protein levels did not significantly predict levels of the intracellular markers. This inconsistent finding may be due to differences in the measurement of glial cell activation via different assays. For example, Western blot analyses are not able to distinguish GFAP in reactive astrocytes from that in quiescent astrocytes. The consequence of this observation is that it is possible that any of the significant differences in GFAP expression between groups, expressed in a minority of active astrocytes, can be weakened by the majority of quiescent astrocytes that express either unchanged or decreased GFAP expression. IHC analysis, on the other hand, predominantly detects increased GFAP expression in reactive astrocytes (as pre-determined by ROI) without being weakened by reduced activation and consequently decreased GFAP expression in quiescent astrocytes. This line of thought is consistent with the development of astrocyte activation in that it is not a simple all-or-none phenomenon. Instead, astrocyte activation is reflective of a continuum of changes that vary according to context and specific signaling patterns (Milligan & Watkins, 2009). Another reason for a lack of significant effects in the correlations between glial cell activity and intracellular marker expression is variability due to a small n. Behavioral correlations to intracellular markers implicate the MAPK/ERK and JAK/STAT pathways in inflammatory responses mediated by estradiol. This finding is supported by studies that demonstrate that ERK is activated in nociceptors by noxious stimuli like electrical stimulation, NGF, and capsaicin (Delcroix et al., 2003; Dai et al., 2002),

and STAT is activated in a time-dependent manner in response to peripheral nerve injury (Schwaiger et al., 2000; Qiu et al., 2005; Bareyre et al., 2011).

Future studies should continue to explore the relationships between specific intracellular markers and glial activity in a larger sample, and it would be interesting to compare this data to correlations with ER activity, both peripherally and centrally. As seen in this study, estradiol significantly mediates spinal cord dorsal horn activity in the development of inflammatory pain. But, many other studies have shown estradiol's widespread effects in other brain regions like the cerebral cortex, hypothalamus, brainstem, and hippocampus: areas of the brain that allow this complex hormone to influence emotions, learning and memory, cognition, motor coordination and pain sensitivity (Roepke et al., 2011). Estradiol may exert these widespread effects by regulating gene expression via intracellular estrogen receptors or by interacting with cell membrane receptors to rapidly alter neuronal-glia communication and regulate second messenger systems (Roepke et al., 2011). Since the perception of pain is the product of intricate peripheral and central processing, it would be remiss to ignore the higher-order effects of estradiol in the brain on the development and maintenance of pathological states of pain. An investigation of these widespread effects can lead to a better understanding of estradiol's neuroprotective effects.

Another interesting avenue of future research is to explore the effects of opioid and toll-like receptor (TLR) activity in response to glial activation. TLR-mediated glial activation has been found to be important in neuropathic pain and opioid-mediated analgesia, and recent research has found that opioid agonists display TLR4 agonistic activity and may therefore help to regulate glial responses (Hutchinson et al., 2007). Also, studies have shown that mu-opioid receptor antagonists induce anti-hyperalgesic behaviors (Cecarelli et al., 2004).

As demonstrated in the present study, estradiol treatment dramatically alters the morphology and consequent activation patterns of glial cells in response to inflammation, inducing significant anti-hyperalgesic effects in nociceptive behavioral responses and in the spinal cord dorsal horn. Figure 5.1 shows a proposed model for estradiol's mediation of glial intracellular responses and Figure 5.2 shows an overall proposed model illustrating a potential mechanism by which estradiol exerts its anti-inflammatory effects from injury site to brain. In response to tissue injury, estradiol acts at multiple levels of the pain pathway to decrease inflammation. Estradiol's reduced macrophage activation at the injury site coupled with dampened glial cell activation in the spinal cord dorsal horn stifle the pro-inflammatory events that occur at the intracellular level in glial cells along different second messenger pathways.

For instance, glial activation increases intracellular flow of Ca^{2+} via NMDA channels leading to production of NO by NOS. NO increases neuronal excitability in the spinal cord, which boosts glutamate release and stimulates the subsequent release of more inflammatory mediators from sensory neurons (McMahon et al., 2005; Kidd & Urban, 2001). Also, intracellular flow of the inflammatory mediator substance P via the NK1 receptor activates the MAPK pathway, which in turn can cause significant transcriptional changes that alter pain responses. Other inflammatory mediators activate different pathways. Specifically, neurotrophic factors activate the cAMP/pKA pathway and IL-6 activates the JAK/STAT pathway to induce transcriptional changes. Another potential estradiol-mediated pathway is the mu-opioid pathway that stimulates pKA expression, resulting in further transcriptional changes. These intracellular changes can in turn modify and/or be modified by ER receptor activity in higher-order centers of the brain to mediate the ultimate perception of pain.

In summary, our research demonstrates the importance of studying estradiol's dynamic neuroimmune effects on inflammation, especially in the context of glial cell activity. Chronic inflammatory illnesses are dynamically regulated by glial-neuronal communication and both the development and duration of these pain states are robustly influenced by changes in endogenous estrogen levels. Understanding this complex interplay of factors that contribute to pain will add to our general knowledge of gender-specific pain processing and help us improve current treatments in hormone replacement therapy for post-menopausal women.

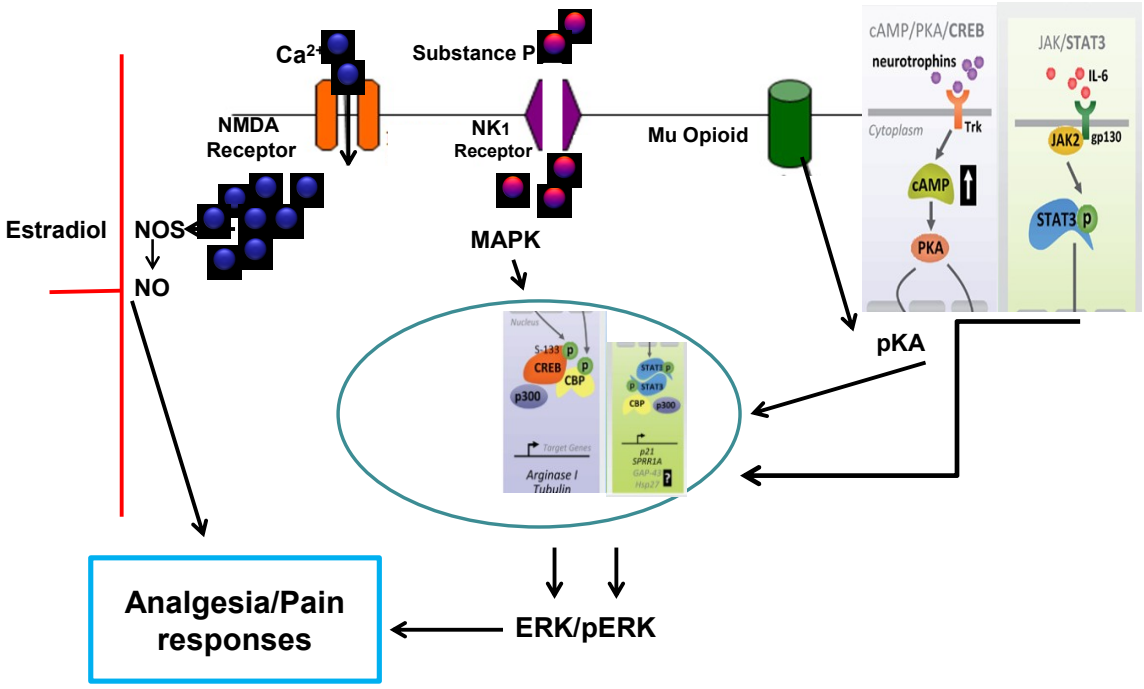

Figure 5.1. Proposed model for estradiol-mediated glial intracellular activity. Estradiol-mediated glial activation increases glial intracellular flow of Ca^{2+} via NMDA channels leading to production of NO by NOS. NO increases neuronal excitability in the spinal cord, which boosts glutamate release and stimulates the subsequent release of more inflammatory mediators from sensory neurons. Also, intracellular flow of the inflammatory mediator substance P via the NK1 receptor activates the MAPK pathway, which in turn can cause significant transcriptional changes that alter pain responses. Other inflammatory mediators activate different pathways. Specifically, neurotrophic factors activate the cAMP/pKA pathway and IL-6 activates the JAK/STAT pathway to induce transcriptional changes. Another potential estradiol-mediated pathway is the mu-opioid pathway that stimulates pKA expression, resulting in further transcriptional changes

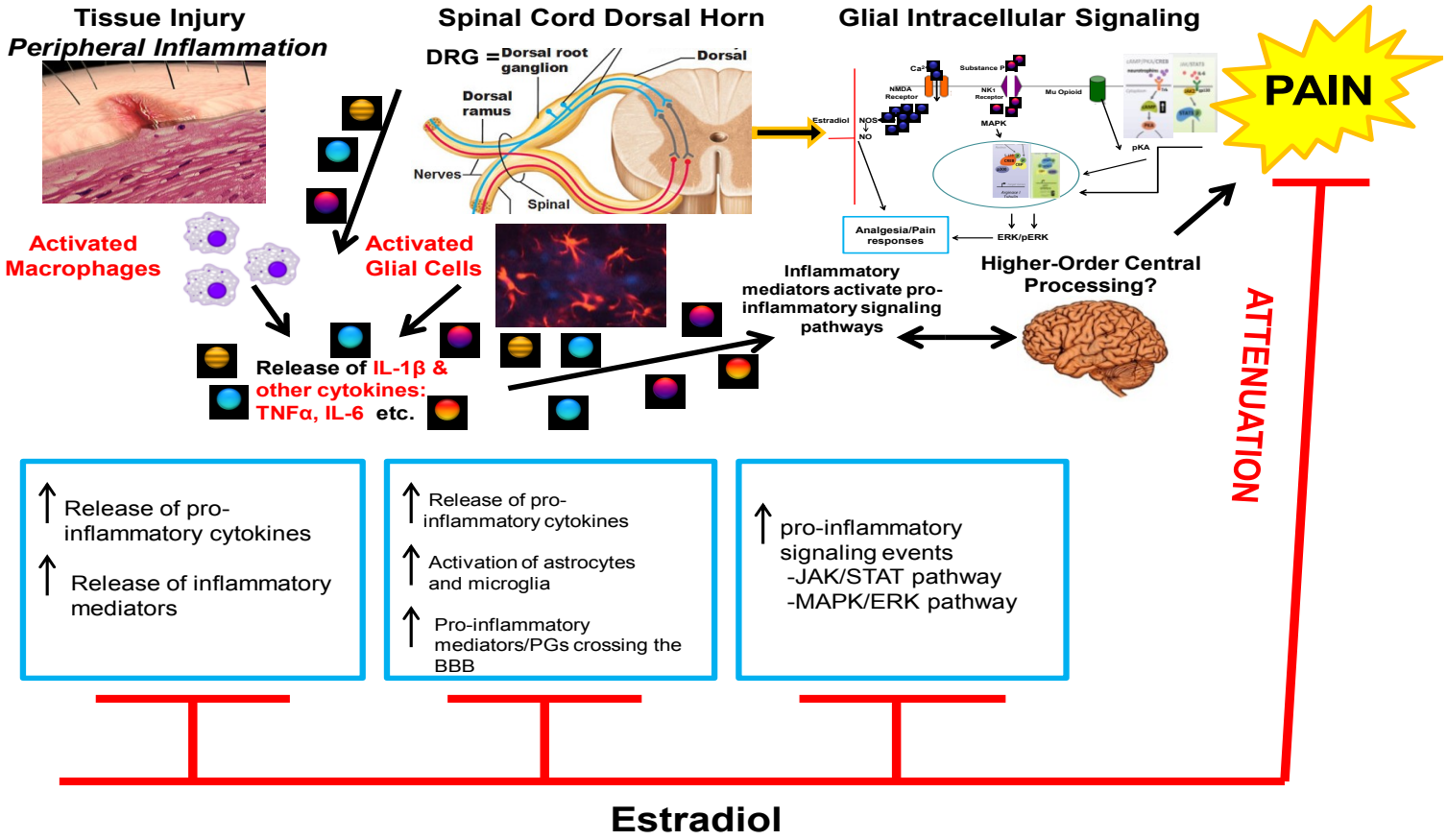

Figure 5.2. Overall proposed model for estradiol's mediation of the inflammatory pain pathway. The inverted T's represent inhibition and arrows represent activation/stimulation. Estradiol's anti-inflammatory effects at injury site, spinal cord dorsal horn, and glial intracellular signaling, with potential role in the contribution of higher order central processing to pain perception, result in attenuated behavioral responses to inflammation.

REFERENCES

Abraham H, Losonczy A, Czeh G, Lazar G. (2001). Rapid activation of microglial cells by hypoxia, kainic acid, and potassium ions in slice preparations of the rat hippocampus. *Brain Res,* 906:115–126.

Abrahamsen, B., Zhao, J., Asante, C.O., Cendan, C.M., Marsh, S., Martinez-Barbera, J.P., et al. (2008). The cell and molecular basis of mechanical, cold, and inflammatory pain. Science, 321, 702-705.

Angst, M.S., Clark, J.D., Carvalho, B., Tingle, M., Schmelz, M., & Yeomans, D.C. (2008). Cytokine profile in human skin in response to experimental inflammation, noxious stimulation, and administration of a COX-inhibitor: A microdialysis study. Pain, 139(1), 15-27.

Bacci A, Verderio C, Pravettoni E, Matteoli M. (1999). The role of glial cells in synaptic function. Philos Trans R Soc Lond B Biol Sci, 354:403–409.

Basbaum, A.I., & Jessell, T.M. (2000). The perception of pain. In E.R. Kandell, J.H. Schwartz, & T.M. Jessell, (Eds.), Principles of Neural Science, 4/e (pp.472-491). New York: McGraw-Hill.

Beggs S, Salter MW. (2007). Stereological and somatotopic analysis of the spinal microglial response to peripheral nerve injury. *Brain Behav Immun,* 21:624–633.

Bennett, G.J. Animal models of pain. In: Kruger, L. (ed.) Methods of Pain Research, Boca Raton, FL: CRC Press; 2001: 67-92.

Berkley, K. J. (1997). Sex differences in pain. Behavioral and Brain Sciences, 20, 371-380.

Brahmachari S, Fung YK, Pahan K. (2006). Induction of glial fibrillary acidic protein expression in astrocytes by nitric oxide. *J Neurosci,* 26:4930–4939.

Cahoy JD, Emery B, Kaushal A, et al. (2008). A transcriptome database for astrocytes, neurons, and oligodendrocytes: a new resource for understanding brain development and function. *J Neurosci,* 28:264–278.

Ceccarelli, I., Fiorenzani, P., Massafra, C., & Aloisi, A.M. (2003a). Long-term ovariectomy changes formalin-induced licking in female rats: the role of estrogens. Reproductive Biology and Endocrinology, 1, 24-33.

Ceccarelli, I., Scaramuzzino, A., Massafra, C., & Aloisi, A.M. (2003b). The behavioral and neuronal effects induced by repetitive nociceptive stimulation are affected by gonadal hormones in male rats. Pain, 104, 35-47.

Chichorro, J.G., Lorenzetti, B.B., & Zampronio, A.R. (2004). Involvement of bradykinin, cytokines, sympathetic amines and prostaglandins in formalin-induced orofacial nociception in rats. British Journal of Pharmacology, 141, 1175-1184.

Costigan, M., & Woolf, C.J. (2000). Pain: Molecular mechanisms. The Journal of Pain, 1(3), 35-44.

Coutaux, A., Adam, F., Willer, J-C., & Le Bars, D. (2005). Hyperalgesia and allodynia: Peripheral mechanisms. Joint Bone Spine, 72, 359-371.

Coyle DE. (1998). Partial peripheral nerve injury leads to activation of astroglia and microglia which parallels the development of allodynic behavior. *Glia,* 23:75–83.

Cunha, F.Q., Poole, S,. Lorenzetti, B.B., Beiga, F.H., Ferreira, S.H. (1999). Cytokine-mediated inflammatory hyperalgesia limited by interleukin-4. British Journal of Pharmacology, 126, 45-50.

Cunha, T.M., Verri, Jr., W.A., Silva, J.S., Poole, S., Cunha, F.Q., & Ferreria, S.H. (2005). A cascade of cytokines mediates mechanical inflammatory hypernociception in mice. Proceedings of the National Academy of Sciences, 102, 1755-1760.

Cuzzocrea S, Santagati S, Sautebin L, Mazzon E, Calabrò G, Serraino I, Caputi AP, Maggi A. (2000). 17 beta-estradiol antiinflammatory activity in carrageenan-induced pleurisy. *Endocrinology*, 141(4):1455-63.

Cuzzocrea S, Mazzon E, Sautebin L, Serraino I, Dugo L, Calabró G, Caputi AP, Maggi A.(2001). The protective role of endogenous estrogens in carrageenan-induced lung injury in the rat. *Mol Med*, 7(7):478-87.

Cuzzocrea S, Genovese T, Mazzon E, Esposito E, Di Paola R, Muià C, Crisafulli C, Peli A, Bramanti P, Chaudry IH. (2008). *Shock*, 29(3):362-71.

Davalos D, Grutzendler J, Yang G, et al. (2005). ATP mediates rapid microglial response to local brain injury in vivo. *Nat Neurosci,* 8:752–758.

DeLeo, J.A., Colburn, R.W., & Rickman, A.J. (1997). Cytokine and growth factor immunohistochemical spinal profiles in two animal models of mononeuropathy. Brain Research, 759, 50-57.

DeLeo JA, Colburn RW. Proinflammatory cytokines and glial cells: their role in neuropathic pain. (1998) In: Walkins LRaM SF, ed. *Cytokines and Pain*. Basel: Birkhauser: 159–181.

Dinarello CA. (1999). *Overview of Inflammatory Cytokines and Their Role in Pain.* Berlin: Birkhauser.

Ferreira SH, Lorenzetti BB, Bristow AF, Poole S (1998). Interleukin-1 beta as a potent hyperalgesic agent antagonized by a tripeptide analogue. *Nature,* 334:698–700.

Fiocchetti, M., Ascenzi, P. , Marino, M. (2012). Neuroprotective Effects of 17β-Estradiol Rely on Estrogen Receptor Membrane Initiated Signals. *Front Physiol* 3:73-83.

Gardell LR, Hyldtoft L, Del Tredici AL, Andersen CB, Fairbairn LC, Lund BW, Gustafsson M, Brann MR, Olsson R, Piu F. (2008). Differential modulation of inflammatory pain by a selective estrogen receptor beta agonist. *Eur J Pharmacol*, 11;592(1-3):158-9.

Garrison CJ, Dougherty PM, Carlton SM. (1994). GFAP expression in lumbar spinal cord of naive and neuropathic rats treated with MK-801. *Exp Neurol,* 129:237–243.

Gaumond, I., Arsenault, P., & Marchand, S. (2005). Specificity of female and male sex hormones on excitatory and inhibitory phases of formalin-induced nociceptive responses. Brain Research, 1052, 105-111.

Gold, M., Reichling, D., Shuster, M., & Levine, J. (1996). Hyperalgesic agents increase a tetrodotoxin-resistent Na^+ current in nociceptors. Proceedings of the National Academy of Sciences, 93(3), 1108-1112.

Gupta, S., Mehrotra, S., Villalon, C.M., Perusquia, M., Saxena, P.R., VanDenBrink, A.M. (2007). Potential role of female sex hormones in the pathophysiology of migraine. Pharmacology & Therapeutics, 113, 321-340.

Guo W, Wang H, Watanabe M, et al. (2007). Glial-cytokineneuronal interactions underlying the mechanisms of persistent pain. *J Neurosci,* 27:6006–6018.

Hansson E. (2006). Could chronic pain and spread of pain sensation be induced and maintained by glial activation? *Acta Physiol (Oxf),* 187:321–327.

Hertz L, Hansson E. (2007) *Roles of Astrocytes and Microglia in Pain Memory*. Seattle, WA: IASP press.

Holguin A, O'Connor KA, Biedenkapp J, et al. (2004). HIV-1 gp120 stimulates proinflammatory cytokine-mediated pain facilitation via activation of nitric oxide synthase-I (nNOS). *Pain,* 110:517–530.

Hopkins, S.J. (2007). Central nervous system recognition of peripheral inflammation: a neural, hormonal collaboration. Acta Biomedica, 231-247.

Jergova S, Cizkova D. (2007). Microglial activation in different models of peripheral nerve injury of the rat. *J Mol Histol,* 38:245–251.

Kidd, B.L., & Urban, L.A. (2001). Mechanisms of inflammatory pain. British Journal of Anaesthesia, 87(1), 3-11.

Kuba, T., Kemen, L.M., & Quinones-Jenab, V. (2005). Estradiol administration mediates the inflammatory response to formalin in female rats. Brain Research, 1047, 119-122.

Kuba, T., & Quinones-Jenab, V. (2005). The role of female gonadal hormones in behavioral sex differences in persistent and chronic pain: Clinical versus preclinical studies. Brain Research Bulletin, 66, 179-188.

Kuba, T., Wu, H.-B. K., Nazarian, A., Festa, E.D., Barr, G.A., Jenab, S., et al. (2006). Estradiol and progesterone differentially regulate formalin-induced nociception in ovariectomized female rats. Hormones and Behavior, 49, 441-449.

Lawson LJ, Perry VH, Dri P, Gordon S. (1990). Heterogeneity in the distribution and morphology of microglia in the normal adult mouse brain. (*Neuroscience.* 1990;39:151–170.

Loram, L.C., Fuller, A., Fick, L.G., Cartmell, T., Poole, S., & Mitchell, D. (2006). Cytokine profile during carrageenan-induced inflammatory hyperalgesia in rat muscle and hind paw. The Journal of Pain, 8, 127-136.

Macfarlane, T.V., Blinkhorn, A., Worthington, H.V., Davies, R.M., & Macfarlane, G.J. (2002). Sex hormonal factors and chronic widespread pain: a population study among women. Rheumatology, 41, 454-457.

Mannino, C.A., South, S.M., Quinones-Jenab, V., & Inturrisi, C.E. (2006). Estradiol replacement in ovariectomized rats is antihyperalgesic in the formalin test. The Journal of Pain,8, 334-342.

Marshall, J.S., Leal-Berumen, I., Nielsen, L., Glibetic, M., & Jordana, M. (1996). Interleukin (IL)-10 inhibits long-term IL-6 production but not preformed mediator release from rat peritoneal mast cells. The Journal of Clinical Investigation, 97(4), 1122-1128.

Martin, V.T., & Behbehani, M. (2006). Ovarian hormones and migraine headache: Understanding mechanisms and pathogenesis—Part 2. Headache, 46, 365-386.

McHugh, J.M., & McHugh, W.B. (2000). Pain: Neuroanatomy, chemical mediators, and clinical implications. American Association of Critical-Care Nurses Clinical Issues, 11(2), 168-178.

McMahon, S., Cafferty, W., & Marchand, F. (2005). Immune and glial cell factors as pain mediators and modulators. Experimental Neurology, 192(2), 444-462.

McRoberts, J., Li, J., Ennes, H., Mayer, E. (2007). Sex-dependent differences in the activity and modulation of NMDA receptors in rat DRG neurons. *Neuroscience* 148(4): 1015–1020.

Meller ST, Gebhart GF. (1993). Nitric oxide (NO) and nociceptive processing in the spinal cord. *Pain,* 52:127–136.

Mertz, P.M., DeWitt, D.L., Stetler-Stevenson, W.G., & Wahl, L.M. (1994). Interleukin 10 suppression of monocyte prostaglanding H synthase-2. The Journal of Biological Chemistry, 269(33), 21322-21329.

Meyer, R.A., Ringkamp, M., Campbell, J.N., & Raja, S.N. (2005). Peripheral mechanisms of cutaneous nociception. In S. McMahon & M. Koltzenburg (Eds.), Wall and Melzack's Textbook of Pain, 5/e (pp.3-27). New York: Elsevier Health Sciences.

Miller AJ, Luheshi GN, Rothwell NJ, Hopkins SJ. (1997). Local cytokine induction by LPS in the rat air pouch and its relationship to the febrile response. *Am J Physiol,* 272: R857–R861.

Milligan, E.D., & Watkins, L.R. (2009). Pathological and protective roles of glia in chronic pain. Nature Reviews, 10, 23-36.

Miyoshi K, Obata K, Kondo T, Okamura H, Noguchi K. (2008). Interleukin-18-mediated microglia/astrocyte interaction in the spinal cord enhances neuropathic pain processingafter nerve injury. *J Neurosci,* 28:12775–12787.

Moalem, G., & Tracey, D.J. (2006). Immune and inflammatory mechanisms in neuropathic pain. Brain Research Reviews, 51, 240-264.

Nakajima K, Kohsaka S. (2001). Microglia: activation and their significance in the central nervous system. *J Biochem,* 130:169–175.

Neumann, S., Doubell, T.P., Leslie, T., & Woolf, C.J. (1996). Inflammatory pain hypersensitivity mediated by phenotypic switch in myelinated primary sensory neurons. Nature, 384, 360-364.

Perkins MN, Kelly D, Davis AJ. (1995). Bradykinin B1 and B2 receptor mechanisms and cytokine-induced hyperalgesia in the rat. *Can J Physiol Pharmacol,* 73:832–836.

Petrenko AB, Yamakura T, Baba H, Shimoji K. (2003). The role of N-methyl-D-aspartate (NMDA) receptors in pain: a review. *Anesth Analg.* 2003;97:1108–1116.

Pozzi S, Benedusi V, Maggi A, Vegeto E. (2006). Estrogen action in neuroprotection and brain inflammation. *Ann NY Acad Sci*, 1089:302-23

Ren, K., & Dubner, R. (1999). Inflammatory models of pain and hyperalgesia. ILAR Journal Online: Animal Models of Pain, 40(3), 1-7.

Riedel, W., & Neeck, G. (2001). Nociception, pain, and antinociception: Current concepts. Zeitschrift für Rheumatologie, 60, 404-415.

Rittner, H.L., Machelska, H., & Stein, C. (2005). Leukocytes in the regulation of pain and analgesia. Journal of Leukocyte Biology, 78, 1215-1222.

Rittner, H.L., & Stein, C. (2005). Involvement of cytokines, chemokines, and adhesion molecules in opioid analgesia. European Journal of Pain, 9, 109-112.

Rivest S. (1999). What is the cellular source of prostaglandins in the brain in response to systemic inflammation? Facts and controversies. *Mol Psychiatry,* 4:500–507.

Roepke, T., Ronnekleiv, O., Kelly, M. (2011). Physiological consequences of membrane-initiated estrogen signaling in the brain. *Front Biosci* 16: 1560-1573.

Saab, C.Y., Waxman, S.G., & Hains, B.C. (2008). Alarm of curse? The pain of neuroinflammation. Brain Research Reviews, 58, 226-235.

Safieh-Garabedian B, Poole S, Allchorne A, Winter J, Woolf CJ. (1995). Contribution of interleukin-1 beta to the inflammation-induced increase in nerve growth factor levelsand inflammatory hyperalgesia. *Br J Pharmacol,* 115: 1265–1275.

Schafers, M., & Sorkin, L. (2008). Effect of cytokines on neuronal excitability. Neuroscience Letters, 437, 188-193.

Schindler R, Mancilla J, Endres S, Ghorbani R, Clark SC, Dinarello CA. (1990). Correlations and interactions in the production of interleukin-6 (IL-6), IL-1, and tumor necrosis factor (TNF) in human blood mononuclear cells: IL-6 suppresses IL-1 and TNF. *Blood,* 75:40–47.

Sommer, C., & Kress, M. (2004). Recent findings on how proinflammatory cytokines cause pain: peripheral mechanisms in inflammatory and neuropathic hyperalgesia. Neuroscience Letters, 361, 184-187.

Stoll G, Jander S. (1999). The role of microglia and macrophages in the pathophysiology of the CNS. *Prog Neurobiol,* 58:233–247.

Sweitzer, S.M., Arruda, J.L., & DeLeo, J.A. The cytokine challenge: Methods for the detection of central cytokines in rodent models of persistent pain. In: Kruger, L. (ed.) Methods of Pain Research, Boca Raton, FL: CRC Press; 2001: 109-132.

Tall, J.M., & Crisp, T. (2004). Effects of gender and gonadal hormones on nociceptive responses to intraplantar carrageenan in the rat. Neuroscience Letters, 354, 239-241.

teVelde, A.A., Huijbens, R.J.F., Heije, K., de Vries, J.E., & Figdor, C.G. (1990). Interleukin-4 (IL-4) inhibits secretion of IL-1β, tumor necrosis factor α, and IL-6 in human monocytes. Blood, 76, 1392-1397.

Meller ST, Gebhart GF. Nitric oxide (NO) and nociceptive processing in the spinal cord. *Pain.* 1993;52:127–136.

Brahmachari S, Fung YK, Pahan K. Induction of glial fibrillary acidic protein expression in astrocytes by nitric oxide. *J Neurosci.* 2006;26:4930–4939.

Hansson E. Could chronic pain and spread of pain sensation be induced and maintained by glial activation? *Acta Physiol (Oxf).* 2006;187:321–327.

Abraham H, Losonczy A, Czeh G, Lazar G. Rapid activation of microglial cells by hypoxia, kainic acid, and potassium ions in slice preparations of the rat hippocampus.
Brain Res. 2001;906:115–126

Carbonaro V, Caraci F, Giuffrida ML, Merlo S, Canonico PL, Drago F, Copani A, Sortino MA. Enhanced expression of ERalpha in astrocytes modifies the response of cortical neurons to beta-amyloid toxicity. Neurobiol Dis 2009; 33: 415–421.

Perea G, Navarrete M, Araque A. Tripartite synapses: astrocytes process and control synaptic information. Trends Neurosci 2009; 32: 421–431.

Freudenberg MA, Tchaptchet S, Keck S, Fejer G, Huber M, Schutze N, Beutler B, Galanos C. Lipopolysaccharide sensing an important factor in the innate immune response to Gram-negative bacterial infections: benefits and hazards of LPS hypersensitivity. Immunobiology 2008; 213: 193–203.

Serbina, N. V., T. Jia, T. M. Hohl, E. G. Pamer. 2008. Monocyte-mediated defense against microbial pathogens. Annu. Rev. Immunol. 26: 421–452.

Taylor, P. R., L. Martinez-Pomares, M. Stacey, H. H. Lin, G. D. Brown, S. Gordon. 2005. Macrophage receptors and immune recognition. Annu. Rev. Immunol. 23: 901–944.

Scholz, J. & Woolf, C. J. The neuropathic pain triad: neurons, immune cells, and glia. Nature Neurosci. 10, 1361–1368 (2007).

Haydon, P. G. Glia: listening and talking to the synapse. Nature Rev. Neurosci. 2, 185–193 (2001).

Carlsten H, Nilsson N, Jonsson R, Backman K, Holmdahl R, Tarkowski A 1992 Estrogen accelerates immune complex glomerulonephritis but ameliorates T cell mediated vasculitis and sialadenitis in autoimmune MRL Ipr/mice. Cell Immunol 144:190–198

Josefsson E, Tarkowski A 1997 Suppression of type II collagen-induced arthritis by the endogenous oestrogen metabolite 2-methoxyestradiol. Arthritis Rheum 40:154–63

Shirai M, Sato A, Chida K 1995 The influence of ovarian hormones on the granulomatous inflammatory process in the rat lung. Eur Respir J 8:272–277

Hayashi T, Yamada K, Esaki T, Muto E, Chaudhuri G, Iguchi A 1998 Physiological concentrations of 17β-estradiol inhibit the synthesis of nitric oxide synthase in macrophages via a receptor-mediated system. J Cardiovasc Pharmacol 31:292–298

Xiaoya Wang,1 Richard J. Traub,2,3 and Anne Z. Murphy1,3 Am J Physiol Regul Integr Comp Physiol. 2006 August; 291(2): R300–R306. Published online 2006 February 23. Persistent Pain Model Reveals Sex Difference in Morphine Potency.

Dayna R. Loyd, Xioaya Wang, Anne Z. Murphy J Sex Differences in Mu Opioid Receptor Expression in the Rat Midbrain Periaqueductal Gray are Essential for Eliciting Sex Differences

in Morphine Analgesia Neurosci. Author manuscript; available in PMC 2010 February 10. 2008 December 24; 28(52): 14007.

Lawson LJ, Perry VH, Dri P, Gordon S. Heterogeneity in the distribution and morphology of microglia in the normal adult mouse brain. *Neuroscience.* 1990;39:151– 170.

Nakajima K, Kohsaka S. Microglia: activation and their significance in the central nervous system. *J Biochem.* 2001;130:169–175.

Stoll G, Jander S. The role of microglia and macrophages in the pathophysiology of the CNS. *Prog Neurobiol.* 1999;58:233–247.

Garrison CJ, Dougherty PM, Carlton SM. GFAP expression in lumbar spinal cord of naive and neuropathic rats treated with MK-801. *Exp Neurol.* 1994;129:237–243.

Miyoshi K, Obata K, Kondo T, Okamura H, Noguchi K. Interleukin-18-mediated microglia/astrocyte interaction in the spinal cord enhances neuropathic pain processing after nerve injury. *J Neurosci.* 2008;28:12775–12787.

Dinarello CA. *Overview of Inflammatory Cytokines and Their Role in Pain*. Berlin: Birkhause; 1999.

Hertz L, Hansson E. *Roles of Astrocytes and Microgliain Pain Memory*. Seattle, WA: IASP press; 2007.

Petrenko AB, Yamakura T, Baba H, Shimoji K. The role of N-methyl-D-aspartate (NMDA) receptors in pain: a review. *Anesth Analg.* 2003;97:1108–1116.

Hogan QH. Role of decreased sensory neuron membrane calcium currents in the genesis of neuropathic pain. *Croat Med J.* 2007;48:9–21.

Guo W, Wang H, Watanabe M, et al. Glial-cytokineneuronal interactions underlying the mechanisms of persistent pain. *J Neurosci.* 2007;27:6006–6018.

Holguin A, O'Connor KA, Biedenkapp J, et al. HIV-1 gp120 stimulates proinflammatory cytokine-mediated pain facilitation via activation of nitric oxide synthase-I (nNOS). *Pain.* 2004;110:517–530. 90.

Sommer C, Schmidt C, George A. Hyperalgesia in experimental neuropathy is dependent on the TNF receptor 1. *Exp Neurol.* 1998;151:138–142. 91. Dinarello CA. *Overview of Inflammatory Cytokines and Their Role in Pain*. Basel: Birkhauser; 1998.

Ferreira SH, Lorenzetti BB, Bristow AF, Poole S. Interleukin-1 beta as a potent hyperalgesic agent antagonized by a tripeptide analogue. *Nature.* 1988;334:698–700.

Safieh-Garabedian B, Poole S, Allchorne A, Winter J, Woolf CJ. Contribution of interleukin-1 beta to the inflammation-induced increase in nerve growth factor levels and inflammatory hyperalgesia. *Br J Pharmacol.* 1995;115: 1265–1275.

Perkins MN, Kelly D, Davis AJ. Bradykinin B1 and B2 receptor mechanisms and cytokine-induced hyperalgesia in the rat. *Can J Physiol Pharmacol.* 1995;73:832–836.

Tilg H, Trehu E, Atkins MB, Dinarello CA, Mier JW. (1994). Interleukin-6 (IL-6) as an anti-inflammatory cytokine: induction of circulating IL-1 receptor antagonist and soluble tumor necrosis factor receptor p55. *Blood,* 83:113–118.

Uceyler, N., & Sommer, C. (2008). Cytokine regulation in animal models of neuropathic pain and in human diseases. Neuroscience Letters, 437, 194-198.

Vale, et al. (2003). Antinociceptive effects of interleukin-4, -10, and -13 on the writhing response in mice and zymosan-induced knee joint incapacitation in rats. The Journal of Pharmacology and Experimental Therapeutics, 304, 102-108.

Vallejo, R., Tilley, D.M., Vogel, L., & Benyamin, R. (2010). The role of glia and the immune system in the development and maintenance of neuropathic pain. *Pain Practice, 10(3),* 167–184.

Verri, Jr., W.A., Cunha, T.M., Parada, C.A., Poole, S., Cunha, F.Q., & Ferreira, S.H. (2006). Hypernociceptive role of cytokines and chemokines: Targets for analgesic drug development? Pharmacology & Therapeutics, 112, 116-138.

Wagner, R., Janjigian, M., & Myers, R.R. (1998). Anti-inflammatory interleuki-10 therapy in CCI neuropathy decreases thermal hyperalgesia, macrophage recruitment, and endoneurial TNF-α expression. Pain, 74, 35-42.

Watkins, L.R., & Maier, S.F. (1999). Implications of immune-to-brain communication for sickness and pain. Proceedings from the National Academy of Sciences, 96, 7710-7713.

Watkins LR, Maier SF. (2003) Glia: a novel drug discovery target for clinical pain. *Nat Rev Drug Discov,* 2:973–985.

Watkins LR,Milligan ED,Maier SF (2001). Glial activation: a driving force for pathological pain. *Trends Neurosci.* 24:450–455.

Weiseler-Frank, J., Maier, S.F., & Watkins, L.R. (2004). Glial activation and pathological pain. Neurochemistry International, 45, 389-395.

Weiseler-Frank, J., Maier, S.F., & Watkins, L.R. (2005). Central proinflammatory cytokines and pain enhancement. Neurosignals, 14, 166-174.

Xu, X.J., Hao, J.X., Olsson, T., Kristensson, K., van der Meide, P.H., & Wiesenfeld-Hallen, Z. (1994). Intrathecal interferon-gamma facilitates the spinal nociceptive flexor reflex in the rat. Neuroscience Letters, 18, 263-266.

Zhang F, Vadakkan KI, Kim SS, Wu LJ, Shang Y, Zhuo M. (2008). Selective activation of microglia in spinal cord but not higher cortical regions following nerve injury in adultmouse. *Mol Pain,* 4:15.